

**Workshop on
Super-Intense Laser-Atom Physics**

The Fields Institute for Research in
Mathematical Sciences

Toronto, Ontario Canada

December 11-13, 2018

SILAP 2018

<https://silap2018.physics.utoronto.ca/>



Thanks from the Co-Chairs

Many thanks to all those who have contributed to hosting SILAP for 2018!

For the last eight months, the committee has made invaluable contributions in advising and making decisions:

- Martin Centurion, University of Nebraska, USA
- Nam Chang Hee, Gwangju Institute of Science & Technology (GIST), KOREA
- Eric Constant, Institut Lumière Matière, Université Lyon, FRANCE
- Paul Corkum, University of Ottawa, CANADA
- Joseph H. Eberly, University of Rochester, USA
- George Gibson, University of Connecticut, USA
- Gianluca Gregori, University of Oxford, UK
- Misha Ivanov, Max Born Institute, Berlin, GERMANY
- Miroslav Kolesik, University of Arizona, USA
- François Légaré, INRS-EMT, CANADA
- Robert Levis, Temple University, USA
- Ruxin Li, Shanghai Institute of Optics and Fine Mechanics, CHINA
- Gérard Mourou, Ecole Polytechnique, FRANCE
- Frédéric Pérez, Ecole Polytechnique, FRANCE
- Boyd, Robert, University of Rochester, USA
- Olga Smirnova, Max Born Institute, Berlin, GERMANY
- Sam Vinko, University of Oxford, UK

June Rockwell, Bryan Eelhart, and Esther Berzunza from the Fields Institute have very ably provided almost all the logistics for the workshop, including registration and abstract-submission support, coordinating catering for breaks, advising and facilitating both the reception and the dinner. Thanks very much too to the Fields Institute itself for its policy of furnishing all the meeting support including provision of our meeting spaces.

Joane Magnaye, University of Toronto Physics, has given many hours of administrative support, which will continue through reimbursement of travel subsidies for some of the earliest-career participants at the workshop. Thanks to Raul Cunha in Physics for graphic design and printing.

Many thanks to Jules Parent of Amplitude, and to Chris Ebert and John Miles of Coherent, for their generous funding to the workshop, which has gone towards subsidy of student travel.

Last but certainly not least, thanks to all the speakers and attendees of SILAP2018, who bring their science and who will create the actual workshop.

Robin Marjoribanks
Howard Milchberg
Co-Chairs SILAP 2018

WORKSHOP WEBSITE:

<http://silap2018.physics.utoronto.ca>

FIELDS INSTITUTE WIFI:

Network: FieldsWiFi

Password: Mathem@ics! (no T needed...)

General Access Code: December-gc87

2.1 Visitor Information

Checking in

Please pick up your event program package and badge by the reception desk. If you do not see a badge with your name, check in with the receptionist. Please wear your badge during your event so that Fields staff can recognize you as a guest at Fields.

Wireless Connectivity, Printing, & Faxing

To connect to the Fields Wireless Network, choose network **FieldsWiFi** and enter the password **Mathem@ics!** (Note: Do not add a "t" after the "@" sign). Open a web browser and follow the instructions to register your device. If you are a visitor without a Fields Institute Account, please use this month's wireless code, available at the Front Desk.

For detailed instructions and troubleshooting for wireless and wired connectivity, please see the handout available at the reception desk.

Printing instructions can be found on the webpage following login to the Fields Wireless Network.

Local faxing is available in room 345. This machine's receiving number is 416-348-9385.

Building Hours & Contact

222 College St., 2nd Floor
Toronto, Ontario M5T 3J1

Hours: Weekdays, 9 a.m. to 5 p.m.
Telephone: **416-348-9710**

Reimbursement Information

Questions about reimbursements should be directed to Joane Magnaye, jmagnaye@physics.utoronto

Libraries

The University of Toronto's main library is Robarts Library (130 St. George St.). The specialized Math and Statistics Library is located on the 6th floor of the Bahen Center (40 St. George St.).

For more information on the University's libraries, visit: <https://onereach.library.utoronto.ca> or call **416-978-8450**.

Parking

Pay parking is available in an outdoor lot across from the Institute at 236 College St., as well as underground at 213 Huron St. (just north from College St.). More information can be found at <http://map.utoronto.ca/access/parking-lots>.

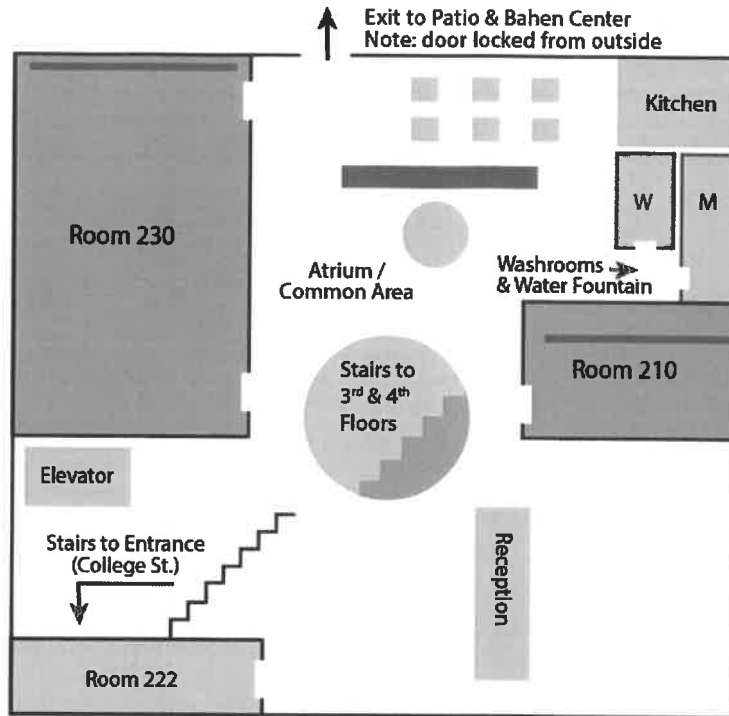
Fire Safety & Emergencies

Should an alarm sound, you are required to leave the building immediately. Do not use the elevator to exit the building when a fire alarm is sounding.

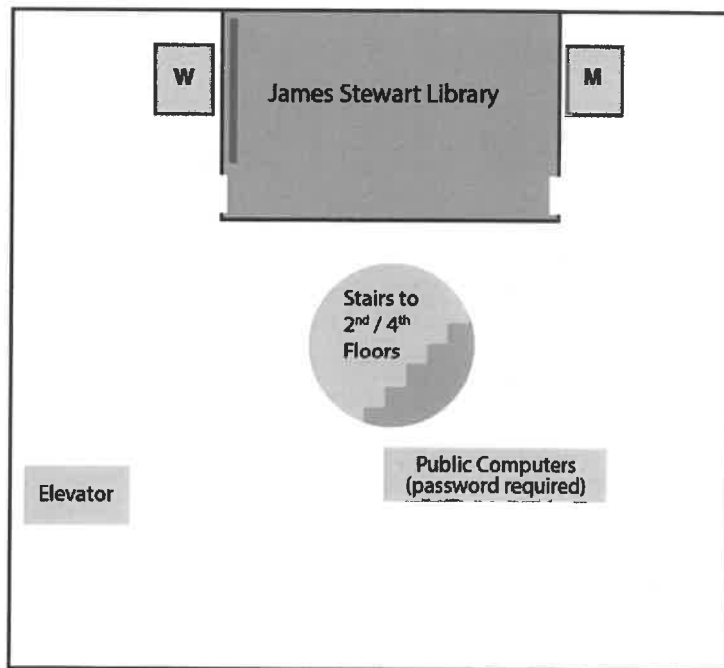
For campus police, dial **416-978-2222**. Dial **911** in an emergency.

2.2 Floor Plan

W: Women's Washroom
M: Men's Washroom



Main (2nd) Floor



3rd Floor

Tuesday, 11 December 2018

8:15 – 9:00	REGISTRATION DESK PACKAGE PICKUP	June Rockwell / Joane Magnaye	
		Presenting Author	Affiliation
9:00 – 9:30	Welcome, Opening Remarks, and Orientation	Co-Chairs	
	<u>High Harmonics and XUV generation</u>	Chair – Paul Corkum	
9:30 – 10:00	Optic-less focusing and spectral filtering of XUV high order harmonics	Mével, Eric	Université de Bordeaux, CNRS, CEA, Centre Lasers Intenses et Appl Invited
10:00 – 10:30	High harmonic generation source for table-top ultrafast magnetic imaging	Légaré, Francois	Institut national de la recherche scientifique Invited
10:30 – 10:50	COFFEE BREAK		
10:50 – 11:10	Phase-matched extreme-ultraviolet frequency-comb generation	Porat, Gil	University of Alberta Contributed
11:10 – 11:40	Giant chiral macroscopic response in high harmonic generation	Ayuso, David	Max-Born-Institut Invited
11:40 – 12:00	Enhancing the Brilliance of Harmonic XUV Radiation with Tailored Driver Beams	Treacher, Daniel	University of Oxford Contributed
12:00 – 13:30	LUNCH – Nearby Restaurants, e.g., see Fields List		
	<u>Electron Dynamics & Ionization</u>	Chair – Robin Marjoribanks	
13:30 – 14:00	Time-resolving electron dynamics in molecules using strong laser fields: coherent probes of charge m	Mauger, Francois	Louisiana State University Invited
14:00 – 14:20	Longitudinal momentum of the electron at the tunnelling exit	Wang, Xu	Graduate School of China Academy of Engineering Physics Contributed
14:20 – 14:40	Characterization of electron wavepackets from strong-field ionization	Liu, Yunquan	Peking University Contributed
14:40 – 15:00	Nondipole effects in atomic dynamic interference	Wang, Mu-Xue	Peking University Contributed
15:00 – 15:20	COFFEE BREAK		
	<u>Relativistically Driven Electron Dynamics</u>	Chair – Francois Legare	
15:20 – 15:50	Polarization-Resolved Nonlinear Thomson Scattering from Laser-Driven Electrons	Peatross, Justin	Brigham Young University Invited
15:50 – 16:20	Magnetic field generation, dynamics and reconnection driven by relativistic intensity laser pulses	Willingale, Louise	University of Michigan Invited
16:20 – 16:50	Relativistic electron dynamics in laser-driven nanowire targets	Marjoribanks, Robin	University of Toronto Invited
18:00 – 19:30	Reception – PreNup Pub		

Wednesday, 12 December 2018

8:40 – 9:00	REGISTRATION DESK PACKAGE PICKUP	June Rockwell / Joane Magnaye		
		Presenting Author	Affiliation	
9:00 – 9:10	Updates and Comments	Co-Chairs		
	<u>Novel Drive and Source-Control Physics</u>	Chair – David Ayuso		
9:10 – 9:40	Topological strong field physics on sub-laser cycle timescale	Jiménez-Galán, Alvaro	Max Born Institut	Invited
9:40 – 10:10	Spatio-temporal optical vortices (STOVs): experiments and simulations	Milchberg, Howard	University of Maryland	Invited
10:10 – 10:30	Nondipole and ellipticity effects in the strong-field ionization physics	Daněk, Jiří	Max-Planck-Institut für Kernphysik	Contributed
10:30 – 10:50	COFFEE BREAK			
	<u>Atom/Molecule Control Physics & Characterization</u>	Chair – Howard Milchberg		
10:50 – 11:20	Unexpected coherent extreme ultraviolet radiation from He atoms exposed to a strong laser field	Kim, Kyung Taec	Gwangju Institute of Science and Technology	Invited
11:20 – 11:50	Strong field physics and high harmonic generation with structured light beams	Corkum, Paul	University of Ottawa	Invited
11:50 – 12:20	Resonantly enhanced inner-orbital ionization in molecular iodine	Gibson, George	University of Connecticut	Invited
12:30 – 14:00	LUNCH – Nearby Restaurants, e.g., see Fields List			
	<u>Electron Dynamics & Ionization – II</u>	Chair – Justin Peatross		
14:00 – 14:30	Photoionization dynamics: Transition and scattering delays	Taiëb, Richard	Sorbone Université	Invited
14:30 – 15:00	Time-dependent multiconfiguration and coupled-cluster methods for intense-laser driven multielectr	Sato, Takeshi	University of Tokyo	Invited
15:00 – 15:20	Hollow core fiber pulse compression using molecular gases	Haddad, Elissa	INRS, Centre Énergie Matériaux et Télécommunications	Contributed
15:30 – 18:00	POSTER SESSION - McLennan Physical Laboratories North Wing			
	Snacks, Beer, Wine			

Thursday, 13 December 2018

8:40 – 9:00	REGISTRATION DESK PACKAGE PICKUP	June Rockwell / Joane Magnaye		
9:00 – 9:10	Updates and Comments	Presenting Author	Affiliation	
	<u>Atomic and Optical Dynamics in Filaments</u>	Co-Chairs		
		Chair – Siegfried Glenzer		
9:10 – 9:40	Spectral interference in shortwave- and mid-infrared laser filaments in gases	Polynkin, Pavel	University of Arizona	Invited
9:40 – 10:00	Light amplification by nearly free electrons in a laser filament	Richter, Maria	Max-Born-Institut	Contributed
10:00 – 10:20	Optical lasing during laser filamentation in the Nitrogen molecular ion: ro-vibrational inversion	Morales, Felipe	Max-Born-Institut	Contributed
10:20 – 10:40	COFFEE BREAK			
	<u>Intense Optical Lasers and Free-Electron Lasers</u>	Chair – George Gibson		
10:40 – 11:10	Exploring matter in extreme conditions with free electron lasers	Glenzer, Siegfried	SLAC National Accelerator Laboratory	Invited
11:10 – 11:30	Transform-limited hard-x-ray lasers pumped by x-ray free-electron lasers	Lyu, Chunhai	Max Planck Institute for Nuclear Physics	Contributed
11:30 – 12:00	Identification of coupling mechanisms between ultraintense laser light and dense plasmas	Leblanc, Adrien	Université Paris-Saclay, CEA Saclay	Invited
12:00 – 12:20	Wakefield acceleration and betatron radiation driven by linearly polarized Laguerre-Gaussian orbital	Longman, Andrew	University of Alberta	Contributed
12:30 – 14:00	LUNCH – Nearby Restaurants, e.g., see Fields List			
	<u>High-Harmonic Spectroscopy and Ionization Dynamics</u>	Chair – Éric Mével		
14:00 – 14:20	High-harmonic spectroscopy of electron-hole dynamics induced by strong-field ionization	Zhao, Jing	National University of Defense Technology	Contributed
14:20 – 14:40	Coherent multichannel dynamics of aligned molecules resolved by two dimensional high-harmonic an	Wang, Xiaowei	National University of Defense Technology	Contributed
14:40 – 15:00	Temporal characterization of a two-color laser field using the tunneling ionization method	Shin, Jeong-uk	Gwangju Institute of Science and Technology	Contributed
15:00 – 15:20	COFFEE BREAK			
	<u>Control and Analysis Using Strong Laser Fields</u>	Chair – Pavel Polynkin		
15:20 – 15:40	Ignatovsky Diffraction: Calculating Vector Fields in an Arbitrarily Tight Laser Focus	Ware, Michael	Brigham Young University	Contributed
15:40 – 16:00	Coupling cryogenic low-Z jets with ultra-intense lasers to observe novel effects induced by relativistic	Curry, Chandra	SLAC National Accelerator Laboratory	Contributed
16:00 – 16:20	Space-Time Resolved Analysis of Electron Repulsion	Glasgow, Scott	Brigham Young University	Contributed
16:20 – 16:40	Remote detection of radioactive material using mid-IR laser-driven electron avalanche	Schwartz, Robert	University of Maryland	Contributed
19:00-22:00	Dinner at Ristorante EVOO	Co-Chairs host		

Super-Intense Laser-Atom Physics 2018
The Fields Institute for Research in Mathematical Sciences
Toronto, Ontario Canada
December 11-13, 2018
<https://silap2018.physics.utoronto.ca/>

TUESDAY, 11 DECEMBER 2018

8:15 – 9:00	REGISTRATION	Package Pick up	June Rockwell / Joane Magnaye
9:00 – 9:30	Welcome, Opening Remarks, and Orientation		Co-Chairs

HIGH HARMONICS AND XUV GENERATION

Chair – Paul Corkum

9:30 – 10:00 Eric Mével K. Veyrinas, C. Valentin, L. Quintard, V. Strelkov, J. Vabek, O. Hort, A. Dubrouil, D. Descamps, F. Burgy, C. Péjot, F. Catoire and E. Constant (Invited) -Université de Bordeaux, CNRS, CEA, Centre Lasers Intenses et Applications, France

Optic-less focusing and spectral filtering of XUV high order harmonics

10:00 – 10:30 Francois Légaré, V. Cardin, T. Balciunas, K. Légaré, N. Jaouen, J. Lüning, A. Baltuska, (Invited) Institut national de la recherche scientifique, Canada

High harmonic generation source for table-top ultrafast magnetic imaging

10:30 – 10:50 **COFFEE BREAK**

10:50 – 11:10 Gil Porat, C.M. Hey, S.B. Schoun, C. Benko, N. Dörre, K.L. Corwin, and J. Ye (Contributed) Department of Electrical and Computer Engineering, University of Alberta, Canada

Phase-matched extreme-ultraviolet frequency-comb generation

11:10 – 11:40 David Ayuso, A. Ordoñez, S. Patchkovskii, P. Declewa, M. Ivanov and O. Smirnova (Invited) Max Born Institute, Germany

Giant chiral macroscopic response in high harmonic generation

Session continues...

11:40 – 12:00 Daniel Treacher, David T. Lloyd, Florian Wiegandt, Kevin O’Keeffe, and Simon M. Hooker (Contributed) University of Oxford, Clarendon Laboratory, UK
Enhancing the Brilliance of Harmonic XUV Radiation with Tailored Driver Beams

12:00 – 13:30 **LUNCH** – Nearby Restaurants, e.g., see Fields List

ELECTRON DYNAMICS & IONIZATION

Chair – Robin Marjoribanks

13:30 – 14:00 Francois Mauger, P.M. Abanador, A.S. Bruner, M. Gordon, T.T. Gorman, S. Khatri, A. Sissay, S. Hernandez, P. Sándor, T.D. Scarborough, P. Agostini, L.F. DiMauro, M.B. Gaarde, R.R. Jones, K. Lopata, K.J. Schafer (Invited), Louisiana State University, USA

Time-resolving electron dynamics in molecules using strong laser fields: coherent probes of charge migration

14:00 – 14:20 Xu Wang, Ruihua Xu and Tao Li (Contributed) Graduate School of China Academy of Engineering Physics, China

Longitudinal momentum of the electron at the tunnelling exit

14:20 – 14:40 Yunquan Liu (Contributed) Peking University, China

Characterization of electron wavepackets from strong-field ionization

14:40 – 15:00 Mu-Xue Wang, Hao Liang, Xiang-Ru Xiao, Si-Ge Chen, Wei-Chao Jiang and Liang-You Peng (Contributed) Peking University, China

Nondipole effects in atomic dynamic interference

15:00 – 15:20 **COFFEE BREAK**

RELATIVISTICALLY DRIVEN ELECTRON DYNAMICS

Chair – François Légaré

15:20 – 15:50 Justin Peatross, B. Pratt, C. Schulzke, and M. Ware (Invited) Brigham Young University, USA

Polarization-Resolved Nonlinear Thomson Scattering from Laser-Driven Electrons

Session continues...

15:50 – 16:20 Louise Willingale, P. T. Campbell, A. Raymond, C. A. J. Palmer, N. Alexander L. Antonelli, A. Bhattacharjee, A. F. A. Bott, H. Chen, V. Chvykov, E. Del Rio, C. Dong, G. Fiksel, P. Fitzsimmonds, W. Fox, G. Gregori, J. Halliday, B. Hou, P. Kordell, K. Krushelnick, Y. Ma, A. Maksimchuk, A. McKelvey, C. Mileham, E. Montgomery, J. Nees, P. M. Nilson, M. Notley, C.P. Ridgers, A. A. Schekochihin, C. Stoeckl, A. G. R. Thomas, E. Tubman, M. S. Wei, G. J. Williams, N. Woolsey, V. Yanovsky, C. Zulick, (Invited) University of Michigan (USA)

Magnetic field generation, dynamics and reconnection driven by relativistic intensity laser pulses

16:20 – 16:50 Robin Marjoribanks, Ludovic Lecherbourg, J. E. Sipe, Gábor Kulcsár, Jeremy Li, Andrew Tan, Sam Vinko, Alan Miscampbell, Oliver Humphries, Justin Wark Anne Héron, Frédéric Pérez (Invited) University of Toronto, Canada

Relativistic electron dynamics in laser-driven nanowire targets

18:00 – 19:30 **RECEPTION– PreNup Pub**

191 College St Toronto, ON M5T 1P9 | Phone: (416) 506-4040

WEDNESDAY, 12 DECEMBER 2018

8:40 – 9:00 REGISTRATION Package Pick up June Rockwell / Joane Magnaye

9:00 – 9:10 Updates and Comments Co-Chairs

NOVEL DRIVE & SOURCE-CONTROL PHYSICS

Chair – David Ayuso

9:10 – 9:40 Alvaro Jiménez-Galán, R.E.F. Silva, B. Amorim, O. Smirnova, and M. Ivanov (Invited) Max Born Institut, Germany

Topological strong field physics on sub-laser cycle timescale

9:40 – 10:10 Howard Milchberg, R S. Zahedpour, S. Hancock, N. Jhajj and J. K. Wahlstrand, (Invited) University of Maryland, USA

Spatio-temporal optical vortices (STOVs): experiments and simulations

10:10 – 10:30 Daněk, Jiří, M. Klaiber, K. Z. Hatsagortsyan, B. Willenberg, J. Maurer, B. W. Mayer, C. R. Phillips, L. Gallmann, U. Keller and C. H. Keitel (Contributed) Max-Planck-Institut für Kernphysik, Germany

Nondipole and ellipticity effects in the strong-field ionization physics

10:30 – 10:50 COFFEE BREAK

ATOM/MOLECULE CONTROL PHYSICS & CHARACTERIZATION

Chair – Howard Milchberg

10:50 – 11:20 Kyung Taec Kim, Hyoek Yun, Je Hoi Mun, Sung In Hwang, Seung Beom Park, Igor A. Ivanov and Chang Hee Nam (Invited) Gwangju Institute of Science and Technology, Korea

Unexpected coherent extreme ultraviolet radiation from He atoms exposed to a strong laser field

11:20 – 11:50 Paul Corkum, Fanqi Kong and Chunmei Zhang (Invited) University of Ottawa, Canada

Strong field physics and high harmonic generation with structured light beams

11:50 – 12:20 George Gibson and D. L. Smith (Invited) University of Connecticut, USA

Resonantly enhanced inner-orbital ionization in molecular iodine

12:30 – 14:00 **LUNCH** – Nearby Restaurants, e.g., see Fields List

ELECTRON DYNAMICS & IONIZATION – II

Chair – Justin Peatross

14:00 – 14:30 Richard Taiëb, M. Labeye, A. Desrier, M. Vacher, A. Maquet, and J. Caillat
(Invited)

Sorbone Université, France

Photoionization dynamics: Transition and scattering delays

14:30 – 15:00 Takeshi Sato (Invited) University of Tokyo, Japan

Time-dependent multiconfiguration and coupled-cluster methods for intense-laser driven multielectron dynamics

15:00 – 15:20 Elissa Haddad, R. Safaei, A. Leblanc, R. Piccoli, Y.-G. Jeong, H. Ibrahim, B.E. Schmidt, R. Morandotti, L. Razzari, F. Légar1, and P. Lassonde (Contributed)

INRS, Centre Énergie Matériaux et Télécommunications, Canada

Hollow core fiber pulse compression using molecular gases

15:30 – 18:00 **POSTER SESSION - McLennan Physical Laboratories North Wing,
Room MP 125**

Snacks, Beer, Wine

THURSDAY, 13 DECEMBER 2018

8:40 – 9:00 REGISTRATION Package Pick up June Rockwell / Joane Magnaye

9:00 – 9:10 Updates and Comments Co-Chairs

ATOMIC AND OPTICAL DYNAMICS IN FILAMENTS:

Chair – Siegfried Glenzer

9:10 – 9:40 Pavel Polynkin (Invited) University of Arizona, USA
Spectral interference in shortwave- and mid-infrared laser filaments in gases

9:40 – 10:00 Maria Richter, Mary Matthews, Felipe Morales, Alexander Patas, Albrecht Lindinger, Julien Gatea, Nicolas Berti, Sylvain Hermelin, Jérôme Kasparian, Timm Bredtmann, Olga Smirnova, Jean-Pierre Wolf and Misha Ivanov (Contributed) Max-Born-Institut, Germany
Light amplification by nearly free electrons in a laser filament

10:00 – 10:20 Felipe Morales, M. Lytova, M. Spanner, M. Richter, O. Smirnova, and M. Ivanov (Contributed) Max-Born-Institut, Germany
Optical lasing during laser filamentation in the Nitrogen molecular ion: ro-vibrational inversion

10:20 – 10:40 COFFEE BREAK

INTENSE OPTICAL LASERS AND FREE-ELECTRON LASERS:

Chair: George Gibson

10:40 – 11:10 Siegfried H. Glenzer, Z. Chen, B. Ofori-Okai et al. (Invited)
SLAC National Accelerator Laboratory, USA
Exploring matter in extreme conditions with free electron lasers

11:10 – 11:30 Chunhai Lyu, S.M. Cavaletto, C.H. Keitel and Z. Harman (Contributed)
Max-Planck-Institut for Nuclear Physics, Germany
Transform-limited hard-x-ray lasers pumped by x-ray free-electron lasers

11:30 – 12:00 Adrien Leblanc, L. Chopineau, G. Blaclard, A. Denoëud, M. Thévenet, J-L. Vay, G. Bonnaud, Ph. Martin, H. Vincenti, and F. Quéré, (Invited)
LIDYL, CEA, CNRS, Université Paris-Saclay, France
Identification of coupling mechanisms between ultraintense laser light and dense plasmas

Session continues...

12:00 – 12:20 Andrew Longman, C. Salgado, G. Zeraouli, J. I. Apiñaniz, J. A. Pérez-Hernández, M. De Marco, C. Z. He, G. Gatti, L. Volpe, W. T. Hill III, and R. Fedosejevs (Contributed) University of Alberta, Canada
Wakefield acceleration and betatron radiation driven by linearly polarized Laguerre-Gaussian orbital angular momentum laser pulses

12:30 – 14:00 **LUNCH** – Nearby Restaurants, e.g., see Fields List

HIGH-HARMONIC SPECTROSCOPY AND IONIZATION DYNAMICS

Chair – Eric Mével

14:00 – 14:20 Jing Zhao, XW Wang and ZX Zhao (Contributed)
National University of Defense Technology, China
High-harmonic spectroscopy of electron-hole dynamics induced by strong-field ionization

14:20 – 14:40 Xiaowei Wang, Yindong Huang, Jing Zhao, and Zengxiu Zhao (Contributed)
National University of Defense Technology, China
Coherent multichannel dynamics of aligned molecules resolved by two dimensional high-harmonic and terahertz spectroscopy

14:40 – 15:00 Jeong-uk Shin, Wosik Cho, and Kyung Taec Kim (Contributed)
Gwangju Institute of Science and Technology, Korea
Temporal characterization of a two-color laser field using the tunneling ionization method

15:00 – 15:20 **COFFEE BREAK**

CONTROL AND ANALYSIS USING STRONG LASER FIELDS

Chair – Pavel Polynkin

15:20 – 15:40 Michael Ware and Justin Peatross (Contributed)
Brigham Young University, USA
Ignatovsky Diffraction: Calculating Vector Fields in an Arbitrarily Tight Laser Focus

15:40 – 16:00 Chandra Curry, M. Gauthier, H-G. Chou, A. Grassi, J. B. Kim, G. Dyer, †, X. Jiao, E. Galtier, G. D. Glenn, S. Goede, R. Mishra, E. McCary, L. Obst, H. J. Quevedo, M. Rehwald, C. Schoenwaelder, Y. Y. Tsui, T. Ziegler, T. Ditmire, K. Zeil, U. Schramm, B. M. Hegelich, ‡, F. Fiuza, and S. H. Glenzer (Contributed)
SLAC National Accelerator Laboratory, USA
Coupling cryogenic low-Z jets with ultra-intense lasers to observe novel effects induced by relativistic transparency.

Session continues...

16:00 – 16:20 Scott Glasgow, and M.J. Ware (Contributed)
Brigham Young University, USA

Space-Time Resolved Analysis of Electron Repulsion

16:20 – 16:40 Robert Schwartz, D. Woodbury, J. Isaacs, P. Sprangle, and H.M. Milchberg
(Contributed) University of Maryland, USA

Remote detection of radioactive material using mid-IR laser-driven electron avalanche

18:00 - 22:00 **Dinner at Ristorante EVOO** Co-Chairs host

138 Avenue Rd, Toronto, ON M5R 2H6 | (647) 560-0381

Contributed and Invited Oral Presentations

Optic-less focusing and spectral filtering of XUV high order harmonics

E. Mével¹, K. Veyrinas¹, C. Valentin¹, L. Quintard¹, V. Strelkov², J. Vabek¹, O. Hort¹, A. Dubrouil¹, D. Descamps¹, F. Burgy¹, C. Péjot¹, F. Catoire¹ and E. Constant³

¹Université de Bordeaux, CNRS, CEA, Centre Lasers Intenses et Applications (CELIA), 43 rue P. Noailles, 33400 Talence, France

²A M Prokhorov General Physics Institute of Russian Academy of Sciences, 38, Vavilova Street, Moscow 119991, Russia.

³Univ Lyon, Université Claude Bernard Lyon 1, CNRS, Institut Lumière Matière (ILM), F-69622 Villeurbanne, France

Corresponding author: eric.mével@u-bordeaux.fr

Abstract

We demonstrate a proper control of the harmonic generation process leading to converging XUV beams without using any optics. The divergence properties vary with the harmonic order. They are controlled by moving a thin gas jet position along a tailored TW IR beam. A Gaussian analytical model reproduces this effect that is predicted to be significant since the XUV foci can be shifted by up to 10 laser Rayleigh ranges as compared to IR focus position. It opens new route for optimizing broadband XUV intensities or selecting a specific XUV range without a set of dispersive and/or low reflectivity optics.

Context

A major challenge in attoscience is to produce XUV intensities high enough to perform attosecond XUV/XUV pump/probe experiments. Joint optimization of both generation efficiency and XUV beam mode is therefore crucial. Additionally, proper XUV spectral selection must be achieved without temporal spreading and/or significant attenuation while filtering out the strong IR driving field. Finally, a broad spectrum must be focused at a same position in order to permit a homogeneous temporal resolution across the studied target.

Experimental results

We show here that one can address those concerns by directly producing high order harmonics as converging beams without any optics [1]. Such an effect occurs when the gas jet is placed upstream the laser focus where the IR converging wave front transferred to the harmonic wavefront dominates on the diverging contribution due to the transverse gradient of the harmonic phase. Experimental evidence are obtained by using a thin gas jet and our corrected wavefront-and thus nearly perfect Gaussian ($M^2=1.04$)-TW ECLIPSE Ti:Sapph. Laser in CELIA. The divergence properties of harmonics have been studied as a function of the jet position and of the harmonic order. By introducing a spatial chirp in the IR beam, one was also able to distinguish converging and diverging harmonics since the direction of the XUV chirp observed in the far field is reversed or preserved respectively (see Fig. 1).

Simulations

A simple Gaussian analytical model allows us to nicely reproduces the measured XUV far field sizes and their evolution with the jet position and thus to identify key control parameters. SFA based numerical simulations corroborates the findings.

First applications and conclusions

By placing a 140 μm pinhole 37 cm after the IR focus, it was possible to tune the transmitted XUV spectra by varying the jet position. Transmittance can reach up to 80 % with a 9:1 contrast and an estimated IR attenuation larger than 99%. Recent SWORD [2] measurement has been performed to determine the position and the size of the harmonic foci. It confirms and quantifies the control of the self-focused harmonics.

Those experiments open new perspectives to select XUV spectra and obtain high XUV intensities without or with less optics or metallic filters. More advanced IR beam shaping are foreseen to achieve optimized broadband optic-less focusing compatible with homogeneous attosecond resolution.

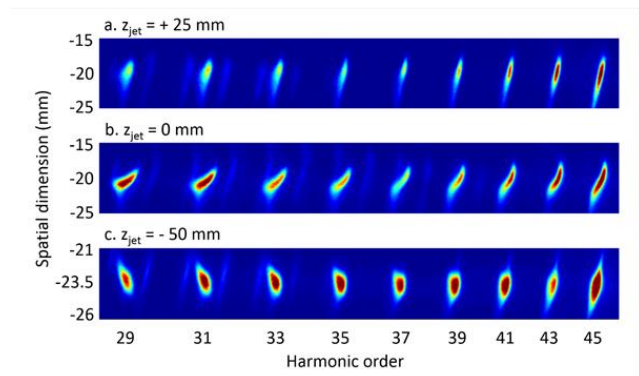


Fig. 1. Far field spatially resolved high-order harmonic spectra obtained with a spatially chirped IR beam. The neon jet is located at various longitudinal positions (a) 25 mm after IR focus, (b) at IR focus and (c) 50 mm before IR focus. The tilt of the harmonic beams is the signature of a spatial chirp in the XUV beams

References

- [1] L. Quintard *et al.* (<http://arxiv.org/abs/1810.07282>)
- [2] E. Frumker *et al.*, Opt. Express 20, 13870 (2012)

High harmonic generation source for table-top ultrafast magnetic imaging

V. Cardin¹, T. Balciunas², K. Légaré¹, N. Jaouen³, J. Lüning⁴, A. Baltuska², and F. Légaré¹

¹Institut national de la recherche scientifique, Varennes, QC, Canada.

²Institute of Photonics, TU Wien, Vienna, Austria.

³Laboratoire de Chimie Physique Matière et Rayonnement, UPMC, Paris, France.

⁴Synchrotron SOLEIL, Saint-Aubin, France.

Corresponding author: legare@emt.inrs.ca

Abstract

We generate harmonics in neon, reaching the cobalt M-edge absorption resonance. A pump-probe scheme then allows us to retrieve demagnetization curves by observing resonant X-ray magnetic scattering on a multilayer cobalt/platinum sample. Using this setup, we are investigating the underlying physics of ultrafast demagnetization by changing the pump wavelength and its pulse duration.

The discovery of the ultrafast optical demagnetization by Beaurepaire *et al.* [1], in 1996, has opened the way to faster data manipulation by optical means. This has been a motivation for extensive investigation of the ultrafast optical demagnetization phenomena, yet the mechanisms behind it are still being debated. In the work presented here, we make use of the HHG source of the Advanced Laser Light Source laboratory (ALLS) to probe ultrafast optical demagnetization at the M-edge of cobalt by resonant magnetic X-ray scattering (RXMS). This scheme has been presented for the first time by Vodungbo *et al.* [2], and we have implemented this approach to investigate the fundamental temporal limit of ultrafast magnetization dynamics and its dependence on pump laser wavelength. The sample studied in this work is a [Co/Pt] multilayer film in which the magnetic domains present out-of-plane magnetization vectors. The inset of figure 1 shows a magnetic force microscope image of the sample's magnetic domains. When placed at the focus of a soft X-ray source tuned to the magnetic edge

energy of the sample, light scattering occurs on the magnetic centers. The diffraction peaks have a width and angular distribution dependent on the size and orientation of the magnetic domains, and an intensity dependent on the magnetization vector's amplitude [3]. Through a pump-probe measurements of the diffracted signal, ultrafast magnetization dynamics is tracked as a function of laser parameters, i.e. the pump pulse duration and its wavelength. Preliminary results are under analysed and will be presented at the meeting.

References

1. E. Beaurepaire, J.-C. Merle, A. Daunois, and J.-Y. Bigot, "Ultrafast spin dynamics in ferromagnetic nickel," *Phys. Rev. Lett.* **76**, 4250–4253 (1996).
2. B. Vodungbo *et al.*, "Laser-induced ultrafast demagnetization in the presence of a nanoscale magnetic domain network," *Nat. Commun.* **3** (2012).
3. J. B. Kortright *et al.*, "Soft-x-ray small-angle scattering as a sensitive probe of magnetic and charge heterogeneity," *Physical Review B - Condensed Matter and Materials Physics* **64** (2001).

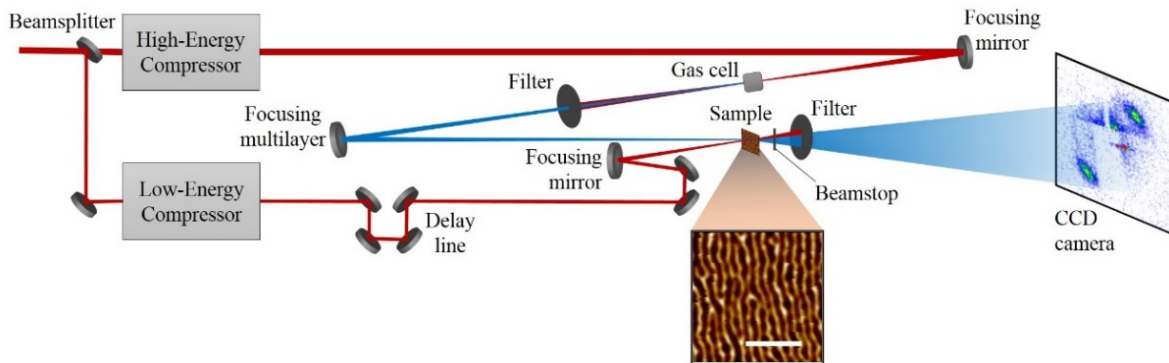


Figure 1 - Layout of the experimental setup for probing ultrafast magnetization dynamics. The sample is positioned with its domains aligned diagonally so that the peaks appear in the corners of the image on the camera. A magnetic force microscope image of the sample is presented in the inset, showing domains with a periodicity of ~ 145 nm. The scale bar represents 1 μm .

Phase-matched extreme-ultraviolet frequency-comb generation

G. Porat^{1,2}, C.M. Heyl^{1,3}, S.B. Schoun¹, C. Benko¹, N. Dörre^{1,4}, K.L. Corwin^{1,5}, and J. Ye¹

¹JILA, NIST and the University of Colorado, 440 UCB, Boulder, CO 80309-0440, USA

²Now at: Department of Electrical and Computer Engineering, University of Alberta, Edmonton, Alberta, T6G 2V4, Canada

³Department of Physics, Lund University, P. O. Box 118, SE-221 00 Lund, Sweden

⁴University of Vienna, Faculty of Physics, VCQ &, QuNaBioS, Boltzmannngasse 5, A-1090 Vienna, Austria

⁵Department of Physics, Kansas State University, Manhattan, Kansas, USA

Corresponding author: gporat@ualberta.ca

Abstract

High-harmonic generation (HHG) in gases is widely used to obtain extreme ultraviolet (XUV) laser radiation. Typically, such lasers operate at low pulse repetition rates (<100 kHz), where phase-matching facilitates efficient HHG. However, high repetition rates (>10 MHz) are necessary where high counting statistics or frequency-comb precision are required. Unfortunately, at high repetition rates, plasma accumulates in the generation volume and prevents phase-matching. We use high-temperature gas mixtures to increase the gas translational velocity and reduce plasma accumulation. We achieve phase-matched HHG at repetition rate of 77 MHz, and generate record power of ~2 mW at 97 nm and ~0.9 mW at 67 nm.

Infrared laser-driven HHG in gases is a well-established method for generating coherent XUV radiation. It is typically achieved using low repetition rate (<100 kHz) laser systems. However, many applications require high repetition rates, e.g., for high counting statistics. Most notably, frequency stabilization for precision XUV frequency comb spectroscopy requires repetition rates $\gg 10$ MHz.

Efficient HHG requires matching the phase velocities of the driving infrared wave and the generated XUV wave. XUV radiation is then generated in-phase along the generation gas and adds up constructively. This is known as phase-matching.

Phase-matched HHG is commonly achieved at low repetition rates, where different contributions to dispersion can be balanced against each other [1]. When the repetition rate exceeds ~10 MHz, phase-matching becomes very challenging. The reason is that the high laser intensities required for HHG ($\sim 10^{14}$ W/cm²) result in plasma generation. At high repetition rates the plasma generated by one pulse does not have time to clear the generation volume before the next pulse arrives and generates more plasma. Therefore, a high-density steady-state accumulation of plasma is formed in the generation volume [2] (see Fig. 1). This high-density plasma is highly dispersive and prevents phase-matching.

We address the steady-state plasma problem by adding a light carrier gas (helium) to the heavy generation gas (xenon). In addition, we heat up the generation gas to ~550°C. Both methods contribute to increasing the gas jet forward velocity, thus reducing the number of consecutive laser pulses that interact with the same atom/ion. The effective gas jet speed is controlled by adjusting the relative amounts of helium and xenon as well as the gas temperature. Note that our laser intensity is too low to ionize helium, so HHG takes place only in xenon.

We applied this method to our XUV comb system, which consists of a 80 W, 77 MHz repetition-rate Yb: fiber frequency comb at a wavelength of 1070 nm, locked to a passive enhancement cavity. Using a 9:1 He:Xe gas mixture, with a backing pressure of ~100 bar applied to a heated quartz nozzle with 50 μ m orifice diameter, we were able to generate ~2 mW and ~0.9 mW at 97 nm and 67 nm, respectively [3]. To the best of our knowledge, this is the highest average power achieved in this wavelength range with a HHG-based source.

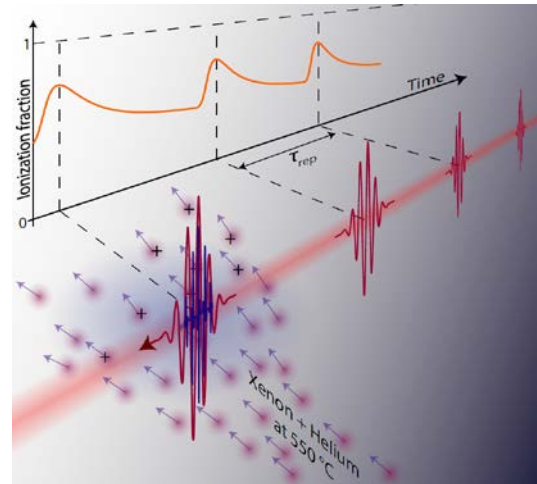


Fig. 1. High-repetition-rate high-harmonic generation inside a gas jet. At high repetition rates (>10 MHz) the interval between consecutive pulses becomes shorter than the plasma transit time through the generation volume, resulting in plasma accumulation, which prevents phase-matching [2]. Heated gas mixes speed up the plasma motion, clearing it between pulses. This facilitates phase-matching and thus much higher efficiency [3].

References

- [1] C.M. Heyl *et al.*, *J. Phys. B* **50**, 013001 (2017).
- [2] T. Allison *et al.*, *Phys. Rev. Lett.* **107**, 183903 (2011).
- [3] G. Porat *et al.*, *Nature Photonics* **12**, 387 (2018).

Giant chiral macroscopic response in high harmonic generation

D. Ayuso¹, A. Ordoñez¹, S. Patchkovskii¹, P. Decleva², M. Ivanov^{1,3,4} and O. Smirnova^{1,5}

¹ Max-Born-Institut, Max-Born-Str. 2A, 12489 Berlin, Germany

² Dipartimento di Scienze Chimiche e Farmaceutiche, Università degli Studi di Trieste, via L. Giorgieri 1, 34127 Trieste, Italy

³ Institute für Physik, Humboldt-Universität zu Berlin, Newtonstraße 15, D-12489 Berlin, Germany

⁴ Department of Physics, Imperial College London, South Kensington Campus, SW72AZ London, UK

⁵ Technische Universität Berlin, Ernst-Ruska Gebäude, Hardenbergstraße 36A, 10623 Berlin, Germany

Corresponding author: david.ayuso@mbi-berlin.de

Abstract

High harmonic generation records the electronic response of matter to light with sub-femtosecond temporal resolution. Since the XIX-th century, chiral response has been thought to require the interplay of the electric and magnetic components of the light field. Here we show that chiral response in high harmonic generation from randomly oriented chiral molecules can be triggered exclusively by the electric field, with efficiency surpassing the accepted standards by orders of magnitude. The microscopic chiral response can be mapped into a giant background free macroscopic chiral signal, discriminating between left-handed and right-handed molecules at the level of 200% of chiral dichroism.

General Information

Chirality is an ubiquitous property of matter, from its elementary constituents to molecules, solids and biological species. Chiral molecules appear in pairs of enantiomers, two virtually identical versions in which their nuclei arrangements present non-superimposable mirror images of each other. Separated only by a mirror, left and right objects are readily distinguished in everyday life, but not in the micro-world. Standard chiroptical techniques [1] rely on the interplay of the electronic response to both the electric and magnetic components of the light field, i.e. on the chiral molecule “feeling” the helix of the light wave. However, the pitch of this light helix is usually too large, resulting in weak chiral response and a justified impression that chiral discrimination is hard, especially on ultrafast time scale. The electric-dipole “revolution” [2-6] is changing this perception. Photoelectron circular dichroism (PECD) was the first optical method to achieve chiral discrimination driven by purely electric dipole interactions [2, 3]. Chiral response in PECD can reach values of few tens of percent, numbers unheard of in chiral discrimination.

High harmonic generation (HHG) has been demonstrated to be a powerful technique for chiral recognition, chiral discrimination and for ultrafast imaging of molecular chirality [7-12]. However, chiral response in HHG still relies on weak magnetic interactions. Here I will show how to bring the dipole revolution to chiral HHG [13,14].

I will start presenting a quantitative model of high harmonic response in the chiral molecule propylene oxide, and the result of applying it to the experimental conditions of [7], with excellent agreement. Then, I will show that the use of a simple optical setup that involves two non-collinear laser

beams can drive a giant chiral macroscopic response in a medium of randomly oriented chiral molecules, in the dipole approximation. This chiral signal vanishes in achiral media, and it is completely separated from the non-chiral optical response in frequency, polarization and space. Furthermore, our work shows that one can achieve complete discrimination between left-handed and right-handed molecules, providing macroscopic background-free chiral signal present in one molecular enantiomer and absent in the other [14]. Which of the two enantiomers exhibits this signal remains under complete control.

The possibility of selectively suppressing the harmonic response in a selected enantiomer while enhancing emission from its mirror image using a simple non-collinear setup allows us to reach the ultimate goal in chiral discrimination: 200% of chiral dichroism. The mechanisms responsible for this giant chiral optical response are general to chiral media in the gas, liquid and condensed phases, thus bringing new opportunities to measure enantiosensitive intensity of optical signals in matter with the ultimate efficiency and with ultrafast time resolution.

References

- [1] N. Berova *et al.*, Wiley, ISBN: 978-0-470-64135-4 (2013)
- [2] B. Ritchie, *Phys. Rev. A* **13**, 1411–1415 (1976)
- [3] I. Powis, *J. Chem. Phys.* **112**, 301–310 (2000)
- [4] P. Fischer *et al.*, *Phys. Rev. Lett.* **85**, 4253–4256 (2000)
- [5] D. Patterson *et al.*, *Nature* **497**, 475–477 (2013)
- [6] S. Beaulieu *et al.*, *Nature Physics* **14**, 484–489 (2018)
- [7] R. Cireasa *et al.*, *Nature Physics* **11**, 654–658 (2015)
- [8] O. Smirnova *et al.*, *J. Phys. B* **48**, 234005 (2015)
- [9] D. Ayuso *et al.* *J. Phys. B* **51** 06LT01 (2018)
- [10] D. Ayuso *et al.*, *J. Phys. B* **51**, 124002 (2018)
- [11] Y. Harada *et al.*, *Phys. Rev. A* **98**, 021401(R)
- [12] D. Baykusheva *et al.*, *Phys. Rev. X* **8**, 031060 (2018)
- [13] O. Neufeld and O. Cohen, *ArXiv* 1807.02630 (2018)
- [14] D. Ayuso *et al.*, *ArXiv* 1809.01632 (2018)

Enhancing the Brilliance of Harmonic XUV Radiation with Tailored Driver Beams

Daniel Treacher¹, David T. Lloyd¹, Florian Wiegandt¹, Kevin O’Keeffe², and Simon M. Hooker¹

1. Department of Physics, University of Oxford, Clarendon Laboratory, Parks Road, Oxford, OX1 3PU, UK

2. College of Science, Department of Physics, Swansea University, Singleton Park, Swansea, SA2 8PP, UK

Corresponding author: daniel.treacher@physics.ox.ac.uk

Abstract

We report on a method that increases the brilliance of higher harmonic radiation by approximately an order of magnitude. A spatial light modulator is used to simultaneously manipulate the size and shape of the focal spot of the driver laser in an HHG setup for a fixed f-number and peak intensity. As the spot size increases the total harmonic flux increases and divergence decreases, thus improving the harmonic brilliance. These results offer an alternative approach for achieving high flux, low divergence, table-top sources of short wavelength radiation with applications in ultrafast imaging.

General Information

High harmonic generation (HHG) is an established method for producing highly coherent radiation in the vacuum ultraviolet and soft x-ray spectral regions with femtosecond and attosecond pulse durations [1]. HHG has applications ranging from seeding free electron lasers, to lensless imaging [2].

The extreme nonlinear interactions which occur during the HHG process mean that small variations in the parameters of the driving laser can have a dramatic influence on the spatial properties and conversion efficiency of the resulting harmonic beam.

Typically the size of the HHG interaction region is controlled by either adjusting the $f/\#$ of the focussing geometry or by altering the longitudinal location of the generating medium relative to the driver focus.

For applications such as lensless imaging with harmonics, loose focussing arrangements have been used to satisfy the demand for high flux and low divergence [3]. However, in many situations, the route toward brighter sources is hindered by the spatial limitations in laboratories for long focal length lenses. Typical focal lengths may exceed 1 m, limited by the maximum experimental footprint.

By introducing a liquid-crystal-on-silicon phase-only spatial light modulator (SLM), the spatial profile of the driver beam at focus can be manipulated [4]. Here we use a binary phase mask to transform the focal spot from Gaussian into a supergaussian profile whilst preserving a flat phase front at focus.

This method preserves the $f/\#$ and hence footprint of the set-up while increasing the radius of the focal spot, w_0 . If the peak intensity is held constant, this enlarges the harmonic source size and hence increases the harmonic flux.

We define the supergaussian intensity distribution as $I(r) = I_0 e^{-\left(\frac{r}{w_0}\right)^p}$, where I_0 , r , and p are the peak intensity, radial coordinate and supergaussian power, or ‘ p value’, respectively. In this study we consider $2 \lesssim p \lesssim 3.5$, above which the shaping achieved in our driver focus degrades due to the operation of the

binary phase mask and size of the SLM chip.

We quantify the average brilliance as $B = \frac{N}{\Delta t \cdot d\Omega \cdot w_0 \cdot \left(\frac{\Delta\nu}{\nu}\right)}$, where for small divergence angles, $d\Omega \approx \frac{\pi w(z)^2}{z^2}$ [5]. Here, N , Δt , $d\Omega$, $\Delta\nu/\nu$, $w(z)$ and z represent the number of photons, time interval, solid angle, fraction of bandwidth, beam radius and source to detector distance respectively.

For increasing p , it was observed that N and $d\Omega$ increase and decrease respectively. We record a 5-fold increase in the photon flux for the optimal value of p . This increase is commensurate with an approximately 5-fold increase in the source size.

With further refinement of the shaping, we anticipate even larger improvements in the harmonic brilliance. Such scaling has only previously been achieved at the expense of a far larger experimental footprint. Thus our work opens a new route for producing bright table-top sources of soft x-rays.

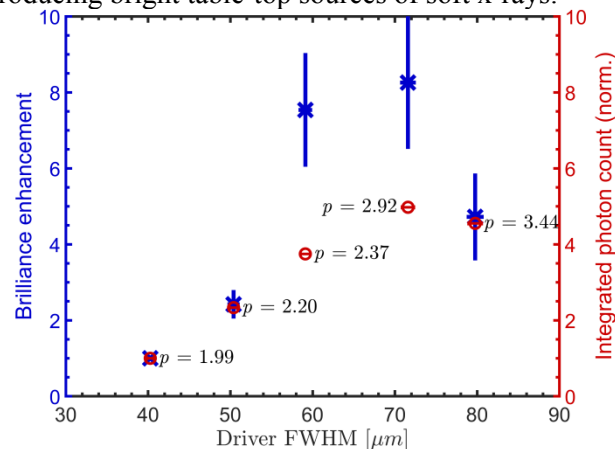


Fig.1. Measured brilliance enhancement (blue asterisks) and integrated photon flux (red circles) for the 25th harmonic as a function of the 800 nm driver beam size. A fixed focal length of 0.5m was used.

References

- [1] M.Gaarde *et al.*, **41**, 13, *J Phys B-At Mol Opt* (2008).
- [2] B. Abbey *et al.*, **5**, 7, *Nat Photon* (2011).
- [3] E. Takahashi *et al.*, **4**, 2691, *Nature Comms* (2013).
- [4] L. Romero *et al.*, **13**, 4, *JOSA-AI* (1996).
- [5] R. Spitzenteufel *et al.*, **96**, 1, *Appl Phys A-Mater* (2009).

Time-resolving electron dynamics in molecules using strong laser fields: coherent probes of charge migration

F. Mauger¹, P.M. Abanador¹, A.S. Bruner², M. Gordon³, T.T. Gorman⁴, S. Khatri³, A. Sissay², S. Hernandez², P. Sándor³, T.D. Scarborough⁴, P. Agostini⁴, L.F. DiMauro⁴, M.B. Gaarde¹, R.R. Jones³, K. Lopata², K.J. Schafer¹

¹ Department of Physics and Astronomy, Louisiana State University, Baton Rouge, Louisiana 70803, USA

² Department of Chemistry, Louisiana State University, Baton Rouge, Louisiana 70803, USA

³ Department of Physics, University of Virginia, Charlottesville, Virginia 22904, USA

⁴ Department of Physics, The Ohio State University, Columbus, Ohio 43210, USA

Corresponding author: fmauger@phys.lus.edu

Abstract

Probing the electronic structure and dynamics of molecules on the attosecond time scale is a formidable challenge that requires state-of-the-art experimental setups and new theoretical tools and models. In this presentation, I will discuss results of a collaborative effort between Louisiana State University, the Ohio State University, and University of Virginia to build such experimental and theoretical probes to observe the earliest stages of electron-mediated structural rearrangement – charge migration, which typically takes place on a sub-femtosecond time scale.

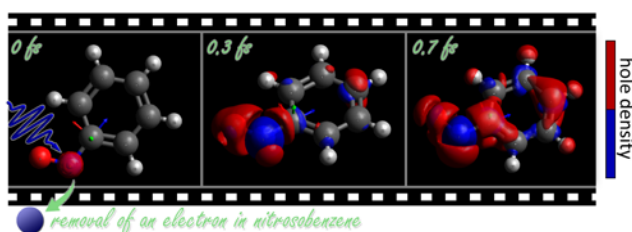


Fig. 1. Snapshots of the electron-hole density in nitrosobenzene following the sudden removal of a core electron on the nitrogen site, computed with TDDFT [1].

When forced out of equilibrium, electrons in matter can respond exceedingly fast, on time-scales approaching the attosecond (see Fig. 1). At this time scale, the dynamics are inherently quantum, and they are not yet impacted by the weaker coupling to a system “bath” that involves large numbers of additional degrees of freedom. This potentially complex quantum evolution can expose correlations between electrons and holes that are otherwise hidden in the static properties of the system.

Probing the electronic structure and dynamics of molecules on the attosecond time scale is a formidable challenge that requires state-of-the-art experimental setups and new theoretical tools and models. In this contribution, we discuss time-resolving electron molecular structure using strong laser fields. We present a picture of charge migration that combines strong-field dynamics [2, 3] with the quantum-chemistry-derived electronic structure of complex molecules [4], backed up by direct numerical simulations [5, 6]. Using a related set of molecules as examples, we compare experimental measurements with the results of our theoretical models and associated numerical simulations to unveil the time-dependent electronic structure [7-10].

More generally, we report results of a collaborative effort between Louisiana State University (LSU), the Ohio State University (OSU),

and University of Virginia (UVA) to build experimental and theoretical approaches [1-10] to observe the earliest stages of electron-mediated structural rearrangement – charge migration, which typically takes place on a sub-femtosecond time scale (see Fig. 2).

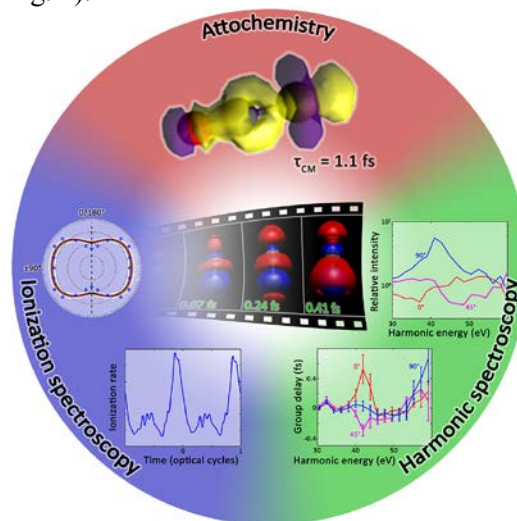


Fig. 2. Illustration of the integrated theory-experiments collaborative effort between LSU, OSU and UVA, with recent results on OCS molecules: (top) Calculations of charge migration modes [5], (right) measurements of the amplitude and phase of harmonics from aligned OCS [9], and (left) measurements and calculations of ionization from aligned OCS. [7].

Our references

- [1] A. Bruner *et al.*, *J. Phys. Chem. Lett.* **8**, 3991 (2017).
- [2] F. Mauger *et al.*, *Phys. Rev. A* **93**, 043815 (2016).
- [3] F. Mauger *et al.*, *Phys. Rev. A* **97**, 043407 (2018).
- [4] A. Sissay *et al.*, *J. Chem. Phys.* **145**, 094105 (2016).
- [5] A. Bruner *et al.*, *in preparation* (2017).
- [6] P.M. Abanador *et al.*, *in preparation* (2018).
- [7] P. Sándor *et al.*, *Phys. Rev. A* **98**, 043425 (2018).
- [8] T.D. Scarborough *et al.*, *Appl. Sci.* **8**, 1129 (2018).
- [9] T.T. Gorman *et al.*, *in preparation* (2018).
- [10] P. Sándor *et al.*, *in preparation* (2018).

Longitudinal momentum of the electron at the tunnelling exit

Ruihua Xu¹, Tao Li², and Xu Wang¹

¹ Graduate School of China Academy of Engineering Physics, Beijing 100193, China

² Beijing Computational Science Research Center, Beijing 100193, China

Corresponding author: xwang@gscaep.ac.cn

Abstract

The longitudinal tunnelling-exit momentum of the electron in strong-field tunnelling ionization is shown to be nonzero even in the static or the adiabatic limit. This nonzero momentum is a purely quantum mechanical effect determined by the shape of the wave function in the vicinity of the tunnelling-exit point. Nonadiabaticity or finite wavelength may increase this momentum substantially, and the detailed value depends on both the atomic and the laser parameters.

Introduction

The longitudinal momentum of the electron at the tunnelling exit is a useful quantity to make sense of the tunnelling ionization process. It was usually assumed to be zero from a classical argument, but recent experiments show that it must be nonzero in order to explain the measured electron momentum distributions [1-3].

The following questions arise from the theoretical point of view: In quantum mechanics what is the definition of electron momentum at specified positions (e.g., the tunnelling exit)? That is, what momentum are we exactly talking about quantum mechanically? How can the electron momentum be nonzero at a point with zero kinetic energy (by definition)? What determines the value of the longitudinal momentum at the tunnelling exit?

The flow momentum of the probability fluid

The flow momentum of the probability fluid [4] is a sensible quantum mechanical definition for tunnelling-exit momentum. The time evolution of a wave function can be viewed as a dynamic flow of the probability fluid in real space. A wave function can be written as

$$\Psi(x, t) = A(x, t)e^{i\phi(x, t)}$$

with $A(x, t) \geq 0$ the amplitude and $\phi(x, t)$ the phase function, both of which are real.

The probability current can be obtained (in a.u.)

$$j(x, t) = \frac{i}{2} \left[\Psi(x, t) \frac{\partial}{\partial x} \Psi^*(x, t) - c. c. \right] = \rho(x, t) \frac{\partial \phi(x, t)}{\partial x}$$

where $\rho(x, t)$ is the probability density. In analogy to the classical fluid equation $j(x, t) = \rho(x, t)v(x, t)$, one sees that the flow velocity or momentum is the spatial derivative of the phase function

$$p(x, t) = \frac{\partial \phi(x, t)}{\partial x}$$

We emphasize that the flow momentum is legally defined at each position.

We numerically solve the time-dependent Schrödinger equation to get the 3D wave function

$$i \frac{\partial}{\partial t} \Psi(\vec{r}, t) = [\hat{H}_0 + \hat{H}_I] \Psi(\vec{r}, t)$$

with $\hat{H}_0 = -\frac{1}{2} \frac{d^2}{dr^2} + \frac{\hat{L}^2}{2r^2} + V(r)$ the field-free atomic Hamiltonian and $\hat{H}_I = F(t)r \cos\theta$ the laser-atom interaction. $V(r)$ is the Green-Sellin-Zachor (GSZ) model potential [5] based on a single-active-electron approximation.

Numerical results

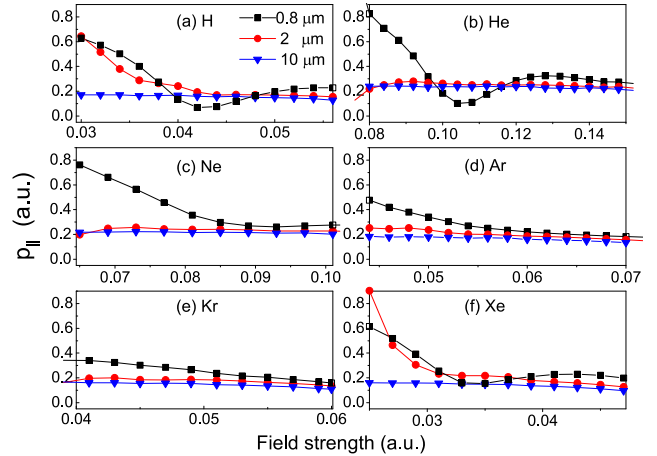


Fig. 1. Tunneling-exit longitudinal momentum for six model atoms, each with three wavelengths. Even with $\lambda = 10 \mu\text{m}$ where the static/adiabatic limit is expected to hold, p_{\parallel} is not zero, but has values around 0.2 a.u. for all the six model atoms. Shorter wavelengths introduce nonadiabatic effects, and in general lead to larger p_{\parallel} values [6].

References

- [1] D. Comtois *et al.*, J. Phys. B 38, 1923 (2005).
- [2] A. N. Pfeiffer *et al.*, Phys. Rev. Lett. 109, 083002 (2012).
- [3] L. Fechner *et al.*, Phys. Rev. Lett. 112, 213001 (2014).
- [4] X. Wang *et al.*, J. Phys. B 51, 084002 (2018).
- [5] A. E. S. Green *et al.*, Phys. Rev. 184,1 (1969).
- [6] R. Xu *et al.*, Phys. Rev. A *in press* (2018)

Characterization of electron wavepackets from strong-field ionization

Yunquan Liu

1. School of Physics and State Key Laboratory for Mesoscopic Physics, Peking University, Beijing 100871, China

2. Collaborative Innovation Center of Quantum Matter, Beijing 100871, China

Author e-mail address: yunquan.liu@pku.edu.cn

We will present the study on the nonadiabatic effect of strong-field ionization and the experimental characterization of electron wavepackets from strong-field ionization.

In the presentation, I will talk about our recent works on the characterization of electron wavepackets from strong-field ionization of atoms. In theory, we have developed a subcycle nonadiabatic strong-field tunneling theory and have derived the position of tunnel exit, the transverse and longitudinal momentum distributions at the tunnel exit, and the ionization rate in an instantaneous laser field. These tunneling coordinates are shown to nonadiabatically couple with each other in an instantaneous laser field when the electron tunnels through the Coulomb barrier. We have further incorporated the nonadiabatic tunneling theory with the quantum-trajectory Monte Carlo approach to investigate the nonadiabatic effect on the photoelectron angular distributions. The simulated photoelectron angular distributions with the nonadiabatic corrections have been validated by comparison with the *ab initio* results through numerically solving the time-dependent Schrödinger equation [1,2]. Experimentally, we have performed the ellipticity-dependent measurement on electron momentum distributions and have verified the nonadiabatic effect [3].

intensity is 1.2×10^{14} W/cm² and the ellipticity is $\varepsilon = 0.6$.

Beside characterization of momentum distributions of electron wavepackets, we have also tried to understand the sub-barrier phase of electron wavepackets by strong-field ionization using the orthogonal polarized fields [4]. In order to measure the phase structure, we recently used the two-color co-rotating circularly polarized fields to probe the phase and amplitude of electron wavepackets [5]. Along the line, the position of tunneling exit, momentum distributions and the initial phase structure of electron wavepackets have been studied.

References:

- [1] M. Li et al., Phys. Rev. A 93, 013402(2016).
- [2] M. Han et al., Phys. Rev. A 95, 023406(2017)
- [2] M. Li et al. Phys. Rev. A 95, 053425(2017).
- [4] M. Han et al., Phys. Rev. Lett. 120, 073202 (2018).
- [5] M. Han et al., Phys. Rev. Lett. 120, 073202 (2018).

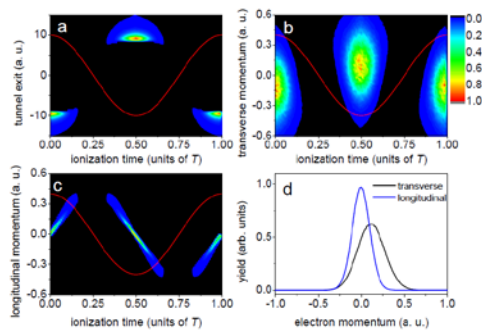


Fig. 1 Non-adiabatic tunneling coordinates of Ar atoms in elliptically polarized laser fields. (a), The distribution of the tunnel exit with respect to the ionization time. (b) and (c) show the initial transverse momentum and the initial longitudinal momentum distribution at the tunnel exit with respect to the ionization time, respectively. The red curves show the laser field along the major axis (z direction) in arbitrary units. The ionization probability is color-coded from red (high) to blue (low). (d), the half-cycle-averaged transverse momentum distribution and initial longitudinal momentum distribution at the tunnel exit. The

Nondipole effects in atomic dynamic interference

Mu-Xue Wang¹, Hao Liang¹, Xiang-Ru Xiao¹, Si-Ge Chen¹, Wei-Chao Jiang² and Liang-You Peng^{1,3}

¹ State Key Laboratory for Mesoscopic Physics and Collaborative Innovation Center of Quantum Matter, School of Physics, Peking University, Beijing 100871, China

² College of Physics and Energy, Shenzhen University, Shenzhen 518060, China

³ Collaborative Innovation Center of Extreme Optics, Shanxi University, Taiyuan, Shanxi 030006, China

Corresponding author: jiang.wei.chao@szu.edu.cn and liangyou.peng@pku.edu.cn

Abstract

Nondipole effects in the atomic dynamic interference are investigated by numerically solving the time-dependent Schrödinger equation of hydrogen. Momentum shifts of photoelectrons in the opposite direction of the laser propagation are founded. The origin of such momentum shifts is attributed to the nondipole phase difference between the two electron wave packets ejected in the rising and falling edge of the laser pulse, which will interfere with each other and result in the final fringe pattern. One consequence of such momentum shifts is that they can smooth out the peak splitting induced by the dynamic interference in the photoelectron energy spectrum.

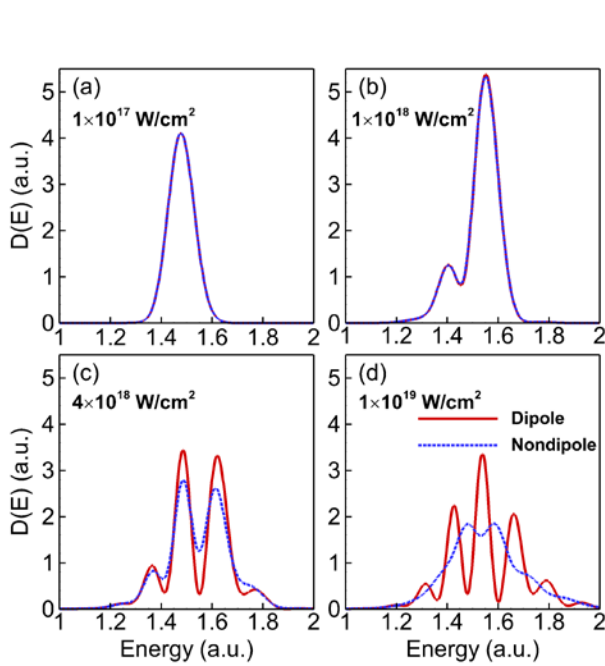


Fig. 1. The photoelectron energy distribution for the 1s state of hydrogen exposed to linearly polarized Gaussian-shaped pulses with a carrier frequency of $\omega = 53.6$ eV and FWHM of 7 cycles at four different laser intensities.

Nondipole effects in dynamic interference become obvious as the pulse intensity increases in results of photoelectron energy spectra in Fig. 1. The peak splitting's being smoothed out in Fig. 1(d) is related to the nondipole momentum shifts in Fig. 2. Through an analytic expression, the origin of such momentum shifts is attributed to the nondipole phase difference between the two electron wave packets ejected in the rising edge and the falling edge of the laser pulse, which will interfere with each other and result in the final fringe pattern.

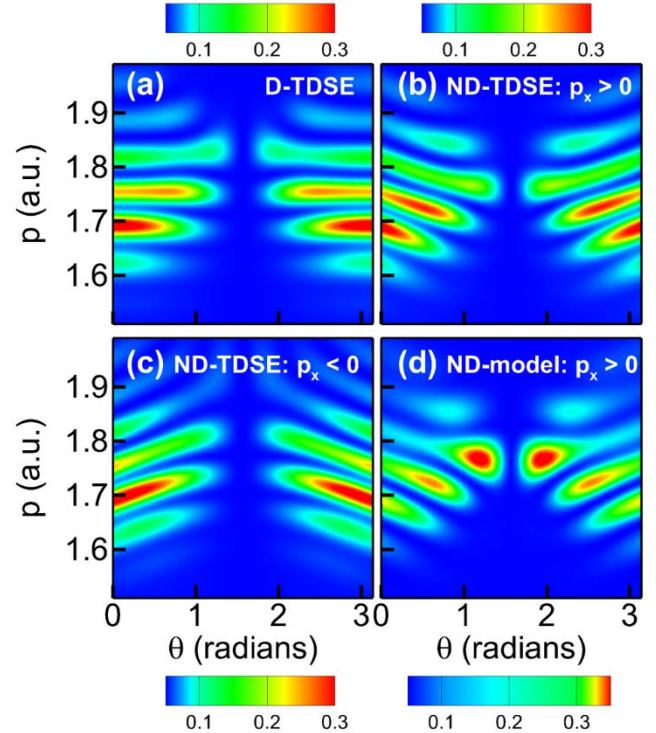


Fig. 2. The 2D photoelectron momentum distributions in the laser-polarization-propagation plane at the same laser intensity in Fig. 1(d) for: (a) the dipole TDSE calculation, (b)-(c) the nondipole TDSE calculation, and (d) the semi-analytical model results.

References

- [1] P. V. Demekhin and L. S. Cederbaum, *Phys. Rev. Lett.* **108**, 253001 (2012).
- [2] M. Bagheri, U. Saalman, and J. M. Rost, *Phys. Rev. Lett.* **118**, 143202 (2017).
- [3] W.-C. Jiang and J. Burgdörfer, *Opt. Express* **26**, 19921 (2018).
- [4] M.-X. Wang *et al.*, *Phys. Rev. A* **96**, 043414 (2017).

Polarization-Resolved Nonlinear Thomson Scattering from Laser-Driven Electrons

J. Peatross, B. Pratt, C. Schulzke, and M. Ware

Department of Physics and Astronomy, Brigham Young University, Provo, UT 84602, USA

Corresponding author: peat@byu.edu

Abstract

We outline an experiment for measuring polarization-resolved fundamental, second, and third harmonic photons scattered from low-density electrons in a Ti:sapphire laser focus, at intensities above 10^{18} W/cm². Different components of the well-known figure-8 electron motion may be associated with orthogonal polarization components of the scattered light.

Introduction

In their landmark analysis nearly a half-century ago, Sarachick and Schappert described trajectories of and radiation from classical electrons in an intense laser field.[1] In the average rest frame, an electron oscillates along a well-known figure-8 path, owing to both the electric and magnetic forces of the laser field. At relativistic intensities, electrons scatter both odd and even harmonics into the far field. This relativistic nonlinear Thomson scattering was first observed by the Umstadter group in a 1-atm plasma in the 1990's.[2] They measured second and third harmonics scattering in directions perpendicular to the focus. To our knowledge, the polarization of this scattered light has not previously been analyzed, either experimentally or theoretically.

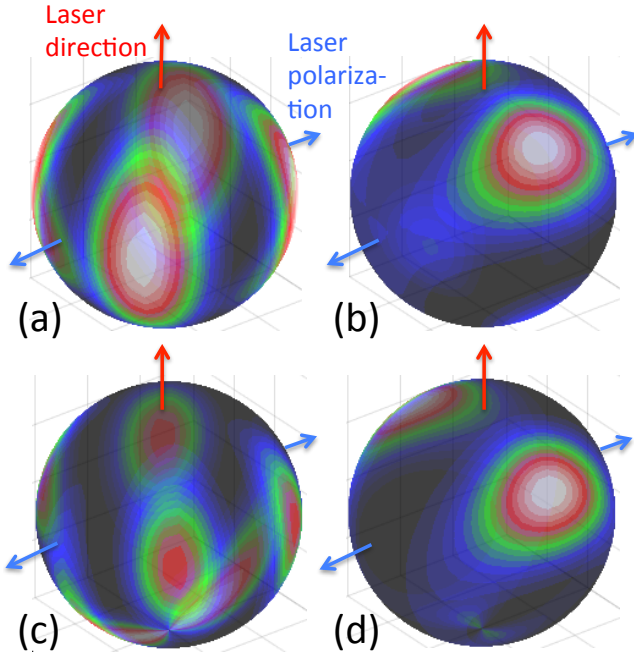


Fig. 1. (a) Azimuthal and (b) longitudinal polarization components of second-harmonic Thomson scattering emitted in all directions. Repeated in (c) and (d) for the third harmonic.

Figure 1 shows polarization components of the emission patterns for second and third harmonic light, resolved along ‘latitude’ and ‘longitude’ lines. The free electrons are stimulated by linearly polarized 800 nm laser light at 1.5×10^{18} W/cm². The added

dimension of polarization gives insight into different aspects of the figure-8 electron motion.

Experiment

We describe ongoing experiments on low-density targets (i.e. $<10^{-4}$ Torr), where we count fundamental, second, and third-harmonic photons scattered by free electrons in an intense laser focus. Figure 2 shows the expected polarization-resolved angular distribution of the emission in a plane perpendicular to the laser beam (same parameters as Fig. 1). Plot 2(b) shows the spatial distribution of total emission (previously measured), and plots (c) and (d) show the resolved polarization components that we are attempting to measure. Acknowledgement: NSF 1708185.

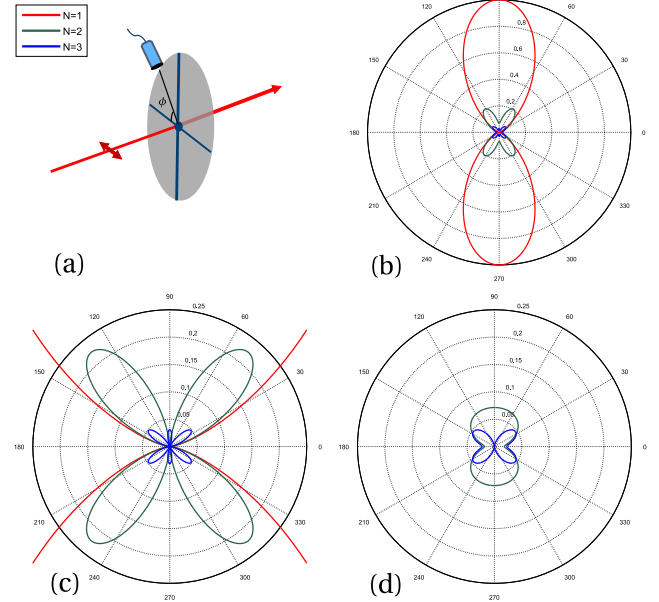


Fig. 2. (a) Schematic of nonlinear Thomson-scattering measurements. (b) Total light emission as a function of detector angle for N=1,2,3 harmonics. Zoomed in (c) azimuthal and (d) longitudinal polarization-resolved emission.

References

- [1] E. S. Sarachik and G. T. Schappert, “Classical Theory of the Scattering of Intense Laser Radiation by Free Electrons,” *Phys. Rev. D* **1**, 2738-2753 (1970).
- [2] Chen, S. Y., Maksimchuk, A., and Umstadter, D. “Experimental observation of relativistic nonlinear Thomson scattering,” *Nature* **396**, 653-655 (1998).

Magnetic field generation, dynamics and reconnection driven by relativistic intensity laser pulses

P. T. Campbell¹, A. Raymond¹, C. A. J. Palmer², N. Alexander³, L. Antonelli⁴, A. Bhattacharjee⁵, A. F. A. Bott², H. Chen⁶, V. Chvykov¹, E. Del Rio³, C. Dong⁵, G. Fiksel¹, P. Fitzsimmonds³, W. Fox⁵, G. Gregori², J. Halliday⁷, B. Hou¹, P. Kordell¹, K. Krushelnick¹, Y. Ma¹, A. Maksimchuk¹, A. McKelvey¹, C. Mileham⁹, E. Montgomery⁸, J. Nees¹, P. M. Nilson⁹, M. Notley⁸, C.P. Ridgers⁴, A. A. Schekochihin², C. Stoeckl⁹, A. G. R. Thomas¹, E. Tubman⁷, M. S. Wei^{3,9}, G. J. Williams⁶, N. Woolsey⁴, V. Yanovsky¹, C. Zulick¹, L. Willingale¹

¹ Center for Ultrafast Optical Science, University of Michigan, Ann Arbor, MI, USA

² Clarendon Laboratory, University of Oxford, Parks Road, Oxford, OX1 3PU, UK

³ General Atomics, San Diego, CA, USA

⁴ Department of Physics, York Plasma Institute, University of York, York YO10 5DD, UK

⁵ Princeton Plasma Physics Laboratory, Princeton, NJ, USA

⁶ Lawrence Livermore National Laboratory, Livermore, CA, USA

⁷ Blackett Laboratory, Imperial College London, SW7 2BZ, UK

⁸ Central Laser Facility, STFC Rutherford-Appleton Laboratory, Chilton, Didcot, Oxfordshire, OX11 0QX, UK

⁹ Laboratory for Laser Energetics, Rochester, NY, USA

Corresponding author: wlouise@umich.edu

Abstract

Relativistic intensity laser pulses are used to heat a relativistic electron population that can drive a magnetic reconnection geometry under unique conditions. The dynamics of these fields is observed experimentally using proton radiography. Measurements of the emitted x-rays (spatial, spectral and temporal), as well as non-thermal electron spectra, provide evidence for magnetic reconnection. Three-dimensional particle-in-cell modelling shows good agreement with the observations and shows the magnetic energy density within the surface plasma can exceed the rest mass energy density.

The chirped pulse amplification (CPA) technique can produce light pulses focused to intensities where the electric field oscillates electrons at relativistic velocities. The currents due to the relativistic electrons can generate huge, dynamic fields within a laboratory plasma. Plasma dynamics in astrophysical plasmas are strongly impacted by magnetic field topology. However, direct measurements of the outer space plasma and field conditions are challenging, so laboratory studies of magnetic dynamics and reconnection provide an important platform for testing theories and characterizing different regimes. The extremely energetic class of astrophysical phenomena – including high-energy pulsar winds, gamma ray bursts, and jets from galactic nuclei – have plasma conditions where the energy density of the magnetic fields exceeds the rest mass energy density. This defines the cold magnetization parameter, $\sigma_{\text{cold}} = B^2/(\mu_0 n_e m_e c^2) > 1$.

Experimental measurements, along with numerical modelling, of short-pulse, high-intensity laser-plasma interactions that produce extremely strong magnetic fields (>100 T) in a plasma such that $\sigma_{\text{cold}} > 1$. The generation and dynamics of these magnetic fields under different target conditions is studied using proton radiography and relativistic-intensity laser-driven magnetic reconnection experiments are performed. X-ray imaging allows the observation of the fast electron dynamics. Evidence of magnetic

reconnection was identified by the plasma's X-ray emission patterns, changes to the electron spectrum, and by measuring the reconnection timescales.

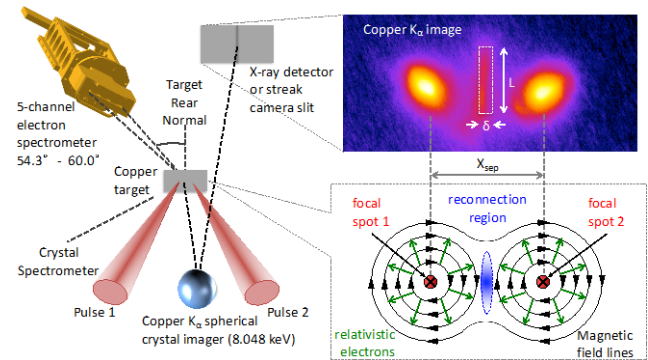


Fig. 1. A schematic of the experimental geometry. A typical K_{α} image is shown with the reconnection layer highlighted in the dashed box. A physical picture of the interaction illustrates the two azimuthal magnetic fields expanding into the reconnection region. Taken from [1].

References

- [1] A. Raymond, C. F. Dong, A. McKelvey, C. Zulick, N. Alexander, A. Bhattacharjee, P. T. Campbell, H. Chen, V. Chvykov, E. Del Rio, P. Fitzsimmonds, W. Fox, B. Hou, A. Maksimchuk, C. Mileham, J. Nees, P. M. Nilson, C. Stoeckl, A. G. R. Thomas, M. S. Wei, V. Yanovsky, K. Krushelnick, and L. Willingale, *Physical Review E*, **98**, 043207 (2018).

Relativistic electron dynamics in laser-driven nanowire targets

Robin Marjoribanks¹, Ludovic Lecherbourg¹, J. E. Sipe¹, Gábor Kulcsár¹, Jeremy Li¹, Andrew Tan¹, Sam Vinko², Alan Miscampbell², Oliver Humphries², Justin Wark², Anne Héron³, Frédéric Pérez⁴

¹Department of Physics, University of Toronto, 60 Saint George St., Toronto, ON M5S-1A7, Canada

²Department of Physics, Clarendon Laboratories, University of Oxford, UK

³CPhT – CNRS, Ecole Polytechnique

⁴LULI – CNRS, Ecole Polytechnique

Corresponding author: marj@physics.utoronto.ca

Abstract

Nickel nanowires present >95% optical absorption in a long $\sim 1 \mu\text{m}$ effective skin-depth. Partly this is due to the strong optical anisotropy of these oriented nanostructures: dielectric in the transverse direction and conductor along the optical axis. Under intense irradiation, and especially at relativistic optical intensities, nanowires can be stripped of electrons and Colomb-explode as if they were 70nm macromolecules. Optical absorption and free-electron dynamics are analysed in an effective-dielectric model and by particle-in-cell simulation, with an aim to blend descriptions.

Introduction

Since our introduction of end-standing nanowires as laser-plasma targets in 2000 [1], and subsequent description of the dynamics of their interaction of ultra-intense laser pulses [2], several groups have shown their great relevance in high energy-density physics [3,4,5] even the production of thermonuclear neutrons [6]. Our recent experiments on the LCLS x-ray free-electron laser have used Ni nanowires in order to produce volumetric heating of homogeneous laser-produced plasmas of controllable density and temperature, for precise measurements of ionization potential depression (IPD) in near solid-density [5].

Much understanding of has come from 2D and 3D particle-in-cell (PIC) simulations. We have also used

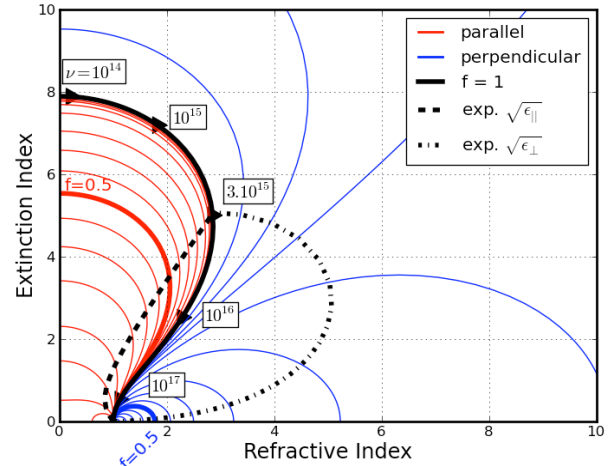


Fig. 2. The refractive index and the extinction index as functions of the electron-ion collision rate, for different fill-factors in the parallel (red curves) and perpendicular (blue curves) cases, for $\lambda = 1.0 \mu\text{m}$ ($\omega_p > \omega$). Along the solid black curve, which represents bulk metal ($f = 1$), we indicate different values of the electron-ion collision rate.

effective-dielectric methods to model small-signal absorption, and extended that with a plasma-model dielectric function. Our aim is to include the relativistic index of refraction due to strong oscillating electron currents, as the laser penetrates deep into an average density far above critical.

References

- [1] G. Kulcsár, D. AlMawlawi, F. W. Budnik, P. R. Herman, M. Moskovits, L. Zhao, and R. S. Marjoribanks, *Phys. Rev. Lett.* **84**:5149, (2000).
- [2] R.S. Marjoribanks, *LPHYS'12 Workshop*, Calgary, AB, Canada, 23-27 July (2012).
- [3] T. Nishikawa et al. *Appl. Phys. B* **78**, 885–890 (2004)21. S. Mondal et al. *Phys. Rev. B* **83**,035408 (2011)
- [4] A.V. Ovchinnikov et al. *Laser Particle Beams* **29**,249–254 (2011)
- [5] M.A. Purvis *et al.*, *Nature Photonics*, v. 7, DOI: 10.1038/NPHOTON.2013.217 (2013)
- [6] A. Curtis *et al.*, *Nature Communications* **9**, 1077 (2018)

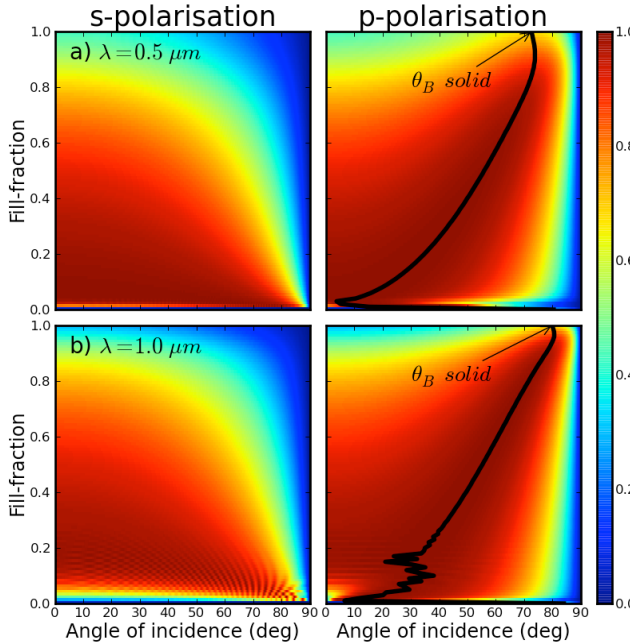


Fig. 1. Modelled absorption of very large ($\sim 20\mu\text{m}$) thickness layers s - and p -polarization, as a function of fill-fraction and angle of incidence, and for two different wavelengths: a) $\lambda = 0.5 \mu\text{m}$, b) $1 \mu\text{m}$.

Topological strong field physics on sub-laser cycle timescale

R.E.F. Silva^{1,2}, A. Jiménez-Galán¹, B. Amorim³, O. Smirnova^{1,4}, M. Ivanov^{1,5,6}

¹ Max Born Institut, Max Born Strasse 2A, D-12489 Berlin, Germany

² Department of Theoretical Condensed Matter Physics, Universidad Autónoma de Madrid, E-28048, Madrid, Spain

³ CeFEMA, Instituto Superior Técnico, Universidade de Lisboa, Av. Rovisco Pais, 1049-001 Lisboa, Portugal

⁴ Technische Universität Berlin, Ernst Ruska Gebäude, Hardenbergstraße 36A, 10623 Berlin, Germany

⁵ Department of Physics, Humboldt University, Newtonstraße 15, D-12489 Berlin, Germany

⁶ Blackett Laboratory, Imperial College London, South Kensington Campus, SW7 2AZ London, United Kingdom

Corresponding author: jimenez@mbi-berlin.de

Abstract

The topological state of matter is intimately linked with dynamics, as manifested via the chiral edge currents in topological insulators. But is there an inherent time scale, associated with topology? We use unique properties of primary electronic response to strong non-resonant optical fields to address this question.

Quantum materials encompass a rich variety of systems with fascinating features. One of them is the topological phase transition, upon which an insulator becomes conducting, supporting robust currents around the insulator's edges [1,2]. “Protected” by the topological invariants of the bulk, the chiral edge states are robust to perturbations, making them appealing for applications, for example in dissipationless devices or topologically robust semiconductors. However, and surprisingly, the ultrafast dynamics of non-equilibrium electronic response to intense optical fields in these materials has remained virtually unexplored. Yet, understanding these dynamics is not only fundamentally interesting. It is also crucial for light-wave electronics in topological materials.

Attosecond science has made major progress in understanding ultrafast electron dynamics in solids [3,4]. Yet, so far it has mostly focused on the role of the band structure. The role of the topological properties, such as the Berry curvature and the topological invariants of condensed matter systems, on the attosecond dynamics of electronic response has been hardly explored. Does the highly non-equilibrium electron dynamics in the bulk, driven by a strong laser field, encode the topological properties on the sub-laser cycle time-scale? How do the Berry curvature and the Chern number affect the first step in the nonlinear response – the field-driven injection of electrons across the bandgap?

In this talk, I will answer these questions using the paradigmatic example of the topological insulator, the Haldane system [5]. I will show how the topological state of the system controls its attosecond, highly non-equilibrium electronic response to strong low-frequency laser fields, in bulk. Topological effects can be identified on the directionality and the attosecond

timing of an electron current injected into the conduction band by the oscillating electric field of an intense light pulse.

I will further show that the highly nonlinear optical response to strong fields, the high harmonic emission, displays topologically-dependent attosecond delays, and that the helicities of the emitted harmonics can record the phase diagram of the system and its topological invariants.

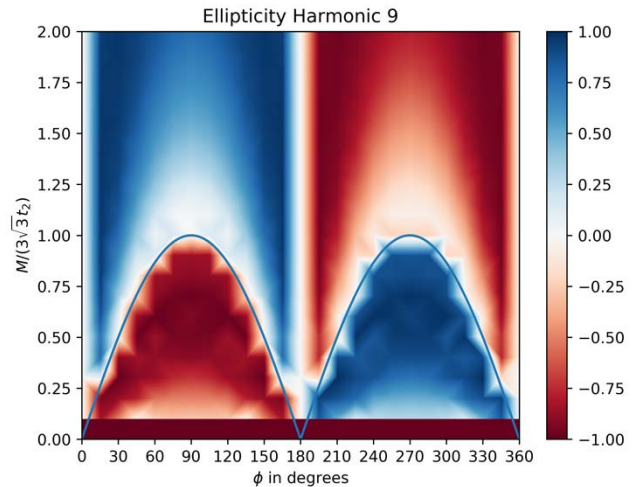


Fig. 1. Helicity of harmonics in topological insulators. The helicity of the high harmonics maps the phase diagram of the Haldane system. The blue solid line marks the topological phase transition, separating the trivial phase (above) from the topological phase (below).

References

- [1] M.Z. Hasan & C.L. Kane, *Rev. Mod. Phys.* **82** 3045 (2010).
- [2] X.L. Qi & S.C. Zhang, *Rev. Mod. Phys.* **83** 1057 (2011).
- [3] G. Vampa *et al.*, *Nature* **522** 462 (2015).
- [4] S.Y. Kruchinin *et al.*, *Rev. Mod. Phys.* **90** 021002 (2018).
- [5] F.D.M. Haldane, *Phys. Rev. Lett.* **61** 2015 (1988).

Spatio-temporal optical vortices (STOVs): experiments and simulations

R S. Zahedpour, S. Hancock, N. Jhajj, J. K. Wahlstrand, and H.M. Milchberg

Institute for Research in Electronics and Applied Physics, University of Maryland, College Park, MD 20742, USA

Corresponding author: milch@umd.edu

Abstract

We have recently introduced the concept of spatio-temporal optical vortices (STOVs), simulating and measuring these structures [1]. STOVs are fundamental to electromagnetic power flow in all self-focusing collapse and self-guiding scenarios, and conserve topological charge, making them robust. More recently, we have generated STOVs in nonlinear propagation in glass, measuring them in 2D (space) +1 (time) and, separately, we have generated them linearly.

We have recently shown experimentally and theoretically that spatio-temporal optical vortices (STOVs) are fundamental to the electromagnetic energy flow in the nonlinear propagation of femtosecond filaments [1]. STOVs arise naturally and necessarily from self-focusing collapse arrest, which occurs both in air filaments, when collapse arrest is due to ionization [2], and in relativistic filaments in plasmas, where collapse arrest is due to ponderomotive force-driven evacuation of electron density from the filament core [3].

behind the object plane. The filament ‘core’ lies inside the dark intensity ring – the intensity null of the STOV – and the ‘reservoir’ lies outside. Note the vortex-like 2π phase shift of the core between panels (ii) and (iii).

More recently, we have developed a method for controlled embedding of STOVs in ultrashort laser pulses without having to engineer and control the complex process of self-focusing collapse arrest. We present our recent experiments probing the nonlinear propagation of these unusual and unique optical structures – now prepared in advance – in gas and transparent solid samples, along with 3D simulations using a version of the unidirectional pulse propagation algorithm [4]. Figure 2 shows generation and measurement of a ‘line-STOV’, where the vortex axis is perpendicular to the propagation direction.

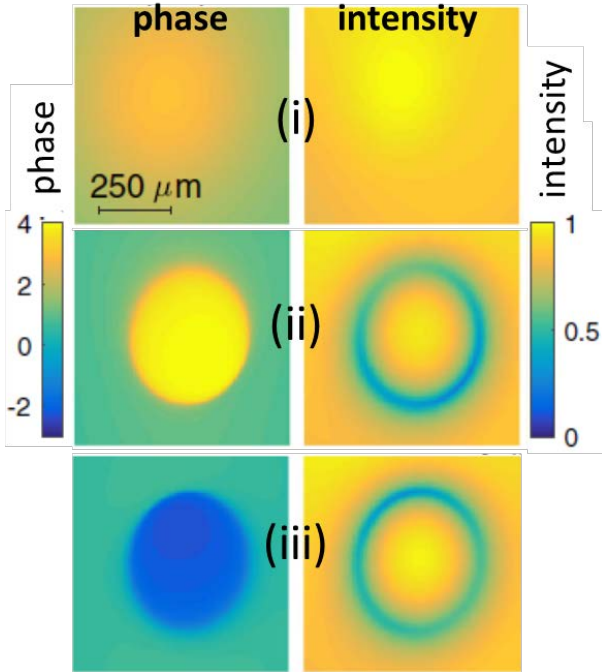


Figure 1. Retrieved spatial phase (radians) and intensity (arbitrary units) images at the collapse location $z = 165$ cm, $P/P_{cr} = 4.4$ for (i) a pre-collapse beam and (ii) and (iii) beams where a vortex ring is on either side of the reference central wavelength of $\lambda=800$ nm (from ref. [1]).

Figure 1 shows the transverse intensity and phase profiles of a femtosecond air filament measured mid-flight at the collapse location ($z=165$ cm) for $P/P_{cr} = 4.4$. The shot-to-shot fluctuations at this z -location show (i) no collapse, (ii) collapse and STOV slightly ahead of the object plane and (iii) collapse and STOV slightly

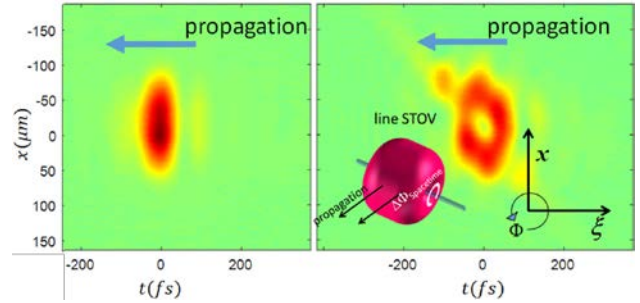


Figure 2. Generation of a 1D STOV. Left panel: input pulse. Right panel: output pulse, showing field null and vortex axis perpendicular to the pulse propagation direction.

Acknowledgements: This work is funded by the AFOSR and NSF.

References

- [1] N.Jhajj, I. Larkin, E.W. Rosenthal, S. Zahedpour, J.K. Wahlstrand, and H.M. Milchberg, *Phys. Rev. X* **6**, 031037 (2016).
- [2] A. Couairon and A. Mysyrowicz, *Phys. Rep.* **441**, 47 (2007).
- [3] H.M. Milchberg, plenary talk, Advanced Accelerator ConceptsWorkshop 2016.
- [4] A. Couairon, E. Brambilla, T. Corti, D. Majus, O. de J. Ramirez-Gongora, and M. Kolesik, *Eur. Phys. J. Special Topics* **199**, 5 (2011).

Nondipole and ellipticity effects in the strong-field ionization physics

**J. Daněk¹, M. Klaiber¹, K. Z. Hatsagortsyan¹, B. Willenberg², J. Maurer²,
B. W. Mayer², C. R. Phillips², L. Gallmann², U. Keller² and C. H. Keitel¹**

¹Max-Planck-Institut für Kernphysik, Saupfercheckweg 1, 69117 Heidelberg, Germany

²Department of Physics, ETH Zurich, 8093, Zurich, Switzerland

Corresponding author: jiri.danek@mpi-hd.mpg.de

Abstract

We investigate the role of the nondipole effects for the case of strong field ionization of atoms with linearly and elliptically polarized mid-IR lasers and provide an intuitive picture for the interplay between the nondipole effects and the Coulomb focusing while explaining experimental spectra. Further, we demonstrate the important role of high-order recollisions for the final electron momenta and observed features in the photoelectron momentum distribution (PMD). Moreover, we show that nonzero ellipticity introduces a similar interplay as the nondipole effects leading to experimental separation of direct and rescattered electrons, which can be used to quantify Coulomb focusing and the wave-packet width.

Introduction

The recent advent of tabletop mid-IR laser technology brings us to the limits of our current theoretical understanding of strong-field ionization based on the dipole approximation. With the larger laser wavelengths the nondipole effects increase and become experimentally observable.

The most prominent experiment manifesting the breakdown of the dipole limit with a linearly polarized laser revealed a rather counterintuitive negative shift of the central cusp [1], which was due to the interplay between the Coulomb-focusing and the non-dipole effects. Recently, the same interplay was observed in experiments with elliptically polarized lasers revealing a simultaneous existence of an outstanding ridge created only by the rescattered electrons on the background of the well-known lobes consisting of direct electrons [2] in the PMD.

In order to provide an insight into electron dynamics and the nature of the interplay, we have developed a perturbative analytical model, where we address the Coulomb focusing effects by calculating the Coulomb momentum transfer at every single recollision along the electron's classical trajectory.

Within our model we are able to explain not only the nature of the counterintuitive bend of the central cusp but also its energy-dependence. For the latter the high-order recollisions also play a significant role and even cause a decrease of the shift at low energies [3].

Further, the high-order recollisions have been shown to have a significant effect also in the dipole case and cannot be omitted for proper investigation of electrons final momenta in the dipole limit either [4].

As the last application of our model we address the photoelectron spectra in the elliptically polarized case. Small values of ellipticity introduce a drift along the minor axis of polarization already in the dipole case, which is, in fact, similar to the magnetic drift acting along the laser field propagation direction of the nondipole case and leads therefore to a similar interplay responsible for a creation of the central ridge structure of rescattered electrons with characteristic deformation. The central structure and its shape are of similar origin as in the non-dipole case and the role of high-order recollisions can be again clearly identified [5].

Moreover, the nondipole peak offset manifests a transition from negative to positive values due to this interplay when the polarization varies from linear to circular [2]. Our model led to deeper understanding of the interplays which allowed for extraction of values of the Coulomb focusing and tunneled wave-packet width from the experiment [2].

References

- [1] A. Ludwig et al., *Breakdown of the Dipole Approximation in Strong-Field Ionization*, Phys. Rev. Lett. **113**, 243001 (2014).
- [2] J. Maurer et al., *Probing the ionization wave packet and recollision dynamics with an elliptically polarized strong laser field in the nondipole regime*, Phys. Rev. A **97**, 013404 (2018).
- [3] J. Daněk et al., *Analytical approach to Coulomb focusing in strong-field ionization. I. Nondipole effects*, Phys. Rev. A **97**, 063409 (2018).
- [4] J. Daněk et al., *Analytical approach to Coulomb focusing in strong-field ionization. II. Multiple recollisions*, Phys. Rev. A **97**, 063410 (2018).
- [5] J. Daněk et al., *Interplay between Coulomb-focusing and non-dipole effects in strong-field ionization with elliptical polarization*, J. Phys. B: At. Mol. Opt. Phys. **51**, 114001 (2018).

Unexpected coherent extreme ultraviolet radiation from He atoms exposed to a strong laser field

Hyoeek Yun¹, Je Hoi Mun¹, Sung In Hwang¹, Seung Beom Park¹, Igor A. Ivanov¹,
Chang Hee Nam^{1,2}, and **Kyung Taec Kim**^{1,2}

¹ Center for Relativistic Laser Science, Institute for Basic Science, Gwangju 61005, Korea

² Department of Physics and Photon Science, Gwangju Institute of Science and Technology, Gwangju 61005, Korea
Corresponding author: kyungtaec@gist.ac.kr

Abstract

We report the observation of an unexpected coherent extreme ultraviolet (EUV) radiation from He atoms exposed to a strong laser field. The atoms are coherently excited through frustrated tunnelling ionization. The coherent EUV radiation is emitted from the excited atoms through free induction decay. The intensity of the radiation is strongly modulated depending on the carrier-envelope-phase and ellipticity of the driving laser pulse. The propagation direction of the radiation can be controlled using a spatially-chirped laser beam. The coherent EUV radiation can be used as a light source for the applications such as EUV imaging and ultrafast pump-probe spectroscopy.

An atom can be excited when it is exposed to a light field. The excitation of an atom from the ground state to an excited state, which often requires much higher energy than the photon energy of a visible or an IR laser pulse, can be made by absorbing multiple photons. This multi-photon absorption has been considered as a main route for the excitation of an atom in an intense laser field.

Recently, Nubbemeyer et al., showed that there is another path for the excitation of an atom [1]. In a strong laser field, an electron can tunnel out through the potential barrier of the atom, and it is accelerated in the laser field. When the laser field off, the electron can be left near the atom with an almost zero kinetic energy. Then, the electron can recombine to an excited state of the atom. This strong field excitation is often referred as frustrated tunnelling ionization (FTI) which explains the survival of a significant amount of neutral atoms in a strong laser field.

In this work, we report that frustrated tunnelling ionization results in a coherent EUV emission which has not been observed so far [2]. The coherent property of the EUV radiation has been tested using an intense few-cycle laser pulse. The intensity of the EUV radiation showed a strong dependence on the carrier-envelop-phase and the ellipticity of the driving laser pulse. The intensity of the EUV radiation was strongest when the linearly polarized laser pulse is used. The intensity of the EUV radiation decreased as the ellipticity of the laser pulse increased. These behaviours show the coherent property of the EUV radiation.

The EUV radiation emitted through FTI has been

tested further using the attosecond lighthouse method in which a spatially-chirped laser beam is used. Since the wavelength of the laser beam is gradually changed across the beam, an individual atom interacts with the laser field at different wavelengths. The electron path from ionization to recombination in the process of FTI increases for the long wavelength field. The longer the wavelength is, the more the phase is accumulated. Therefore, the wavefront of the FTI radiation is tilted, resulting in the change of the propagation direction of the FTI radiation. The change of the propagation direction is a clear sign of the frustrated tunnelling since it shows the effect of the phase accumulated along the electron path after tunnelling.

In summary, the coherent property of the EUV radiation has been tested for the laser parameters such as the carrier-envelop-phase and the ellipticity. The propagation direction of the coherent EUV radiation generated through FTI could be controlled using the attosecond lighthouse technique. The EUV radiation generated through FTI can be used as a light source for the applications such as EUV imaging and ultrafast pump-probe spectroscopy.

References

- [1] T. Nubbemeyer, K. Gorling, A. Saenz, U. Eichmann, and W. Sandner, "Strong-Field Tunneling without Ionization," *Phys. Rev. Lett.* 101, 233001 (2008).
- [2] H. Yun *et al.*, "Coherent extreme ultraviolet emission generated through frustrated tunneling ionization," *Nat. Photonics* 12, 620–624, (2018).

Strong field physics and high harmonic generation with structured light beams

Paul Corkum, Fanqi Kong and Chunmei Zhang
Joint Attosecond Science Laboratory
University of Ottawa and National Research Council of Canada
Max Planck Centre for Extreme and Quantum Optics

Abstract

In the infrared it is possible to transform a Gaussian beam into structured light beams –beams with orbital angular momentum and “vector beams” (vector beams are beams with complex polarization states). We use structured light beams for high-harmonic generation and we also show that, like Gaussian beams, cylindrical symmetric vector beams can be compressed in hollow core fibers.

There are two general approaches to producing circularly polarized soft X-rays. (1) It is possible to use two circularly polarized co-propagating beams of different handedness with one being the second harmonic of the other. (2) One can also use either a structured fundamental beam or two beams with the same frequency but different direction of propagation. The key challenge is to find which approach is optimal for reaching very short wavelengths. Favoring the vector beam approach is the cut-off law which favors longer wavelength light and the scaling of the two color approach with long wavelength drivers.

We will show that high power vector beams open a new pathway to creating circular polarized harmonics that we demonstrate experimentally [1].

The underlying technology is to transform high power infrared or visible beams into structured beams. We achieve this transformation using Q-plates and we show that, once created, a cylindrically symmetric vector beam can be compressed using conventional hollow core fiber compression. These few cycle pulses can then be exploited in high intensity experiments [2].

We also produce XUV beams with orbital angular momentum, generated by high harmonic conversion. Like spin angular momentum, we confirm that orbital angular momentum is conserved during the conversion [3] (in fact total angular momentum is also conserved [4]) and we show how the conservation of angular momentum leads to a method for coupling a controlled orbital angular momentum on any harmonic [5].

In the visible, orbital angular momentum beams are very important for advanced microscopy and for quantum optics. Our results open a pathway for attosecond science with similarly structured light.

References

1. F. Kong, C. Zhang, H. Larocque, Z. Li, F. Bouchard, D. H. Ko, G. Brown, A. Korobenko, T. J. Hammond, R. W. Boyd, E. Karimi & P. B. Corkum, “Vectorizing the spatial structure of high-harmonic radiation from gas,” submitted to *Nature Comm.*
2. F. Kong, H. Larocque, E. Karimi, P. B. Corkum and C. Zhang, “Generating few-cycle radially polarized pulses”, submitted to *Optica*.
3. G. Gariépy, J. Leach, K. T. Kim, T. J. Hammond, E. Frumker, R. W. Boyd, and P. B. Corkum, “Creating High-Harmonic Beams with Controlled Orbital Angular Momentum”, *Phys. Rev. Lett.* **113**, 153901 (2014)
4. F. Kong, C. Zhang, H. Larocque, F. Bouchard, Z. Li, M. Taucer, G. Brown, T. J. Hammond, R. W. Boyd, E. Karimi & P. B. Corkum, “Spin constrained orbital angular momentum control in high-harmonic generation,” *Physics Review Letters* (**submitted**)
5. F. Kong, C. Zhang, F. Bouchard, Z. Li, G. G. Brown, D. H. Ko, T. J. Hammond, L. Arissian, R. W. Boyd, E. Karimi, and P. B. Corkum, “Controlling the orbital angular momentum of high harmonic vortices”, *Nat. Commun.* **8**, 14970 (2017)

Resonantly enhanced inner-orbital ionization in molecular iodine

G. N. Gibson and D. L. Smith

Department of Physics, University of Connecticut, 2152 Hillside Road, Storrs, CT 06269, USA

Corresponding author: george.gibson@uconn.edu

Abstract

Many experiments have shown evidence of deep inner-orbital ionization resulting from the strong-field interaction with diatomic molecules. In general, these deep inner-orbitals correspond to the ones formed from the s-electrons, as opposed to the less-bound p-electrons. In this talk, we present new data on the resonant enhancement of inner-orbital ionization iodine. When the transition from the highest-occupied molecular orbital (HOMO) to the lowest-unoccupied molecular orbital (LUMO) is driven, we find a strong enhancement of ionization from the HOMO-3 and HOMO-4 orbitals.

Introduction

For atoms and light molecules in strong laser fields, most ionization comes from the least bound electron in either the outer shell for atoms or the HOMO for molecules [1]. The influence of inner orbitals can be seen in the strong-field molecular interaction, but the angularly averaged ionization rate from the inner orbitals is small (<10%) [2]. We have shown in previous experiments that this is not the case for iodine. In fact, the branching ratio for ionization of the inner orbitals can exceed 90%[3]. We have also recently observed a dramatic wavelength dependence to the ionization rates of the different orbitals [4]. Both of these results run counter to a simple tunneling model of strong field ionization, in that tunneling ionization strongly prefers the least bound electron and predicts no wavelength dependence [5].

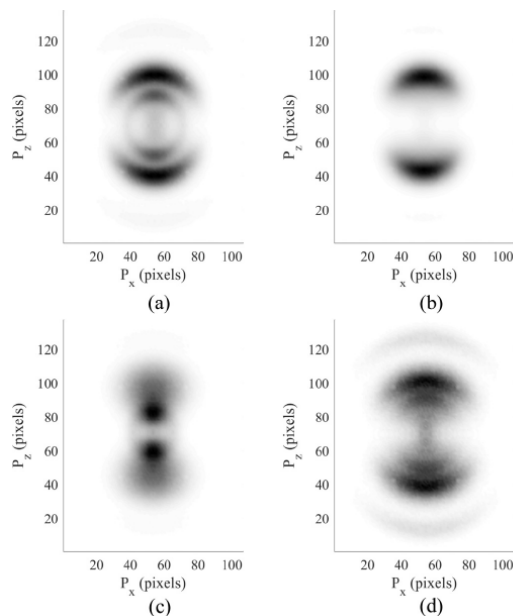
In this talk, we report results on the single ionization of I_2 in the vicinity of the X to B state resonance in the neutral molecule. Since the X–B transitions involves driving an electron from the HOMO to the LUMO, one might expect that ionizing I_2 at this resonance would simply enhance the ionization rate of the HOMO, as that electron would be promoted to the LUMO, where it should easily ionize. However, it turns out the results are significantly more complicated and counter-intuitive. We divide the ionization signal into two parts: one corresponding to ionization of the HOMO, the HOMO-1, and HOMO-2, leading to the population of the X, A, and B states of the molecular ion, respectively [6]. We refer to this part as outer-orbital ionization (OOI). The other part of the ionization signal corresponds to deeply bound inner orbitals, or inner-orbital ionization (IOI). Both signals show a strong resonant behavior around the X to B transition, but the peaks in the two signals as a function of wavelength are slightly different. As a result, the branching ratio into the IOI channel shows a dispersion-type profile with the peak of the branching ratio exceeding 98%. At this point, the resonant interaction does not increase the ionization rate of the HOMO, but rather enhances the ionization

rate of the inner orbital electrons. We speculate that driving the neutral molecule on a one-photon resonance creates a strong dipole that couples to the inner orbitals, leading to their large ionization rates, compared to the outer orbitals.

Results

Figure 1 shows VMI images around the X to B state resonance in I_2 (530 nm). This is a dramatic wavelength dependence, not often see in strong-field ionization. The significance of these results will be discussed in the talk.

Fig. 1. Four I^+ VMI images at wavelengths of (a) 489 nm,



(b) the peak in the IOI signal at 519 nm, (c) the peak in the OOI signal at 580 nm, and (d) 670 nm.

References

- [1] B. K. McFarland, et al., *Science* 322, 1232 (2008).
- [2] H. Akagi, et al., *Science* 325, 1364 (2009).
- [3] H. Chen, et al., *Phys. Rev. Lett.* 109, 193002 (2012).
- [4] D. L. Smith, et al., *Phys. Rev. A* 95, 013410 (2017).
- [5] M. V. Ammosov, et al., *Sov. Phys. JETP* 64, 1191 (1986).
- [6] M. C. R. Cockett, et al., *J. Chem. Phys.* 105, 3347 (1996).

Photoionization dynamics: Transition and scattering delays

M. Labeye¹, A. Desrier¹, M. Vacher², A. Maquet¹, J. Caillat¹ and R. Taïeb¹

¹ Sorbonne Université, CNRS, UMR 7614, Laboratoire de Chimie Physique Matière et Rayonnement, Paris, France

² Department of Chemistry—Ångström, Uppsala University, Box 538, SE-751 21 Uppsala, Sweden

Corresponding author: richard.taieb@upmc.fr

Abstract

We review various aspects of photoemission dynamics in the case of 1 and 2-photon ionisation for atoms and molecules. Numerical experiments on model atoms are used to show how the group delay associated with the transition phase is actually representative of the early dynamics of the detected photoelectron wave packets. Then we address the question of measuring these transition delays using a standard interferometric technique of experimental attosecond physics, so-called RABBIT, and its implication on reconstructing time-dependant electronic wavepackets.

Resolving electron motion in atoms and molecules on its natural attosecond (as) scale is way beyond the temporal resolution of available detection devices. The techniques developed to achieve such attosecond resolution thus rely on interferometric setups [1]. In fact, the reported times are actually group delays derived from phase measurements, involving coherent photoemission processes. Therefore, the analysis of the experimental data and the related theoretical development ask for rigorous and unambiguous definitions and interpretations of these phases, and of the inferred group delays [2].

It is now accepted that a "scattering delay" [4] affects the dynamics of any photoemission process. However, the simplicity of the underlying physics is not fully recognized yet. Formally, such delays are imprinted in the phase shifts of the photoelectron wave-functions, which are commonly expressed on the basis of incoming waves. In this framework, the "scattering phase" associated to photoemission appears as the argument of the transition amplitude, thus obscuring the significance of the delay - which may be misinterpreted for example as a transition duration.

Here, we will present the benefits of working with the continuum wave-functions selected by the transitions (scwf) [2,3], which (i) carry all the information related to the continuum reached by photoabsorption, (ii) are defined independently of the arbitrary basis one chooses to work with and (iii) are real valued for single-photon transitions. They provide a clear-cut interpretation of the scattering delays.

In higher order processes, the scwf comes with an additional complex phase, as soon as the transition is resonant. We will show that the group delay associated with that phase can now be interpreted as a "transition delay", and how it can be accessed experimentally in a straightforward reinterpretation of the rabbit interferometric technique, initially designed for the characterization of coherent xuv pulses.

Furthermore, using an extension of the RABBIT method, i.e. the so-called "Rainbow-RABBIT", we can reconstruct *in time* the photoelectron wave-packet and follow *in time* how the spectrum is built in Helium atom [5] and in chiral molecule [6].

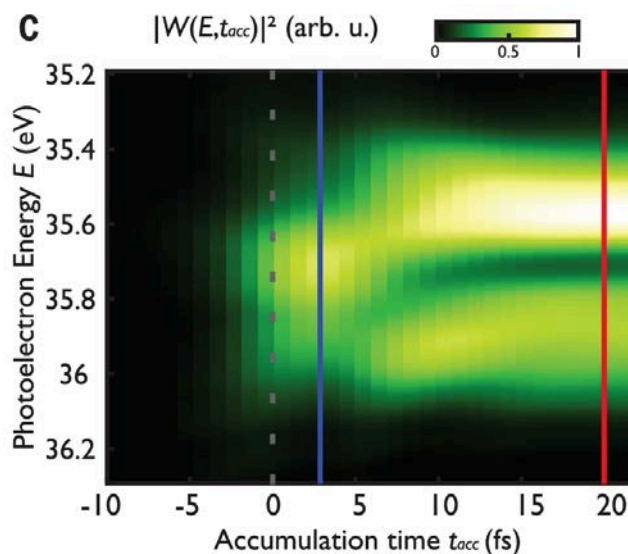


Fig. 1. Reconstruction of the timeresolved buildup of the resonant spectrum using the time-energy. The photoelectron spectrum is plotted as a function of the accumulation time t_{acc} used in the inverse Fourier transform [1].

References

- [1] S. Haessler et al., *Phys. Rev. A* **80** 011404 (2009); M. Schultze et al., *Science* **328** 1658 (2010) ; K. Klunder et al., *Phys. Rev. Lett.* **106** 143002 (2011).
- [2] J. Caillat et al., *Phys. Rev. Lett.* **106** 093002 (2011); R. Gaillac et al., *Phys. Rev. A* **93** 013410 (2016); M. Vacher et al., *J. of Optics* **19** 12401 (2017).
- [3] H. Park et al., *J. Chem. Phys.* **104** 4554 (1996).
- [4] E. P. Wigner, *Phys. Rev.* **98** 145 (1955).
- [5] V. Gruson et al., *Science* **354**, 734 (2016).
- [6] S. Beaulieu et al., *Science* **258**, 1288 (2017).

Time-dependent multiconfiguration and coupled-cluster methods for intense-laser driven multielectron dynamics

Takeshi Sato^{1, 2, 3}

¹ Department of Nuclear Engineering and Management, Graduate School of Engineering, The University of Tokyo, 7-3-1 Hongo, Bunkyo-ku, Tokyo 113-8656, Japan

² Photon Science Center, Graduate School of Engineering, The University of Tokyo, 7-3-1 Hongo, Bunkyo-ku, Tokyo 113-8656, Japan

³ Research Institute for Photon Science and Laser Technology, Graduate School of Engineering, The University of Tokyo, 7-3-1 Hongo, Bunkyo-ku, Tokyo 113-8656, Japan

Corresponding author: sato@atto.t.u-tokyo.ac.jp

Abstract

We have developed time-dependent wavefunction-based methods such as time-dependent complete-active-space self-consistent-field (TD-CASSCF) method and time-dependent optimized coupled-cluster (TD-OCC) method for *ab initio* descriptions of intense laser-matter interactions. This report describes our methodology development, computer implementation, and applications to correlated electron dynamics in atoms and molecules.

An important goal of high field physics and attosecond science is the direct measurement and control of electron dynamics in atoms and molecules. To theoretically investigate multielectron dynamics in intense laser fields, the multiconfiguration time-dependent Hartree-Fock (MCTDHF) method has been developed [1-2], which, though powerful, suffers from the exponential increase of the computational cost with respect to the number of electrons.

To circumvent this difficulty, we have developed time-dependent multiconfiguration self-consistent-field methods such as time-dependent complete-active-space self-consistent-field (TD-CASSCF) [3] and time-dependent occupation-restricted multiple-active-space (TD-ORMAS) methods [4], which enables *ab initio* description, beyond mean-field treatments such as time-dependent Hartree-Fock (TDHF) and time-dependent density functional theory (TDDFT), of many-electron atoms and molecules for a broad range of laser parameters. (See Fig. 1 and 2.)

Furthermore, we have recently formulated a radically advanced theoretical method based on the cluster expansion of the wavefunction using time-dependent orbitals, called time-dependent optimized coupled-cluster (TD-OCC) method [5]. The TD-OCC is a time-dependent, orbital-optimized generalization of the highly-successful stationary coupled-cluster method in quantum chemistry. It is a gauge-invariant, polynomial-cost scaling, and size-extensive alternative to the MCTDHF method. In this talk, I briefly introduce theoretical background and computer implementations of these methods and report their applications to intense-laser driven correlated electron dynamics in atoms and molecules.

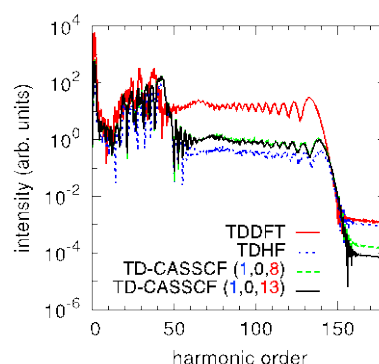


Fig. 1. HHG spectrum of Ne exposed to a laser pulse with a wavelength of 800 nm, a peak intensity of 10^{15} W/cm², and the foot-to-foot pulse duration of two optical cycles, obtained with TDDFT, TDHF and TD-CASSCF with various active spaces [3].

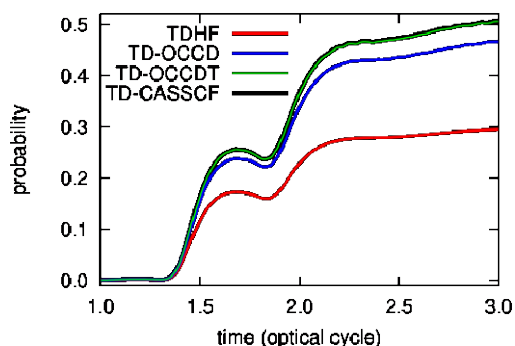


Fig. 2. Single ionization probabilities, as a function of time, of Ar atom exposed to a laser pulse with a wavelength of 800 nm and an intensity of 6×10^{14} W/cm², computed with TDHF, TD-OCC, and TD-CASSCF methods. [5].

References

- [1] T. Kato and H. Kono, *Chem. Phys. Lett.* **392**, 533 (2004).
- [2] J. Caillat *et al*, *Phys. Rev. A* **71**, 012712 (2005).
- [3] T. Sato and K. L. Ishikawa, *Phys. Rev. A* **88**, 023402 (2013).
- [4] T. Sato and K. L. Ishikawa, *Phys. Rev. A* **91**, 023417 (2015).
- [5] T. Sato *et al*, *J. Chem. Phys.* **148** 051101(2018).

Hollow core fiber pulse compression using molecular gases

E. Haddad¹, R. Safaei¹, A. Leblanc¹, R. Piccoli¹, Y.-G. Jeong¹, H. Ibrahim¹, B.E. Schmidt², R. Morandotti^{1,3}, L. Razzari¹, F. Légaré¹, and P. Lassonde¹

¹ INRS, Centre Énergie Matériaux et Télécommunications, 1650 Blvd. Lionel-Boulet, Varennes, QC J3X 1S2, Canada

² Few-cycle Inc., 2890 Rue de Beaurivage, Montreal, QC H1L 5W5, Canada

³ ITMO University, St. Petersburg 199034, Russia

Corresponding author: elissa.haddad@emt.inrs.ca

Abstract

We demonstrate that hydrofluorocarbon molecular gases can be used as an alternative to atomic noble gases to efficiently compress relatively low energy pulses with a hollow core fiber setup. Compression of a 1030 nm, 200 μ J, 170 fs initial pulse to a sub-five-cycle duration of 15.6 fs is achieved.

Introduction

Pulse compression based on non-linear propagation in a gas-filled hollow core fiber (HCF) is amongst the common techniques to generate few-cycle laser pulses [1]. Although very efficient, the major disadvantage of this method is the need to use expensive noble gases like krypton or xenon to compress low energy pulses [2-4]. Our latest results confirm that certain molecular gases, hydrofluorocarbons, represent an affordable and efficient alternative to the traditional atomic gases [5]. Such gases bear the potential to generalize HCF compression to high repetition rate, low intensity laser systems [6].

Spectral broadening of Ti:Sa pulses

We studied the nonlinear properties of 3 molecular gases: 2 hydrofluorocarbons – R152a ($C_2H_4F_2$) and R134a ($C_2H_2F_4$) – and ethylene (C_2H_4). The spectral broadening through these media in a 1-m-long HCF was measured as a function of pressure for different pulse energies. Two typically employed atomic gases, krypton and argon, were used as references.

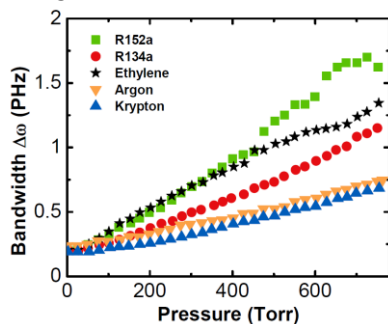


Fig. 1. Spectral broadening of a 120 μ J (except for argon, 240 μ J) pulse as a function of pressure for all gases.

Fig. 1 shows the spectral broadening for an initial pulse of 120 μ J (except for argon, 240 μ J) from a Ti:Sa laser at 800 nm with a 2.5 kHz repetition rate. The greater slopes for the molecular gases indicate a much stronger nonlinear response compared to the atomic ones. Although ethylene seems to efficiently

broaden laser pulses, important ionization was observed compared to the other gases, which suggests that it might not allow proper compression.

Pulse compression

To demonstrate the potential of hydrofluorocarbon gases for compression of low intensity and high average power lasers, typically ytterbium-based systems, we compressed 1030 nm, 200 μ J, 170 fs pulses from a Yb:KGW laser using a folded 4f stretcher/compressor after propagation through a 6-m-long HCF filled with R134a (pressure of 2000 Torr). Temporal characterization was achieved using second-harmonic generation frequency-resolved optical gating (SHG-FROG) and the retrieved pulse duration of 15.6 fs (sub-five-cycle) is shown in Fig. 2.

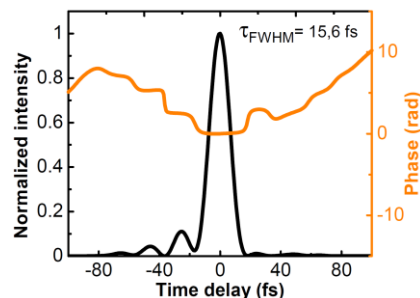


Fig. 2. Retrieved pulse in the time domain with its phase after compression in R134a ($E = 200 \mu$ J, $p = 2000$ Torr).

Our most recent results show that it is possible to compress pulses of energy as low as tens of microjoules using these hydrofluorocarbon gases. We believe this affordable and simple yet very efficient approach will greatly facilitate compression of very high repetition rate and low intensity laser systems.

References

- [1] M. Nisoli, S.D. Silvestri, and O. Svelto, *Applied Physics Letters* **68**, 2793 (1996).
- [2] B.F. Mansour, H. Anis, D. Zeidler, P.B. Corkum, and D.M. Villeneuve, *Optics Letters* **31**, 3185 (2006).
- [3] V. Cardin *et al.*, *Applied Physics Letters* **107**, 181101 (2015).
- [4] G. Fan *et al.*, *Optica* **3**, 1308 (2016).
- [5] E. Haddad *et al.*, *Optics Express* **26**, 25426 (2018).
- [6] L. Lavenue *et al.*, *Optics Express* **25**, 7530 (2017).

Spectral interference in shortwave- and mid-infrared laser filaments in gases

Pavel Polynkin¹

¹ College of Optical Sciences, The University of Arizona, 1630 E. University Blvd., Tucson, Arizona 85721, USA
Email: ppolynkin@optics.arizona.edu

Abstract

I will discuss experiments and computer simulations on the nonlinear self-channelling (filamentation) of shortwave-infrared and mid-infrared, ultrashort laser pulses in air and argon. The observed spectral interference in the generated white light is found to be robust against pulse-energy fluctuations of the pump laser. The dependence of the interference patterns on the carrier-envelope phase (CEP) of the pump pulses can be used for inline, single-shot measurements of the CEP in CEP-unstable laser sources.

Nonlinear self-channelling of intense, ultrashort laser pulses in gases, known as laser filamentation, has various potential applications ranging from remote sensing in the atmosphere to lightning control. In the last two decades, laser filamentation has been extensively investigated using ultrafast Ti:Sapphire laser systems operating in the near-infrared. Recent developments of ultrafast laser technology enable the extension of these studies to the shortwave-infrared and mid-infrared parts of the optical spectrum. There, filamentation physics is different due to the presence of windows of anomalous dispersion in molecular gases and a much wider spectral range over which the white-light supercontinuum and harmonics of the driver field can be generated and studied.

In this talk, I will discuss experiments and computer simulations on filamentation of two state-of-the-art laser sources: A carrier-envelope phase (CEP) stable, 11 fs OPCPA at 1.7 μm wavelength at the University of Central Florida and a CEP-unstable, 100 fs, mid-infrared OPCPA at 3.9 μm wavelength at

the Technical University of Vienna. In both cases, we observed CEP-dependent interference patterns in the spectra of white light generated through filamentation in air and argon. We interpret these spectral features as the result of interference between different nonlinear source terms generating white light – supercontinuum, harmonic generation and the Brunel mechanism. In spite of the highly nonlinear pulse dynamics, the CEP-coherence is preserved on propagation through the filamentation zone, due to the intensity clamping, which has been shown to be operative in few-cycle pulses.

Acknowledgements

I would like to acknowledge contributions from the research groups of Professors Zenghu Chang (University of Central Florida), Andrius Baltuska and Audrius Pugzlys (Technical University of Vienna), and Miroslav Kolesik (University of Arizona). The author's contribution was supported by the US Air Force Office of Scientific Research under program FA9550-16-1-0013.

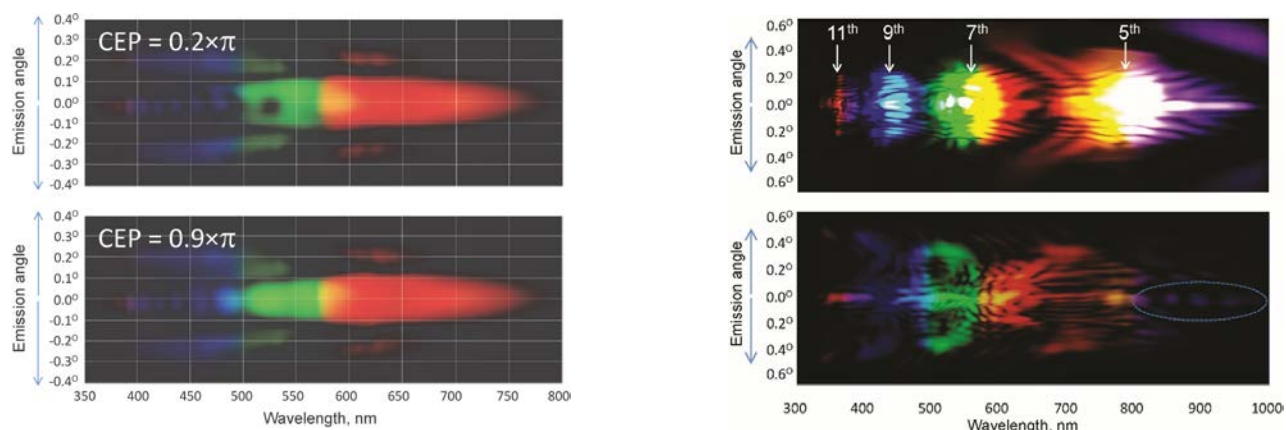


Fig. 1. Left: Angularly-resolved spectra of white light generated through filamentation of 1.4 mJ, 11 fs, CEP-stable laser pulses at 1.7 μm center wavelength in air. The images are averaged over $\sim 1,000$ laser shots. The top and bottom images are for the CEP values corresponding to the most dissimilar spectra. The main CEP-dependent feature is the appearance and disappearance of the spectral hole in the on-axis emission in the vicinity of the 3rd harmonic of the 1.7 μm driver. **Right:** Single-shot spectra of white light generated through filamentation of 30 mJ, 100 fs CEP-unstable laser pulses at 3.9 μm wavelength in air (top) and argon (bottom), both at 1 atm. pressure. Harmonics of up to 11th order are detected. The CEP-dependent spectral fringes due to the interference between 3rd and 5th harmonics are highlighted with the oval in the bottom image.

Light amplification by nearly free electrons in a laser filament

Mary Matthews¹, Felipe Morales², Alexander Patas³, Albrecht Lindinger³, Julien Gateau¹, Nicolas Berti¹, Sylvain Hermelin¹, Jérôme Kasparian¹, Maria Richter^{2,4}, Timm Bredtmann², Olga Smirnova², Jean-Pierre Wolf¹ and Misha Ivanov^{2,5}

¹ GAP, University of Geneva, 22 ch. de Pinchat, 1211 Geneva 4, Switzerland

² Max-Born-Institut, Max Born Straße 2A, 12489 Berlin, Germany

³ Inst. für Exp. Physik, Freie Universität Berlin, Arnimallee 14, 14195 Berlin, Germany

⁴ Departamento de Química, Módulo 13, Universidad Autónoma de Madrid, 28049 Madrid, Spain

⁵ Blackett Laboratory, Imperial College London, South Kensington Campus, SW7 2AZ London, United Kingdom

Corresponding author: maria.richter@mbi-berlin.de

Abstract

Light can be used to modify and control properties of media, as in the case of electromagnetically induced transparency or, more recently, for the generation of slow light or bright coherent extreme ultraviolet and X-ray radiation. Particularly unusual quantum states can be created by light fields with strengths comparable to the Coulomb field which binds valence electrons in atoms: the states describe a nearly free electron oscillating in the laser field yet still loosely bound to the core [1,2]. Using shaped laser pulses, we demonstrate [3] that such states can arise not only in isolated atoms, but also in gases, at and above atmospheric pressure, guiding intense laser pulses, where they can act as a gain medium. The gain is created within just a few cycles of the guided field. The corresponding emission yields signatures of these unusual states, demonstrating a general, new, ultrafast gain mechanism during laser filamentation.

Bound states of nearly free electrons

Since the late 1980s, it has been speculated that when an atom or molecule interacts with an intense light field, whose strength substantially exceeds the ionic Coulomb attraction, new and surprisingly stable states of a hybrid quantum system, “atom + intense light field”, can be formed. The electron becomes nearly but not completely free: rapidly oscillating in the laser field, it still feels residual attraction to the core, which keeps it bound [1,2]. These exotic states are known as the Kramers-Henneberger (KH) states [4], a specific example of laser-dressed states [2]. It took three decades before the existence of such states was indirectly inferred from experiments [2], showing the ability of isolated neutral atoms to survive laser intensities as high as $I \sim 10^{15} - 10^{16}$ W/cm².

But are such unusual stable states really exotic? Can they also form in gases at ambient conditions, at intensities well below 10^{15-16} W/cm²? After all, for *excited* electronic states bound by a few eV, the laser field overpowers the Coulomb attraction to the core already at $I \sim 10^{13-14}$ W/cm². If this is the case, would these exotic stable states manifest inside laser filaments [5]?

The role of nearly free electrons in laser filaments

The formation of the KH states should modify both real [6] and imaginary parts [7] of the refractive index of a laser-driven system. While their response is almost free-electron-like, they do form discrete states and lead to new resonances. Qualitatively, these resonances can be understood as Stark-shifted field-free states, with stability against ionization being their

key distinguishing feature. Crucially, at sufficiently high intensities theory predicts the emergence of population inversion in the higher Rydberg states relative to the lowest excited states [8]. This inversion reflects the increased stability of the KH states and is the signature of the transition into the stabilization regime. If the inversion were created inside a laser filament, it would lead to amplification of the filament spectrum at the transition frequencies between the stabilized states.

"Nearly-free-electron lasing" inside laser filaments

I will describe a combination of experimental and theoretical results [3] which show that the KH states arise not only in isolated atoms, but also in rare gases at and above atmospheric pressure, where they can act as a gain medium during laser filamentation. Using properly shaped laser pulses, gain in these states can be achieved within just a few cycles of the guided field, leading to amplified emission in the visible, at lines peculiar to the laser-dressed atom. Our work suggests that these unusual states of neutral atoms can be exploited to create a general ultrafast gain mechanism during laser filamentation.

References

- [1] J. H. Eberly & K.C. Kulander, *Science* **262**, 1229 (1993).
- [2] U. Eichmann *et al.*, *Nature* **461**, 1261 (2009).
- [3] M. Matthews *et al.*, *Nat. Phys.* **14**, 695 (2018).
- [4] W. C. Henneberger, *Phys. Rev. Lett.* **21**, 838 (1968).
- [5] A. Couairon & A. Mysyrowicz, *Phys. Reports* **441**, 47 (2007).
- [6] M. Richter *et al.*, *New J. Phys.* **15**, 083012, (2013).
- [7] T. Bredtmann *et al.*, *Phys. Rev. A* **93**, 021402 (2016).
- [8] U. Eichmann *et al.*, *Phys. Rev. Lett.* **110**, 203002 (2013).

Optical lasing during laser filamentation in the Nitrogen molecular ion: ro-vibrational inversion

F. Morales¹, M. Lytova², M. Spanner², M. Richter^{1,3}, O. Smirnova¹ and M. Ivanov^{1,4}

¹Max-Born-Institut, Max Born Strasse 2A, D-12489 Berlin, Germany

²National Research Council of Canada, 100 Sussex Drive, Ottawa, ON K1A 0R6, Canada

³Dpto. de Química, Módulo 13, Univ. Autónoma de Madrid, E-28049 Madrid, Spain

⁴Blackett Laboratory, Imperial College London, South Kensington Campus, SW7 2AZ London, United Kingdom

Corresponding author: morales@mbi-berlin.de

Abstract

Inducing and controlling lasing in the open air is an intriguing challenge. Recent experiments on laser filamentation in the air have demonstrated generation of population inversion and lasing at the 391 nm and 428 nm lines in the nitrogen ion, which correspond to transitions between the second excited $B^2\Sigma_u^+$ and the ground $X^2\Sigma_g^+$ electronic states. Importantly, lasing at these transitions appears to be a very general effect, arising during filamentation of virtually any incident radiation, from visible to mid-infrared. We analyze the possible mechanisms that can be responsible for the generation of the population inversion between the $B^2\Sigma_u^+$ and $X^2\Sigma_g^+$ states of N_2^+ , focusing on the interplay between tunnel ionization of neutral nitrogen to different electronic states of the ion, ultrafast laser driven electronic excitations in the ion, molecular vibrations, laser induced alignment and rotations. We show how the combined action of all of these mechanisms can enable population inversion in $B^2\Sigma_u^+$.

Several experiments have shown that a tightly focused laser beam in air produces bright emission lines in the forward emission direction, in particular at 391 nm and 428 nm. These wavelengths correspond to transitions between the second excited (the $B^2\Sigma_u^+$ state) and the ground (the $X^2\Sigma_g^+$ state) states of the N_2^+ molecule [1] (see figure).

By now, several competing explanations of the underlying process of this exciting experimental observation have been offered. The proposed mechanisms are, however, specific to the laser-driven electronic and vibrational dynamics in the nitrogen molecular ion and seem to be dependent on a delicate interplay of the wavelength, the intensity, and the duration of the laser pulse, in contrast to the experimental observations. Moreover, the attempts to provide a unifying physical picture, that supports the experimental findings [see e.g. 2-4], do not report sufficient gain to support spontaneous unseeded lasing.

Besides being a fascinating unresolved physics problem, the complete understanding of this phenomenon, and its control, is of practical relevance as it offers important practical applications, e.g., in the field of remote sensing.

We propose a mechanism that explains the population inversion between the $B^2\Sigma_u^+$ state and the $X^2\Sigma_g^+$ state and is based on the combined effect of several processes: (i) tunnel ionization of neutral nitrogen to the different relevant ionic states, using angular-resolved strong-field ionization rates calculated numerically for the nitrogen molecule, (ii)

laser-induced ultrafast electronic excitations in the ion, (iii) molecular vibrations, (iv) alignment of the molecule induced by the strong laser pulse, and (v) molecular rotation upon ionization.

We find that the strong laser field creates a ro-vibrational 'conveyor belt' carrying the population away from the ground electronic state and enabling population inversion in the high rotational states of the excited $B^2\Sigma_u^+$ state. Our results show that population inversion is not a pre-requisite, but rather that lasing without inversion is possible, thanks to the coherent rotational dynamics in the cation. This new rotational mechanism is not specific to the nitrogen ion and should facilitate gain in other systems.

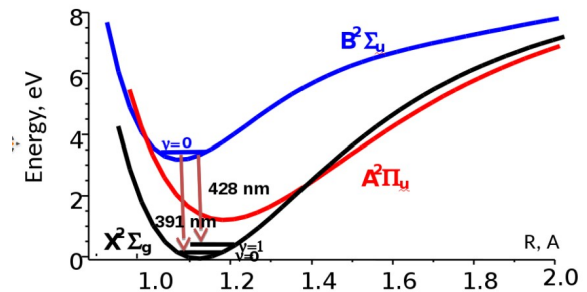


Figure 1: Sketch representation of the two emission lines

References

- [1] Q. Luo *et al.*, *Appl. Phys. B* 76, 337 (2003)
- [2] Y. Liu *et al.* *PRL* 115, 133203 (2015)
- [3] H. Xu *et al.* *Nat. Comm.* 6, 8347 (2015)
- [4] J. Yao *et al.* *PRL* 116, 143007 (2016)

Exploring matter in extreme conditions with free electron lasers

Siegfried H. Glenzer, Z. Chen, B. Ofori-Okai et al.

SLAC National Accelerator Laboratory, 2575 Sand Hill Rd, Menlo Park, CA 94025

glenzer@slac.stanford.edu

Abstract: The Linac Coherent Light Source (LCLS) free electron laser produces the world's brightest x-ray pulses to probe the physical and structural properties of matter on ultrafast time scales. At the Matter in Extreme Conditions (MEC) end station we combine the x-ray beam with high-power lasers that produce short-lived plasma states with high pressures, high temperatures or high densities to study some of the most violent phenomena that occur in astrophysical scenarios and in fusion plasma research. The first data of the collective plasmon scattering spectra from isochorically-heated aluminum obtained with the Linac Coherent Light Source (LCLS) have provided information about the electrical conductivity to temperatures up to 6 eV [1]. The plasmon feature shows significant broadening from which we extract the collision frequency and thus the conductivity. Density functional theory simulations provide excellent agreement with the measured spectra and compare well with the observed scaling of conductivity with temperature [2]. However, recent criticism was voiced regarding both the experiment and theory [3-5]. For example, calculations based on time-dependent theory [3] suggested lower temperatures than quoted in the original paper. Further, questions about the LCLS focal spot size have been raised [4], and, finally, confusion about comparisons with the existing data set from liquid aluminum have arisen [5]. In this presentation, we will 1) show experimental data from LCLS that support the choice of the structure factor used in our calculations, 2) provide evidence for the LCLS focal spot size, and 3) clarify the use of existing isobaric versus isochoric data in the liquid regime [6]. We will then go on and lay out a new experimental program aimed at delivering much improved conductivity data in the warm dense matter regime. For this purpose, we will take advantage of multiple recent experimental capabilities; they are free-electron lasers [7], ultrafast electron diffraction [8], ultrafast pump-probe measurements [9], and single-shot THz spectroscopy [10]. We will present new experimental data demonstrating that these techniques provide well-characterized conditions in concert with the first direct measurements of both ac and dc conductivity in the warm dense matter regime. First results and analysis support the earlier results and reveal a new temperature scaling.

[1] P. Sperling, E. J. Gamboa, H. K. Chung, E. Galtier, H. J. Lee, Y. Omarbakiyeva, H. Reinholz, G. Röpke, U. Zastra, J. Hastings, L. B. Fletcher, and S. H. Glenzer, *Phys. Rev. Lett.* **115**, 115001 (2015).

[2] B. B. L. Witte, L. B. Fletcher, E. Galtier, E. Gamboa, H. J. Lee, U. Zastra, R. Redmer, S. H. Glenzer, and P. Sperling, *Phys. Rev. Lett.* **118**, 225001 (2017).

[3] C. Mo, Z. Fu, W. Kang, P. Zhang, and X. T. He, *Phys. Rev. Lett.* **120**, 205002 (2018).

[4] E. Gamboa, private communication (2018).

[5] M. W. C. Dharma-wardana, D. D. Klug, L. Harbour, and L. J. Lewis, *Phys. Rev. E* **96**, 053206 (2017).

[6] Comment on "Isochoric, isobaric, and ultrafast conductivities of aluminum, lithium, and carbon in the warm dense matter regime", B. B. L. Witte, G. Röpke, P. Neumayer, M. French, P. Sperling, V. Recoules, S. H. Glenzer, and R. Redmer, *Phys. Rev. E* (in review).

[7] D. Koralek, J. B. Kim, P. Brůža, C. B. Curry, Z. Chen, H. A. Bechtel, A. A. Cordones, P. Sperling, S. Toleikis, J. F. Kern, S. P. Moeller, S. H. Glenzer & D. P. DePonte, *Nature Communications* **9**, 1353 (2018).

[8] M. Mo, Z. Chen, R. K. Li, M. Dunning, B. B. L. Witte, J. K. Baldwin, L. B. Fletcher, J. B. Kim, A. Ng, R. Redmer, A. H. Reid, P. Shekhar, X. Z. Shen, M. Shen, K. Sokolowski-Tinten, Y. Y. Tsui, Y. Q. Wang, Q.

Zheng, X. J. Wang, and S. H. Glenzer, *Science* **360**, 1451-1454 (2018).

[9] Z. Chen, M. Mo, L. Souldard, V. Recoules, P. Hering, Y. Y. Tsui, S. H. Glenzer, and A. Ng, *Phys. Rev. Lett.* **121**, 075112 (2018).

[10] B. K. Russell, B. K. Ofori-Okai, Z. Chen, M. C. Hoffmann, Y. Y. Tsui, and S. H. Glenzer, *Optics Express* **25**, 16140 (2017).

Transform-limited hard-x-ray lasers pumped by x-ray free-electron lasers

C. Lyu, S.M. Cavaletto, C.H. Keitel and Z. Harman

Max-Planck-Institut für Nuclear Physics, Saupfercheckweg 1, 69117 Heidelberg, Germany

Corresponding author: chunhai.lyu@mpi-hd.mpg.de

Abstract

We put forward a scheme to generate fully coherent x-ray lasers based on population inversion in highly charged ions, created by fast inner-shell photoionization using x-ray free-electron-laser pulses in a laser-produced plasma. Numerical simulations show that one can obtain femtosecond, transform-limited Gaussian-like x-ray pulses of relative bandwidths by orders of magnitude narrower than in x-ray free-electron-laser pulses for wavelengths down to the sub-ångström regime. Analytical solutions in the small-signal regime show that the duration of x-ray laser pulses is determined by the lifetime of the population inversion.

Introduction

The investigation of the coherent interaction between hard-x-rays and matter demands x-ray sources with high spectral brilliance and good temporal coherence. X-ray lasers pumped by high-intensity x-ray free-electron lasers (XFELs) are good candidates for such applications. Former experiments at SLAC, Stanford [1] and SACLA, Japan [2] had demonstrated such x-ray lasers with neutral atoms where the bandwidth of the lasers were dominated by fast Auger decay processes, leading to a coherence time in the range of 2 fs.

Here, we propose a scheme to obtain x-ray lasers based on stimulated emission in highly charged He-like ions, with the population inversion achieved by photoionization of Li-like ions via intense XFEL pulses [3] (see Fig. 1). The nonexistent of Auger decay channel in these ions significantly increases the coherence time of the outgoing x-ray lasers to the range of 100 fs.

Fig. 1. Scheme of the lasing process. (a) General setup. (b) Level scheme.

We first performed ab initio atomic structure calculations to obtain the transition energies and rates for He-like ions such as Ne^{8+} , Ar^{16+} , Kr^{34+} and Xe^{52+} . We use the FLYCHK code, a collisional-radiative plasma model, to determine the plasma conditions needed to achieve the corresponding ions in a laser-produced plasma. Then the Maxwell-Bloch equations

are applied to describe the lasing dynamics, and are solved both numerically and analytically.

Fig. 2. Evolution of the normalized (a) pulse and (b) spectral profiles of an x-ray laser based on Ar^{16+} (with photon energy of $\omega=3.12$ keV). (c,d) the pulse and spectral profiles at medium length L_c depicted in (a,b) for different XFEL pump pulses presented in (e-h). Blue solid lines in (c,d) are averaged results over 1000 simulations.

Starting with noisy spontaneous emissions, as shown in Figs. 2a,b for numerical simulations, the x-ray pulse gradually evolves into a transform-limited Gaussian profile at medium length of $L=0.75$ mm, with a pulse duration around 200 fs. In the meantime, the intensity of the x-ray laser increases exponentially as it propagates through the medium, and it reaches the saturation intensity at $L=2.3$ mm where an abrupt reduction of the pulse duration and a significant broadening of the spectral width become apparent.

Though there are shot-to-shot fluctuations in the peak intensities, pulse durations and spectral widths at given medium length (see Figs. 2c,d), comparing to the random XFEL pump pulses in Figs. 2e-h, the x-ray laser pulses are always fully coherent with a narrow bandwidth of $\Delta\omega/\omega\approx 10^{-5}$.

References

- [1] N. Rohringer *et al.*, Nature (London) 481, 488 (2012).
- [2] H. Yoneda *et al.*, Nature (London) 524, 446 (2015).
- [3] C. Lyu *et al.*, arXiv:1801.02503 (2018).

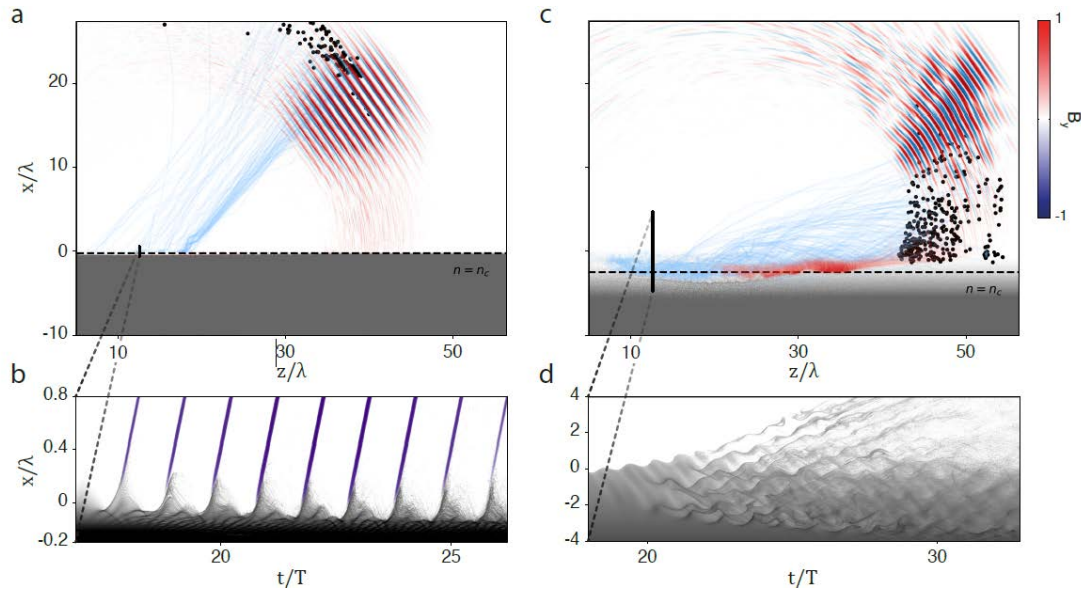
Identification of coupling mechanisms between ultraintense laser light and dense plasmas

L. Chopineau¹, A. Leblanc¹, G. Blaclard^{1,2}, A. Denoeud¹, M. Thévenet²,
J-L. Vay², G. Bonnaud¹, Ph. Martin¹, H. Vincenti¹, and F. Quéré¹,

¹ LIDYL, CEA, CNRS, Université Paris-Saclay, CEA Saclay, 91 191 Gif-sur-Yvette, France
² Lawrence Berkeley National Laboratory, Berkeley, CA 94720, USA

The interaction of intense laser beams with plasmas created on solid targets involves a rich non-linear physics. Because such dense plasmas are reflective for laser light, the coupling with the incident beam occurs within a thin layer at the interface between plasma and vacuum. One of the main paradigms used to understand this coupling, known as Brunel mechanism, is expected to be valid only for very steep plasma surfaces. Despite innumerable studies, its validity range remains uncertain, and the physics involved for smoother plasma-vacuum interfaces is unclear, especially for ultrahigh laser intensities.

We report the first comprehensive experimental and numerical study of the laser-plasma coupling mechanisms as a function of the plasma interface steepness, in the relativistic interaction regime. Our results reveal a clear transition from the temporally-periodic Brunel mechanism to a chaotic dynamic associated to stochastic heating. By revealing the key signatures of these two distinct regimes on experimental observables, we provide an important landmark for the interpretation of future experiments.



2D PIC simulations in the two distinct regimes of laser-plasma coupling. These data are obtained from 2D PIC simulations with different density gradients L ($\lambda/15$ for a and b, and $\lambda/1.5$ for c and d), while all other physical parameters remain the same ($a_0=3.5$, $\theta=55^\circ$). The two upper panels display the complete trajectories of a selected set of expelled high-energy test electrons (orange lines), together with the total y-component of the total B-field (blue to red color map) at a given time after the laser-plasma interaction. The plasma density profile at the end of the interaction is indicated in gray in log scale. The lower panels show the temporal evolution of the plasma electron density (gray-scale color map, in log scale), spatially-resolved along the normal to the target surface, at the center of the focal spot. The emitted attosecond pulses are superimposed to this density map in purple. They are clearly visible in panel b, but are too weak to be observed in panel d.

Wakefield acceleration and betatron radiation driven by linearly polarized Laguerre-Gaussian orbital angular momentum laser pulses

A. Longman¹, C. Salgado², G. Zeraoui², J. I. Apiñaniz², J. A. Pérez-Hernández², M. De Marco², C. Z. He³, G. Gatti², L. Volpe², W. T. Hill III³, and R. Fedosejevs¹

¹ Department of Electrical and Computer Engineering, University of Alberta, 9203 116St NW, Edmonton, AB, T6G 1R1, Canada

² Centro de Láseres Pulsados (CLPU), Calle del Adaja, 8, 37185 Villamayor de la Armunia, Salamanca, Spain

³ Joint Quantum Institute, University of Maryland, College Park, MD 20742, USA

Corresponding author: longman@ualberta.ca

Abstract

In this work, we report on the first results of wakefield accelerated electrons by ultra-intense linearly polarized Laguerre-Gaussian orbital angular momentum (OAM) modes. These modes, generated from the laser pulse after compression in the VEGA2 200TW Ti:Sapphire laser system at the Centro de Láseres Pulsados (CLPU) in Spain used novel off-axis spiral phase mirrors to convert the flat top laser beam to high purity Laguerre-Gaussian beams with $l = +1, -1$ and $+2$, with intensities of over 10^{18} Wcm⁻². Preliminary results of changes in electron and betatron divergence and energy spectrum when compared to the standard TEM₀₀ mode will be presented. These results will be compared to simulations using the 3D Particle in Cell (PIC) code EPOCH.

Introduction

The interaction of high intensity beams carrying orbital angular momentum (OAM) with a plasma has been a growing area of interest in recent years. The ability to introduce orbital angular momentum into a beam in addition to its spin angular momentum opens new avenues for investigating and controlling laser-plasma interactions. Several papers have indicated OAM beams as new possible sources of intense axial magnetic fields [1] and possible enhanced radiation sources in the relativistic intensity regime.

Experiment Design

Using the new VEGA2 30fs 200TW laser system at the Centre for Ultra Intense Pulsed Lasers (CLPU) in Salamanca, Spain, we were able to successfully generate LG₁₀, LG₋₁₀, and LG₂₀ beams at relativistic intensities. To generate these beams, we utilized new off-axis spiral phase mirrors (OAspM) shown in Figure 1. These mirrors are an ideal solution to the problems of mode conversion in large scale laser facilities and can convert a TEM₀₀ mode to an LG₁₀ mode with a conversion efficiency as high as 93% [3]. A fast change out system was employed

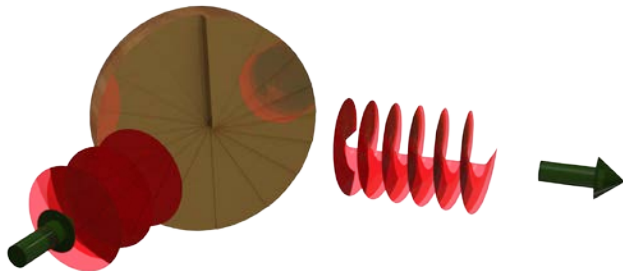


Fig. 1. Computer render of an off-axis spiral phase mirror (OAspM) used to generate high intensity OAM beams [2].

to switch between OAM mirrors enabling comparison of the wakefield electrons with similar laser parameters. These beams were focused into a mixture of helium and nitrogen (99:1) at densities of around 5×10^{18} cm⁻³ and intensities between 2×10^{18} Wcm⁻² and 1×10^{19} Wcm⁻² depending on the mode. Diagnostics were installed to observe various changes in the electron spectra, divergence and flux. The betatron radiation was monitored for its spectral content and divergence.

Results and Simulations

Preliminary analysis of the results has confirmed that higher order OAM modes are able to efficiently drive wakefield accelerated electrons. Electrons with energies more than 400 MeV were observed from both the LG_{±10} and the LG₂₀ modes. A filamentation instability may have caused these modes to break apart into beamlets, as some publications have suggested, resulting in a few electron “spots” in the far field divergence diagnostic. This filamentation instability may be driven by azimuthal asymmetries in the Laguerre-Gaussian beam.

An increase in betatron divergence was observed for increased OAM charge, likely due to an increase in the focal spot size. These measurements are compared with 3D PIC simulations run using EPOCH showing qualitative agreement.

References

- [1] S. Ali, J. R. Davies, and J. T. Mendonca, *Phys. Rev. Lett.* **105**, 035001 (2010).
- [2] A. Longman, and R. Fedosejevs, *U.S. Provisional Patent* #62/508,222 (2018)
- [3] A. Longman, and R. Fedosejevs, *Opt. Express*, 25(15), 17382-17392 (2017)

High-harmonic spectroscopy of electron-hole dynamics induced by strong-field ionization

J. Zhao, XW Wang and ZX Zhao

Department of Physics, National University of Defense Technology, Changsha 410073, Hunan, People's Republic of China

Corresponding author: jzhao@nudt.edu.cn

Abstract

We propose an IR-pump-XUV-probe scheme to investigate multi-electron-hole coherence. Using the laser-induced ionization as a gate for XUV excitation of core electrons, it provides us the opportunity to probe both the core and valence electron dynamics.

Recent advances in attosecond spectroscopy has enabled resolving electron-hole dynamics in real time (Ref.1). The correlated electron-hole dynamics and the resulted coherence are directly related to how fast the ionization is completed. Under strong infrared (IR) laser, ionization ignites from the outermost electron because of its long wavelength. The released valence electron and the created hole are further driven by the intense external fields. How their coherence evolves and whether it can be utilized to probe the core dynamics are among the key questions in attosecond physics or even attosecond chemistry. The combination of the ever-shorter attosecond pulses with the ever-intense infrared lasers helps probing and controlling both inner and outer shell electrons coherently on the equal footing.

In this work, we consider atoms with closed shells subjected to an intense IR laser pulse and a time delayed attosecond pulse (AP) which has a central frequency in resonant with the transition between the inner and valence shells. In the absence of the IR pulse, the direct transition from the inner shell to the valence shell is forbidden due to the Pauli exclusion principle. However, once the IR field induces ionization from the valence shell, the transition is triggered leaving a hole in the inner shell affecting the subsequent rearrangement dynamics. As shown in Fig.1, strong field ionization from the filled valence shell by IR field creates the associated continuum. Concurrently, it opens the subshell allowing the followed resonant transition pumped by the AP, which creates a hole in the core and transfers the continuum into its own. The attosecond light absorption and the resulted emission are thus gated by the ionization, in close analogy to the ionization induced absorption saturation where the transition energy is shifted by ionization. Meanwhile, the opened AP absorption creates coherence between the valence-hole and the core-hole. The transfer of coherence from ionization into both holes leads to multiple paths of HHG: harmonics can be radiated through recombination into the valence shell (path (v)) and the core hole (path (h)) respectively, or it can be generated upon the resonant core-valence transition

accompanied by the transfer of the continua (path (x)).

The emission spectra from the core-valence transition and the core-hole recombination are found modulating strongly as functions of the time delay between the two pulses, suggesting the coherent electron wave packets in multiple continua can be utilized to temporally resolve the core-valence transition in attoseconds. Therefore, using the laser-induced ionization as a gate for XUV excitation of core electrons, it provides us the opportunity to probe both the core and valence electron dynamics by manifesting themselves as a pronounced resonant peak in harmonic spectra and an extended cut-off harmonics. By analyzing the modulation of the spectra with the time-delay between the IR field and the AP, we show that the coherence of the ionization process and the driven core-hole and valence-hole coherence contribute to high-harmonic emission which can be utilized to obtain the multi-electron-hole or multichannel-coherence information.

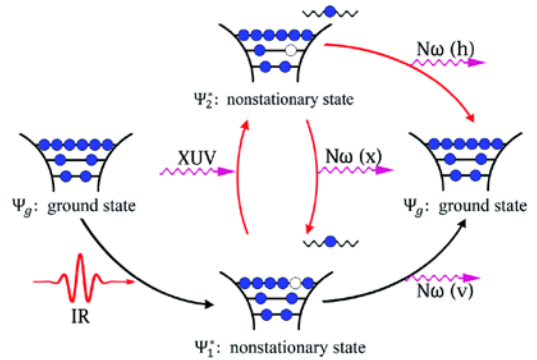


Fig. 1. Illustration of the interaction of the atom with the laser and XUV fields and the related high-harmonic generation processes.

References

- [1] F. Krausz and M. Ivanov, *Rev. Mod. Phys.*, **81**, 163 (2009).
- [2] J. Zhao, J. Yuan and Z. Zhao, *arXiv*: 1510.07947 (2015)

Coherent multichannel dynamics of aligned molecules resolved by two dimensional high-harmonic and terahertz spectroscopy

Yindong Huang, Xiaowei Wang, Jing Zhao, and Zengxiu Zhao

Department of Physics, National University of Defense Technology, Changsha 410073, Hunan, China

Corresponding author: xiaowei.wang@nudt.edu.cn

Abstract

In this work we combine the simultaneous measurement of terahertz wave and high harmonic emission to resolve the coherent multichannel electron dynamics of aligned CO₂ molecules driven by femtosecond laser pulses. Our approach provides a new tool for detecting and resolving these multi-electron phenomena.

Multichannel coherence plays an indispensable role in quantum dynamics. Observing the dynamics in ever larger spectral range provides more depth information on the ignition through ending of the dynamics in full details. To the strong field interaction, joint measurements on high-harmonic and terahertz spectroscopy (HATS) from atoms or molecules provides a new tool in understanding and controlling the electron dynamics from picoseconds to attoseconds. By precisely controlling the dual-color relative phase (50~attoseconds) and the alignment of molecules (2 degrees), we extend the HATS method to two dimensions to resolve the coherence of ionization and to reveal the coherent multichannel dynamics of aligned carbon dioxide in intense laser pulses. Experimental results and theoretical analysis suggest that multiple orbitals participate in the high harmonic generation and there is no phase difference between the different ionization channels. Our 2D-HATS method provides an alternative for the further investigations on multi-electron system and can be utilized as an in site modulator for attosecond pulse shaping.

In this work we combine the simultaneous measurement of terahertz wave and high harmonic emission to resolve the coherent multichannel electron dynamics of aligned CO₂ molecules driven by femtosecond laser pulses. Based on the single electron picture, high harmonic generation (HHG) can be understood by the rescattering model. Within each half optical cycle, the electron is accelerated away from the ion following tunneling ionization, and then driven back to recombine into the original state generating attosecond burst. For multielectron systems, however, the ionization could leave the ions in different configurations. In terms of the concept of molecular orbital (MO), HHG process can start from and end in the same orbitals, either the highest occupied MO (HOMO) or the lower lying MOs (HOMO-1 or

HOMO-2) of CO₂ molecules. As shown in Fig. 1, each participating orbital is associated to a particular channel and the total harmonic emission is their coherent summation. The amplitude and the phase of each channel that are to be scrutinized are related to the ionization, propagation and recombination of electron wave packets. Different from HHG, THz emission can be attributed to the coherent current generated by the continuum electron from all the channels. Combining measurement of both radiations for alignment controlled molecules, it is possible to resolve the coherence between these channels by observing in full details of the related dynamics.

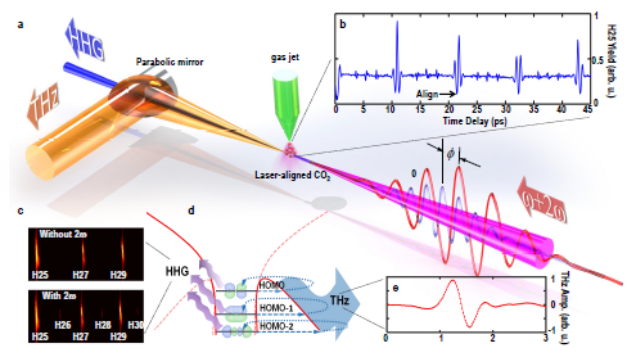


Fig. 1. a. Schematic illustration of the experimental set-up of 2D-HATS. b. Experimental data of the harmonic 25 yield from CO₂ as a function of the alignment and generation pulse delay. c. CCD camera images on the high harmonic spectroscopy with or without the second-harmonic pulse. d. Schematic diagram of the multi-channel participation on the generation process of the even harmonic and the THz wave. e. Typical THz waveform obtained from electro-optic sampling technique.

References

- [1] Y. Huang, *et al*, *Phys. Rev. Lett.* 115, 123002 (2015).
- [2] Y. Huang, *et al*, *J. Phys. B* 235601 (2016)

Temporal characterization of a two-color laser field using the tunneling ionization method

Jeong-uk Shin^{1,2}, Wosik Cho^{1,2}, and Kyung Taec Kim^{1,2,*}

¹Center for Relativistic Laser Science, Institute for Basic Science, Gwangju 61005, Korea

²Dept. of Physics and Photon Science, Gwangju Institute of Science and Technology, Gwangju 61005, Korea

Corresponding author: *kyungtaec@gist.ac.kr

We investigate the validity of the temporal characterization technique called tunneling ionization with a perturbation for time-domain observation of an electric field (TIPTOE) for a two-color laser field that is obtained using a fundamental laser field and its second harmonic field. The ionization yield calculated from the time-dependent Schrodinger equation shows a strong dependence on the relative delay between the fundamental pulse and the second harmonic pulse. The calculation results show that the TIPTOE technique can be applied for a two-color laser field.

The temporal characterization of a laser field is indispensable to study ultrafast light-matter interactions. Several characterization techniques for femtosecond laser pulses have been successfully demonstrated [1, 2]. However, most of them utilize the nonlinearity in second harmonic generation. These techniques can hardly be applied for the two-color laser field which contains both the fundamental and its second harmonic in the laser field.

Recently, the temporal characterization technique that utilizes the extreme nonlinearity of tunnelling ionization has been demonstrated, which is called tunnelling ionization with a perturbation for time-domain observation of an electric field (TIPTOE) [3]. In the TIPTOE method, the ionization yield is measured using two laser pulses, one strong and the other weak. The strong laser field (E_p) ionization gas molecules, and the weak laser field (E_s) perturb the ionization, slightly altering the ionization yield when superposed with the strong pulse.

The instantaneous ionization rate $w(t)$ is only dependent to the field strength of the laser pulse as

$$w(E_f + E_p) \approx w(E_f) + \left. \frac{dw}{dE} \right|_{E=E_f} E_p$$

If the fundamental pulse is not badly chirped, the modulation of the ionization yield at time delay τ between $E_f(t)$ and $E_p(t)$ would be

$$\begin{aligned} \delta N(\tau) &= N(\tau) - N_f(\tau) \\ &= \int_{-\infty}^{\infty} [w(E_f(t) + E_p(t + \tau)) - w(E_f(t))] dt \propto E_p(\tau), \end{aligned}$$

where $N(\tau)$ is the total ionization yield and $N_f(\tau)$ is the ionization yield obtained with the strong laser field only.

The validity of the TIPTOE method for the two-color laser field was test by solving one-dimensional time dependent Schrodinger equation (TDSE). The calculation results show that the accuracy of the TIPTOE measurement for the

two-color laser field strongly depends on the relative phase Δ between two-color pulses as shown Fig. 1. When Δ is zero, the ionization yield fits well with the input pulse. In the case of Δ being half of the cycle of second harmonics, the ionization yield has a flipped and delayed waveform of the input pulse. Thus, a suitable reconstruction process is required to find the input field from the ionization yield modulation.

In summary, we have investigated the applicability of the TIPTOE method for the two-color laser field. The ionization yield modulation reproduce the input pulse when the relative phase between the two laser field is zero. For other relative phases, the input pulse can still be retrieved through a reconstruction process.

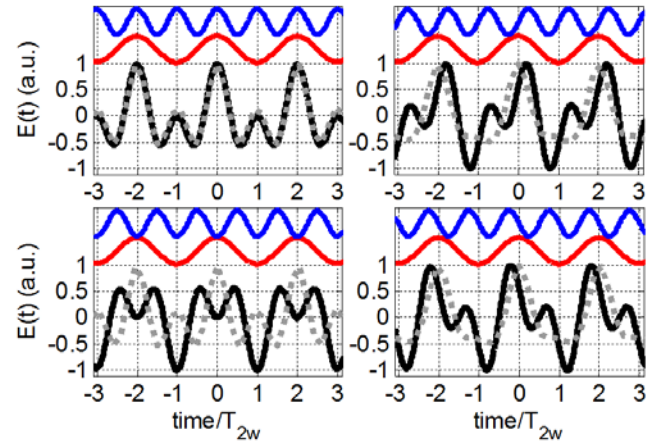


Fig. 1. Comparison of the ionization yield obtained by solving TDSE calculations (grey dotted) and the input pulse (black solid) at four different relative phase. Fundamental pulse (red) and the second harmonics (blue) are shown above.

References

- [1] D. J. Kane et al., *IEEE J. Quantum Electron.* **29**, 571–579 (1993).
- [2] C. Iaconis et al., *Opt. Lett.* **23**, 792–794, (1998).
- [3] S. B. Park et al., *Optica* **5**, 402-408 (2018).

Ignatovsky Diffraction: Calculating Vector Fields in an Arbitrarily Tight Laser Focus

Michael Ware and Justin Peatross

Department of Physics and Astronomy, Brigham Young University, Provo, UT 84602

Abstract

Extremely tight focusing produces a somewhat complicated vector field structure in the focus of a laser pulse. Accurately modelling this vector field requires an integral approach as introduced by Ignatovsky in the 1920s. The Ignatovsky model is an exact solution to Maxwell's equations, and correctly models the vector fields in a laser focus at all focal sizes. Several approximations for vector fields in a laser focus have been introduced and are now in wide use. These approximations provide significantly reduced computational requirements, but at varying costs in accuracy. We compare several of these models to the Ignatovsky model, and show that for most practical cases a model developed by Singh and Erikson in 1994 provides the most accurate results.

Ignatovsky Diffraction

We highlight the under-appreciated (and under-used) work of V. S. Ignatovsky [1] which models vector diffraction for a beam focused by a parabolic mirror or by a lens. Ignatovsky published his work in 1920. Unfortunately, Ignatovsky was executed together with his wife by the Soviets, but his work has influenced the development of vector diffraction in the microscopy community for nearly a century. In [2] we provide a streamlined and accessible derivation of Ignatovsky's results and demonstrate its practicality for use in high-intensity laser physics. For an azimuthally symmetric beam with uniform polarization, the diffraction integral collapses to one dimension, which can be performed numerically with reasonable efficiency.

Although some in the microscopy community have used Ignatovsky diffraction, many in the laser community have sought alternative vector models of a laser focus, apparently without the benefit of Ignatovsky's work. A variety of models have been offered, which often differ markedly from each other. A broad criticism that we make against many of these models is that they start from an *assumed field distribution* in the focal region and attempt to develop vector fields (consistent with Maxwell's equations) in the surrounding region. This approach is at odds with the fact that no experimenter directly controls the focal field distribution. Rather, experimenters typically diagnose and manipulate their incident beam to control the fields at the focusing optic before it converges, diffracts, and interferes to form the focal fields. Moreover, the ability to directly measure vector components of the fields in an intense focus is extremely limited. This makes Ignatovsky diffraction, where the incident field is defined at a focusing optic rather than inside the focus, much more natural and relevant to experimental work.

Other Models

For applications such as computing relativistic trajectories of charged particles in a tightly focused intense beam, one would ideally like a closed analytic formula that adequately represents the vector field components to avoid repeatedly evaluating the integrals used in Ignatovsky diffraction at various positions within the interaction region. We evaluate several of these models and compare them with the results calculated using the Ignatovsky model. We find that a paraxial vector model proposed by Erikson and Singh [3] best agrees with Ignatovsky diffraction (down to $f/2$ optics).

On the other hand, a frequently employed iterative scheme first introduced by Lax in 1975 [4], with the intent of improving beyond the paraxial limit, actually worsens agreement with Ignatovsky. We note also that the Lax expansion produces undesirable divergences in the far field, making that program suspect.

Acknowledgement: NSF 1708185

References

- [1] V. S. Ignatovsky, "Diffraction by a Parabolic Mirror Having Arbitrary Opening," *Trans. Opt. Inst. Petrograd* 1, paper 5 (1920).
- [2] J. Peatross, M. Berrondo, D. Smith, and M. Ware, "Vector fields in a tight laser focus: comparison of models," *Optics Express* 25, 287287 (2016).
- [3] W. L. Erikson and S. Singh, "Polarization Properties of Maxwell-Gaussian Laser Beams," *Phys. Rev. E* 49, 5778-5786 (1994).^[1]_[SEP]
- [4] M. Lax, W. H. Louisell, and W. B. McKnight, "From Maxwell to paraxial wave optics," *Phys. Rev. A* 11, 1365-1370 (1975).

Coupling cryogenic low-Z jets with ultra-intense lasers to observe novel effects induced by relativistic transparency

C. B. Curry^{1,2}, M. Gauthier¹, H-G. Chou¹, A. Grassi¹, J. B. Kim^{1,*}, G. Dyer^{3,†}, X. Jiao³, E. Galtier¹, G. D. Glenn³, S. Goede⁴, R. Mishra¹, E. McCary³, L. Obst⁵, H. J. Quevedo³, M. Rehwald⁵, C. Schoenwaelder^{1,6}, Y. Y. Tsui², T. Ziegler⁵, T. Ditmire³, K. Zeil⁵, U. Schramm⁵, B. M. Hegelich^{3,‡}, F. Fiuza¹, and S. H. Glenzer¹

¹High Energy Density Science Division, SLAC National Accelerator Laboratory, Menlo Park, CA 94025, USA

²Department of Electrical and Computer Engineering, University of Alberta, Edmonton, AB T6G 1H9, Canada

³Department of Physics, University of Texas at Austin, Austin, TX 78712, USA

⁴European XFEL GmbH, 22869 Schenefeld, Germany

⁵Institute of Radiation Physics, Helmholtz-Zentrum Dresden-Rossendorf, 01328 Dresden, Germany

⁶Erlangen Centre of Astroparticle Physics, Friedrich-Alexander University, 91058 Erlangen, Germany

* Present address: KLA-Tencor Corporation, Milpitas, CA 95035, USA

† Present address: SLAC National Accelerator Laboratory, Menlo Park, California, 94025, USA

‡ Present address: Center for Relativistic Laser Science, Institute for Basic Science (IBS), Gwangju 61005, Republic of Korea

Corresponding author: glenzer@slac.stanford.edu

Abstract

To date, most laser-driven ion beam parameters remain suboptimal for the most promising applications in terms of ion energy, spatial control, and brilliance. Particle-in-cell (PIC) simulations have identified more favorable regimes than Target Normal Sheath Acceleration using higher peak laser intensities and advanced target designs. Planar cryogenic low-Z jets have been fielded at the DRACO and the Texas Petawatt laser facilities to explore ion acceleration from TNSA to the relativistic transparency regime where high energy, low divergence ion beams are predicted. First experimental results demonstrate improved control and beam shaping and record peak brilliance setting up a clear path towards high repetition rate applications.

Cryogenic micro-jets are formed by cryogenically cooling a low-Z gas to liquid that is injected into vacuum through a micron-sized aperture [1, 2]. The liquid continues to cool by evaporative cooling and solidifies before breakup due to the Plateau-Rayleigh instability. The high flow velocity and rapid solidification process produces a solid cylindrical (planar) jet by maintaining the circular (rectangular) aperture geometry as shown in Fig. 1. As such, cryogenic low-Z jets, with tunable thickness and near-critical density, can be used to systematically investigate multiple ion acceleration regimes. We have studied the transition from Target Normal Sheath Acceleration to Enhanced Sheath Field (ESF) acceleration using the DRACO laser (3 J, 30 fs) [3-6] and the Texas Petawatt laser (110 J, 135 fs). Experimental observations suggest a direct interaction between the laser pulse and the bulk plasma, a signature of relativistic transparency. These results are compared with 2D/3D Particle-in-Cell (PIC) simulations.

Acknowledgments

We gratefully acknowledge the DRACO and Texas Petawatt laser scientists, technicians, and support staff. This work was part of a larger collaboration with Helmholtz-Zentrum Dresden-Rossendorf and supported by the U.S. Department of Energy Office of Science, Fusion Energy Science under FWP No. 100182, 100237 and 100331, the National Science Foundation under Grant No. 1632708, and by EC Horizon 2020 LASERLAB-EUROPE/LEPP (Contract No. 654148).

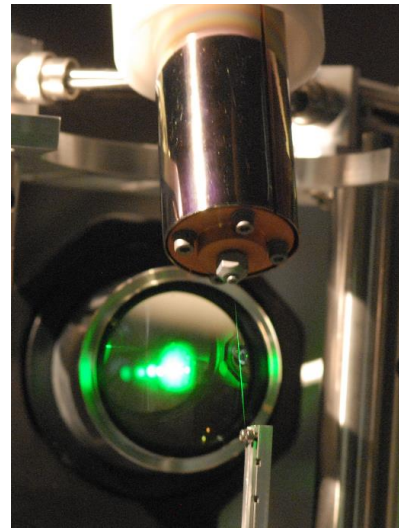


Fig. 1. Photograph of cryogenic hydrogen jet in the Titan chamber at the Jupiter Laser Facility [1]

References

- [1] M. Gauthier, J. B. Kim et al, *Rev. Sci. Instrum.*, (2015)
- [2] J. B. Kim, S. Goede et al, *Rev. Sci. Instrum.*, (2015)
- [3] S. Goede, C. Roedel et al, *Phys. Rev. Lett.*, (2017)
- [4] M. Gauthier, C. B. Curry et al, *Appl. Phys. Lett.*, (2017)
- [5] L. Obst, S. Goede, M. Rehwald et al, *Sci. Rep.*, (2017)
- [6] L. Obst, T. Ziegler et al, *Nat. Commun.*, (2018)

Space-Time Resolved Analysis of Electron Repulsion

Scott Glasgow¹, and M.J. Ware²

¹ Department of Mathematics, 275 TMCB Brigham Young University, Provo UT 84602

² Department of Physics, N283 ESC Brigham Young University, Provo UT 84602

Corresponding author: Glasgow@mathematics.byu.edu

Abstract

We give a qualitatively correct Quantum-Field-Theoretic analysis of basic but nontrivial spatio-temporal features of electron repulsion, demonstrating distinct eras of dynamics. The analysis is not perturbative, and is in the form of full space-time resolved simulations, which are computationally feasible because we consider a scenario in which one spatial dimension captures the qualitatively relevant features of electron repulsion, and because we assume that the coupling between radiation and matter is small enough that effects associated with measuring two or more force-carrying quanta simultaneously, and effects caused by the generation of virtual electron-positron pairs are both qualitatively negligible.

In the past decade, Grobe, Su, et al. have made great strides in producing time-resolved quantum-field-theoretic dynamics [2]. We continue in this vein and generate realistic simulations of electron-electron repulsion via the following model: We consider Schrodinger dynamics

$$i \frac{d}{d\tau} |\Psi\rangle = H_2 |\Psi\rangle$$

where τ measures time in units of $\hbar / m_e c^2$, m_e is the (bare) mass of an electron, and the second-quantized Hamiltonian H_2 is given by

$$H_2 = \int d\xi \left(h_e(\xi) c^\dagger(\xi) c(\xi) + h_\gamma(\xi) a^\dagger(\xi) a(\xi) \right) + \int d\xi \int d\xi' g(\xi', \xi) c^\dagger(\xi') a^\dagger(\xi - \xi') c(\xi) + \text{h.c.}$$

Here $a^\dagger(\xi)$ creates from bare vacuum $| \rangle_a$ a photon $| \xi \rangle_\gamma = a^\dagger(\xi) | \rangle_a$ of well-defined momentum and energy $p = m_e c \xi$, $E = m_e c^2 h_\gamma(\xi) = m_e c^2 | \xi |$, while $c^\dagger(\xi)$ creates a bare electron $| \xi \rangle_e = c^\dagger(\xi) | \rangle_e$ of that momentum with bare energy $E = m_e c^2 h_e(\xi) = m_e c^2 \sqrt{1 + \xi^2}$. The term $g(\xi', \xi) c^\dagger(\xi') a^\dagger(\xi - \xi') c(\xi)$ indicates that $g(\xi', \xi)$ is the rate at which H_2 generates scattering of a bare electron of momentum ξ into a correlated (bare) electron-photon pair state, the electron sporting new momentum ξ' , the photon carrying off the remaining momentum $\xi - \xi'$. The structure of the function $g(\xi', \xi)$ is indicated in [1], and is a consequence of the Lorentz invariance of 3+1 Dimensional QED. To make simulations feasible, we develop a first quantized approximate Hamiltonian $H_1 = P H_2 P$, where P projects the full Fock space of arbitrarily large numbers of photons onto a subspace with no more than one photon, and also projects onto the H_2 -invariant subspace of charge two.

Fig. 1. shows snapshots of the time evolution of

the joint probability distribution for finding one of the electrons at position x and the other at position y , no photon found anywhere. The centres of the electron distributions at time $\tau = 0$ are at $x, y = \pm 4$, where distance is measured in units such that it takes one unit of time τ for light to traverse one unit of space. The initially bare electrons undergo only quantum diffusion for an era. This era is also characterized by the localized bare electrons becoming dressed by an equally localized photon field, as well as generating a radiated photon unneeded for this localized dressing. In the second snapshot in **Fig. 1** a radiated photon from one of the now rather well-dressed electrons finally arrives at the other, and in the next two figures a probability “shock wave” travels through the well-dressed electrons. In the fourth frame the electrons begin to separate, indicating something like the occurrence of Compton scattering between one of the electrons and the photon radiated by the other. In the last snapshot the electrons have moved a significant amount away from each other, and have undergone a good deal of quantum dispersion. Since the numerical simulation involves a “universe” of the size indicated by these frames, subsequent snapshots reveal that the radiated electrons return from the opposite side and push the electrons back together, again via an event like Compton scattering.

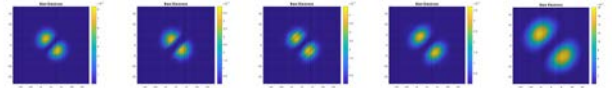


Fig. 1. Time $\tau = 0, 2, 4, 10, 20$ snapshots of the joint probability distribution for finding two electrons and no photons, starting at $\tau = 0$ with no photons and with the electrons most likely to be found at positions $x, y = \pm 4$.

References

- [1] S. Glasgow, D. Smith, L. Pritchett, J. Gardiner, and M. J. Ware, Phys. Rev. A 93, 062106 (2016)
- [2] R. E. Wagner, M. R. Ware, B. T. Shields, Q. Su, and R. Grobe, Phys. Rev. Lett. 106, 023601 (2011).

Remote detection of radioactive material using mid-IR laser-driven electron avalanche

R.M. Schwartz, D. Woodbury, J. Isaacs, P. Sprangle, and H.M. Milchberg
 Department of Physics, University of Maryland, College Park, MD 20742-4111, USA
 Corresponding author: rms344@umd.edu

Abstract

Remote detection of distant, shielded radioactive material is an important goal, but it is made difficult by the finite spatial range of the decay products. Here, we demonstrate a remote detection technique using mid-infrared ($\lambda=3.9\mu\text{m}$) laser-induced avalanche breakdown of air. We discuss several detection schemes, verify observed trends with numerical simulations, and present our latest results to extend the detection range of this technique.

Introduction

Detecting radioactive material at range remains a difficult technical challenge. Conventional methods directly detect radioactive emission whose flux falls off, at best, as the inverse square of the distance from the source. In the immediate vicinity of radioactive material, however, high-energy particles ionize neutral air constituents, elevating the number of free electrons and ions present in the ambient air. This technique uses the enhanced negative ion population surrounding a radioactive source to seed an avalanche breakdown driven by an intense 50ps $3.9\mu\text{m}$ laser [1,2]. Mid-IR pulses efficiently drive avalanche ionization while avoiding multi-photon ionization which masks the enhancement from radiation. Several schemes relying on transmission, backscatter, and plasma fluorescence can be used to detect the presence of radioactive materials near the laser focus.

Experiment and Results

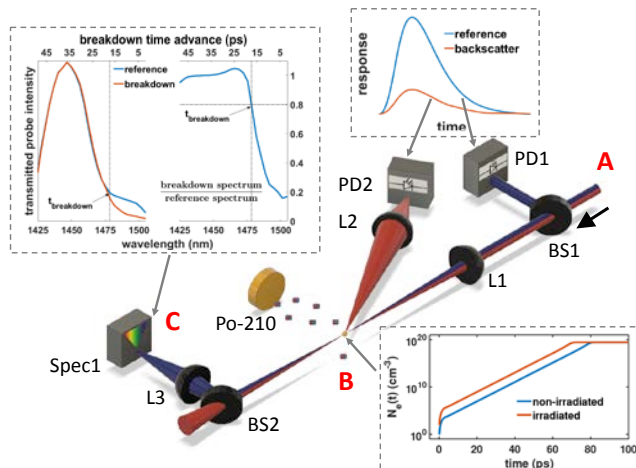


Fig. 1. Experimental Overview. (A) Two photodetectors measure shot-by-shot pump reference energy and backscatter. (B) The rate of avalanche ionization depends on the irradiation from a Po-210 α -emitter. (C) The chirped transmitted probe spectrum measures breakdown time.

Copropagating chirped 50ps $\lambda=3.9\mu\text{m}$ pump and weak 70 ps $1.45\mu\text{m}$ probe pulses are generated in

an OPCPA [3]. The two beams are focused from f/10 to f/25 to pump intensities on the order of 10^{12} W/cm^2 near a Po-210 source emitting 5.3MeV α -particles (Fig 1).

Avalanche ionization seeded by the radioactive source creates a plasma which scatters the pump and probe. The backscattered pump is collected by a PbSe photodetector and the transmitted probe is collected by a NIR InGaAs spectrometer. The backscattered pump energy is correlated with the breakdown rate and the spectrum of the chirped probe provides a measure of the breakdown time. Large enhancements in both measures are seen as the radioactive source approaches the laser focus (Fig. 2). Observed results are in close agreement with our 0-D numerical ionization models.

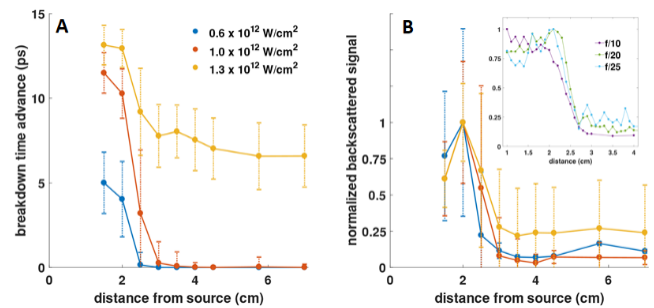


Fig. 2. Breakdown enhancement as a Po-210 source is brought closer to the laser focus leads to (A) faster breakdowns of the time resolved $1.45\mu\text{m}$ transmitted probe and (B) larger backscatter signals of the $3.9\mu\text{m}$ pump. Inset shows various focal geometries with a fixed $0.7 \times 10^{12} \text{ W/cm}^2$ intensity.

Our current work is extending this detection scheme to meter-scale distances using a mid-IR InSb imaging spectrometer to resolve the spectra of the backscattered pump allowing for single-color measurements while still getting the time resolution of the chirped probe.

References

- [1] J. Isaacs, C. Miao, P. Sprangle., *Physics of Plasmas* (2016)
- [2] R.M. Schwartz, D. Woodbury, J. Isaacs, P. Sprangle, H.M. Milchberg., *Science Advances* (in review).
- [3] G. Andriukaitis *et al.*, *Optics Letters* (2011)

POSTER ABSTRACTS

Picosecond time-resolved spectra of enhanced K-shell emission in petawatt-laser-irradiated Ni nanowire arrays

O.S. Humphries¹, M.P. Hill², B. Williams², M.G. Ramsay², P. Allan², C.R.D. Brown², L.M.R. Hobbs², S.F. James², D.J. Hoarty², R.S. Marjoribanks³, J. Park⁴, R. London⁴, R. Tommasini⁴, A. Pukhov⁵, C. Bargsten⁶, R. Hollinger⁶, V. N. Shlyaptsev⁶, M.G. Capeluto⁶, J.J. Rocca⁶, S.M. Vinko¹

¹ Clarendon Laboratory, Department of Physics, University of Oxford, OX1 3PU, UK

² Material Physics Group, AWE Plc, Aldermaston, RG7 4PR, UK

³ Department of Physics, University of Toronto, M5S 1A7, Canada

⁴ Lawrence Livermore National Laboratory, Livermore, CA 94550, USA

⁵ Heinrich Heine University of Düsseldorf, 40225, Düsseldorf, Germany

⁶ Department of Electrical and Computer Engineering, Colorado State University, Fort Collins, CO 80523, USA

Corresponding author: oliver.humphries@physics.ox.ac.uk

Abstract

Nanostructured samples irradiated by intense short pulse lasers present new opportunities to create ultra-high energy density systems at near solid density, with enhanced X-ray emission yields. Here details and analysis of an experimental campaign on the AWE Orion laser to investigate the scaling of nanowire targets to petawatt-scale lasers are presented, which provide first estimates of the conditions achievable at relativistic intensities on nanostructured targets.

Information

Nanostructured samples irradiated by intense short pulse lasers present new opportunities to create ultra-high energy density systems near solid density. These samples have also been shown to enhance X-ray emission yields by over an order of magnitude in certain conditions, making them of interest to X-ray backlighting and radiography applications in laser plasma experiments. Here we present picosecond-resolution streaked nickel K-shell spectra which show the evolution of material conditions within these samples, using data obtained from the AWE Orion laser. The time-resolved emission of different

nanowire target geometries is interpreted using the FLYCHK [3] atomic kinetics code, and compared to a flat foil target. These results provide first estimates of the conditions achievable at relativistic intensities, and will guide future research investigating the electronic structure of heated nanowire samples at the LCLS FEL and the Orion laser.

References

- [1] G. Kulcsár *et al.*, *Physical Review Letters* **84.22:5149** (2000)
- [2] M.A. Purvis *et al.*, *Nature Photonics* **7.10:796** (2013)
- [3] H.-K. Chung *et al.*, *High Energy Density Phys.* **1.1:3** (2005)
- [4] C. Bargsten *et al.*, *Science Advances* **3.1:e1601558** (2017)

Alpha decay in intense laser fields: Calculations using realistic nuclear potentials

Jintao Qi¹, Tao Li², Ruihua Xu¹, Libin Fu¹, and Xu Wang^{1,*}

¹ Graduate School, China Academy of Engineering Physics, Beijing 100193, China

² Beijing Computational Science Research Center, Beijing 100193, China

*Corresponding author: xwang@giscaep.ac.cn

Abstract

We calculate the effect of intense laser fields on nuclear alpha decay process, using realistic and quantitative nuclear potentials. We show that alpha decay rates can indeed be modified by strong laser fields to some finite extent. We also predict that alpha decays with lower decay energies are relatively easier to be modified than those with higher decay energies, due to longer tunneling paths for the laser field to act on. Furthermore, we predict that modifications to angle-resolved penetrability are easier to achieve than modifications to angle-integrated penetrability.

Introduction

The past few decades witness rapid advancements in intense laser technologies. The promising under-constructing extreme light infrastructure (ELI) of Europe is designed to reach peak intensities above 10^{23} W/cm² [1].

Widely accepted as a quantum tunneling process [2], nuclear alpha decay is expected to be modified in the presence of a strong laser field through modifying the potential barrier. We mention works by Misticu and Rizea [3] and by Delion and Ghinescu [4] aiming at providing qualitative understandings. Here we studied the effect of intense laser fields on nuclear alpha decay quantitatively, using realistic and quantitative alpha-nucleus potentials. Our numerical results show that alpha decay can indeed be modified by strong external laser fields to some finite extent. A modification on the alpha particle penetrability (or half life) of 0.1% may be expected for laser intensity 10^{24} W/cm².

Method

(1) The alpha-nucleus potential

$$V(r) = V_N(r) + V_C(r)$$

where $V_C(r) = ZZ/r$ is the Coulomb potential, and

$$V_N(r) = -1100 \exp\left\{-\left[\frac{r-1.17A^{1/3}}{0.574}\right]\right\} \text{ MeV}$$

is a quantitative alpha-nucleus potential [5] by fitting to alpha-nucleus scattering data.

(2) The laser-nucleus interaction

$$V_l(\vec{r}, t) = -Z_{eff}\vec{r} \cdot \vec{\epsilon}(t) = -Z_{eff}r\epsilon(t)\cos\theta$$

where $Z_{eff} = (2A - 4Z)/(A + 4)$ is an effective charge.

The neglect of the magnetic part of the laser field is justified by the fact that the alpha particle moves much slower than (estimated to be a few percent of) the speed of light.

(3) The quasistatic approximation

From a classical picture, the alpha particle needs about 10^{-21} sec to travel through a potential barrier of 10 fm length. This time is much smaller than an optical cycle of strong lasers (on the order of 10^{-15} sec).

During the time that the alpha particle penetrates through the potential barrier, the change of the laser field is negligible and the laser field can be viewed as static.

(4) The penetrability of the alpha particle

The penetrability of the alpha particle through the potential barrier can be calculated using the Wentzel-Kramers-Brillouin (WKB) method as

$$P(\theta, t) = \exp\left(-\frac{2}{\hbar} \int_{R_{in}}^{R_{out}} \sqrt{2\mu[V(r) - Q + V_l(r, \theta, t)]} dr\right)$$

The decay energy Q for the three nuclear elements are 1.97, 5.82, and 8.98 MeV, respectively.

Example Numerical Results

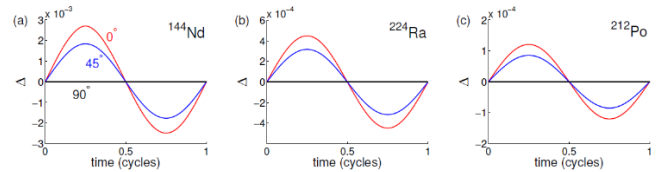


Fig. 1. Laser-induced modifications to the alpha particle penetrability, for laser peak intensity 10^{24} W/cm². Modifications to the alpha penetrability are on the order of 0.1% for ¹⁴⁴Nd and of 0.01% for ²²⁴Ra or ²¹²Po. $\Delta \equiv [P(\epsilon) - P(\epsilon = 0)]/P(\epsilon = 0)$ is the relative change of the penetrability with the laser field.

More results can be found in our preprint [6].

References

- [1] D. Ursescu *et al.*, Proc. SPIE 8780, 87801H-1 (2013).
- [2] G. Gamow, Z. Physik 51, 204 (1928).
- [3] S. Misticu and M. Rizea, J. Phys. G 40, 095101 (2013).
- [4] D. S. Delion and S. A. Ghinescu, Phys. Rev. Lett. 119, 202501 (2017).
- [5] G. Igo, Phys. Rev. Lett. 1, 72 (1958).
- [6] J. Qi *et al.*, arXiv: 1810.07331 (2018).

Impact of ultrafast optical and XFEL laser pulses on nanowire targets, for high energy-density atomic physics studies

Georgia Thomas¹, Alan Miscampbell², Ryan Royle², Oliver Humphries²,
Anne Heron³, Sam Vinko², Robin Marjoribanks¹

¹Department of Physics, University of Toronto, 60 Saint George St., Toronto, ON M5S-1A7, Canada

²Department of Physics, Clarendon Laboratories, University of Oxford, UK

³CPhT – CNRS, Ecole Polytechnique

Corresponding author: marj@physics.utoronto.ca

Abstract

Nickel nanowire targets were introduced as targets for experiments on the Matter in Extreme Conditions (MEC) end-station of the LCLS x-ray free-electron laser (XFEL). An intense femtosecond optical pulse provided laser plasma heating and ionization, and the tuneable output of the synchronized XFEL probed the state of warm dense matter in a detailed study of ionization-potential depression. The studies included this characterization of susceptibility of nanowire targets to low levels of optical laser prepulse.

Introduction

Experiments on the LCLS x-ray free-electron laser have provided newly precise measurements of ionization potential depression (IPD) in solid-density systems heated by high-intensity x-ray pulses in low-Z materials [1,2]. Surprisingly, the standard derived model (Stewart-Pyatt (SP)), used for decades for laser-produced plasmas, is not routinely the best fit: results may be in better agreement with the earlier *ad hoc* Ecker-Kroll (EK) model.

Given the importance of IPD in plasma physics, this disparity is a key scientific question, and has spurred considerable further theoretical work [3–7]. New precise work investigating the physics of IPD in laser-produced plasmas on ORION, at higher temperatures and densities, also shows more continuum lowering than predicted by the SP model, but neither do these results fit the simple EK model successfully applied to the LCLS results [8,9].

We have used nanowire targets, introduced by Marjoribanks in 2000 [10] as laser-plasma targets, to create near-isochoric laser heating, to compare to XFEL isochoric heating of solid targets, in an effort to create an ‘intermediate’ data set, laser-heated but XFEL-probed. We quantified relative absorption of nanowire and flat targets, by imaging scattered light. Experiments were compared to EMI2D particle-in-cell (PIC) simulations. Modelling and experiments both show greatly increased absorption in nanowire targets. We studied the effect of minuscule amounts of prepulse on the integrity of nanowires at the time of peak intensity.

References

- [1] O. Ciricosta et al., *Phys. Rev. Lett.* **109**, 065002, (2012).
- [2] O. Ciricosta et al. *Nat. Commun.* **7**, 11713 (2016).
- [3] S.-K. Son et al., *Phys. Rev. X*, **4**, 031004 (2014).
- [4] B.J.B. Crowley, *High Energy Density Physics*, **13**(0):84 102 (2014).
- [5] S. M. Vinko et al, *Nat. Commun.* **5**, 3533 (2014).

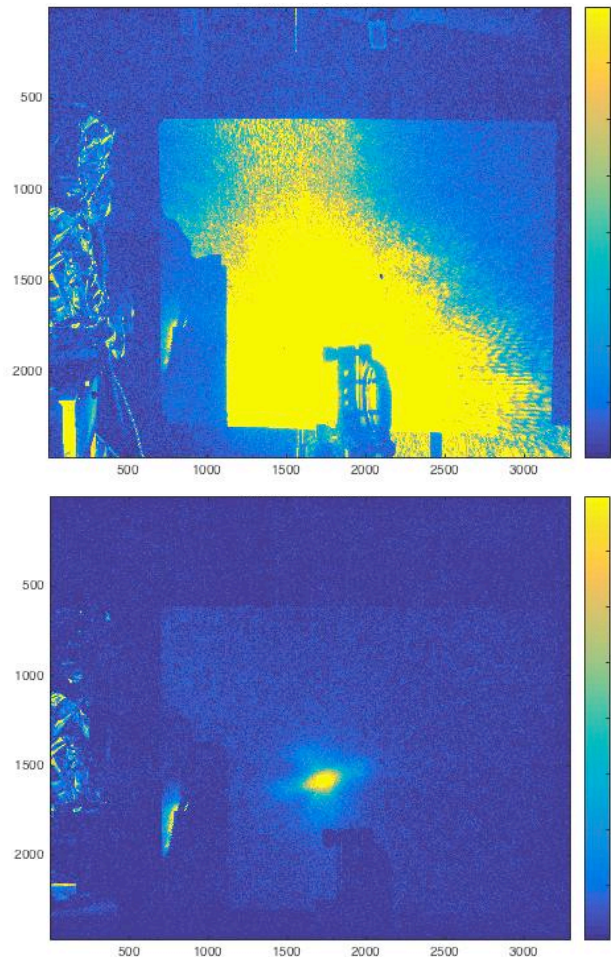


Fig. 1. Reflectometry images of a planar Ni target (top) and nanowire Ni target (bottom) quantify orders-of-magnitude difference in reflected light, and concomitant higher absorption (same intensity scale).

- [6] A. Calisti et al., *Contrib. Plasma Physics*, **55**(5):360365 (2015).
- [7] S. Zhang et al., *Phys. Rev. B* **93**, 115114 (2016).
- [8] D.J. Hoarty et al. *Phys. Rev. Lett.* **110**:265003, (2013).
- [9] T.R. Preston et al., *HEDP* **9**, 258 (2013).
- [10] G. Kulcsár, D. AlMawlawi, F. W. Budnik, P. R. Herman, M. Moskovits, L. Zhao, and R. S. Marjoribanks, *Phys. Rev. Lett.* **84**:5149, (2000).

1.3 Participants

First Name	Last Name	Affiliated Institution
David	Ayuso	Max-Born-Institut
Paul	Corkum	University of Ottawa
Chandra B.	Curry	SLAC National Accelerator Laboratory
Jiří	Daněk	Max-Planck-Institut für Kernphysik
Tom	Dzelzainis	University of Toronto
George	Gibson	University of Connecticut
Scott	Glasgow	Brigham Young University
Siegfried	Glenzer	SLAC National Accelerator Laboratory
Elissa	Haddad	Institut national de la recherche scientifique (INRS)
Oliver	Humphries	University of Oxford
Alvaro	Jimenez-Galan	Max Born Institut Berlin
Kyung Taec	Kim	IBS / GIST
Fanqi	Kong	University of Ottawa
FRANCOIS	LEGARE	Institut national de la recherche scientifique (INRS)
Andrew	Longman	University of Alberta
Chunhai	Lyu	Max-Planck Institute for Nuclear Physics
Robin	Marjoribanks	University of Toronto
FRANCOIS	MAUGER	Louisiana State University
Eric	MEVEL	Universite de Bordeaux
Howard	Milchberg	University of Maryland
Felipe	Morales Moreno	Max-Born Institute Berlin
Justin	Peatross	Brigham Young University
Pavel	Polynkin	University of Arizona
Gil	Porat	University of Alberta
Maria	Richter	Max-Born Institute Berlin
Takeshi	Sato	The University of Tokyo
Robert	Schwartz	University of Maryland
Jeong Uk	Shin	Gwangju Institute of Science and Technology
Richard	TAIEB	Sorbonne Universite
Daniel	Treacher	University of Oxford
Muxue	Wang	Peking University
Xu	Wang	Graduate School of China Academy of Engineering Physics
Michael	Ware	Brigham Young University

2.4 About the Fields Institute

Mandate

The Fields Institute is a center for mathematical research activity - a place where mathematicians from Canada and abroad, from academia, business, industry and financial institutions, can come together to carry out research and formulate problems of mutual interest.

Our mission is to provide a supportive and stimulating environment for mathematics innovation and education. The Fields Institute promotes mathematical activity in Canada and helps to expand the application of mathematics in modern society.

History

Founded in 1992, the Fields Institute was initially located at the University of Waterloo. The Fields Institute officially opened at its 222 College Street location on the campus of the University of Toronto on November 17, 1995. The building the Institute occupies was designed specifically to accommodate its research functions and

activities by Toronto architects Kuwabara Payne McKenna Blumberg.

The Institute is named for Canadian mathematician John Charles Fields (1863-1932), whose will established the International Medal for Outstanding Discoveries in Mathematics, now known as the Fields Medal.

Activities at the Institute

The Fields Institute environment is designed to support and enhance a large spectrum of mathematical activities such as research in pure and applied mathematics, statistics, computer science, and a broad spectrum of other disciplines including engineering, mathematical biology, theoretical physics, economics and mathematical finance, telecommunications, and medicine.

Research activities of the Institute bring together prominent mathematicians from Canada and around the world for periods of intensive collaborative research on topics of current importance. Programs are selected by the Scientific Advisory Panel, an independent group of leading Canadian and international mathematicians.

Publications

The Fields Institute publishes two book series with the American Mathematical Society (AMS):

- The Monograph Series features high-quality research monographs and lecture notes in mathematics and applications of mathematics in science, engineering and industry.

- The Communications Series volumes are conference proceedings of research and survey articles.

Publications in both series often result from activities at the Institute, but we encourage

all authors to consider publishing with us. Our publishing program with the AMS affords authors the advantages of wide distribution and advertising, high quality, and low cost of published material, and a guarantee that all volumes will remain long in print.

All Monographs and Communications volumes are available for purchase from the American Mathematical Society On-line Bookstore:

**[www.ams.org/cgi-bin/bookstore/
bookpromo/fimseries](http://www.ams.org/cgi-bin/bookstore/bookpromo/fimseries)**

3.1 Nearby Restaurants

On Campus

White Cube

Cafeteria-style cafe.
40 St. George St. - 905-616-5973

New College Residence Café

On-campus cafeteria.
40 Willcocks St. - 416-598-2029

Veda

Indian vegan, Halal, and allergen-friendly takeaway.
569 Spadina Cres. - 416-961-9797

Coffee Shops

Second Cup

Inside the Koffler Student Centre beside Fields
40 St. George St. - No phone

Starbucks

At College / Beverley intersection one block east of Fields
205 College St. - 416-341-0101

Tim Hortons

One block west of Fields on College.
455 Spadina Ave. - 416-593-5523

Spadina Avenue

Dumpling House

Chinese restaurant
328 Spadina Ave. - 416-596-8898

Pho Hung

A classic Vietnamese restaurant specializing in pho dishes.
350 Spadina Ave. - 416-593-4274

Goldstone Noodle

Cantonese restaurant
266 Spadina Ave. - 416-596-9053

Rol San

Chinese restaurant featuring dim sum
323 Spadina Ave. - 416-977-1128

Simon Sushi

Japanese restaurant
409 Spadina Ave. - 416-977-2828

Xe Lua

Vietnamese restaurant featuring pho dishes
254 Spadina Ave. - 416-703-8330

College Street

Prenup Pub

Upscale campus pub with large beer selection
191 College St - (416) 506-4040

Izakaya

Japanese sushi and bento boxes
294 College St. - 416.551.6264

Free Times Café

Jewish and Middle Eastern cuisine
320 College St - 416-586-0202

Baldwin Village

Café La Gaffe

French and Mediterranean restaurant
24 Baldwin Street - 416-596-2397

Crepes Club

Featuring both savoury and sweet French crepes.
49 Baldwin St. - 416.357.5404

John's Italian Café

Casual Italian restaurant
27 Baldwin St - 416-596-8848

Kinton Ramen

Specializing in Japanese Ramen.
51 Baldwin St. - 647.748.8900

Kuni Sushi Ya

Sushi restaurant
20 Baldwin St. - 416-260-3188

Sin and Redemption

Casual restaurant and pub
17 Baldwin St. - 416-621-3636

Vegetarian Haven

Vegetarian and vegan restaurant
136 McCaul St. - 416.640.9197

Kensington Market

El Trompo

Mexican food with patio
277 Augusta Ave. - 416-260-0097

Hibiscus

Cafe featuring vegetarian and gluten-free options
238 Augusta Ave. - 416-364-6183

Templeton's

Casual pub fare with patio
319 Augusta Ave. - 416.922.7423

Torito

Spanish tapas restaurant
276 Augusta Ave. - 416.961.7373

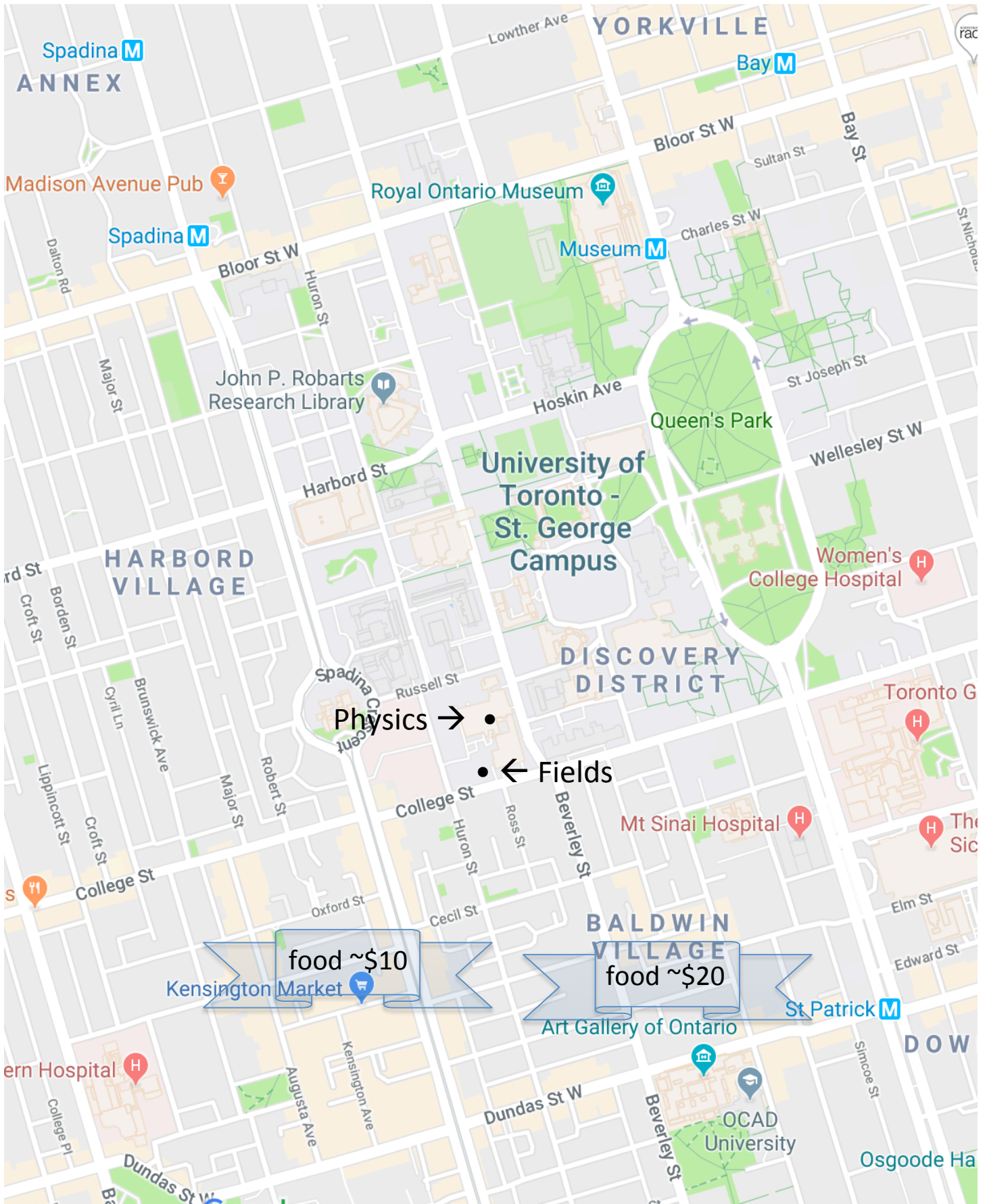
Trinity Common

Bar and restaurant
303 Augusta Ave. - 647-346-3030

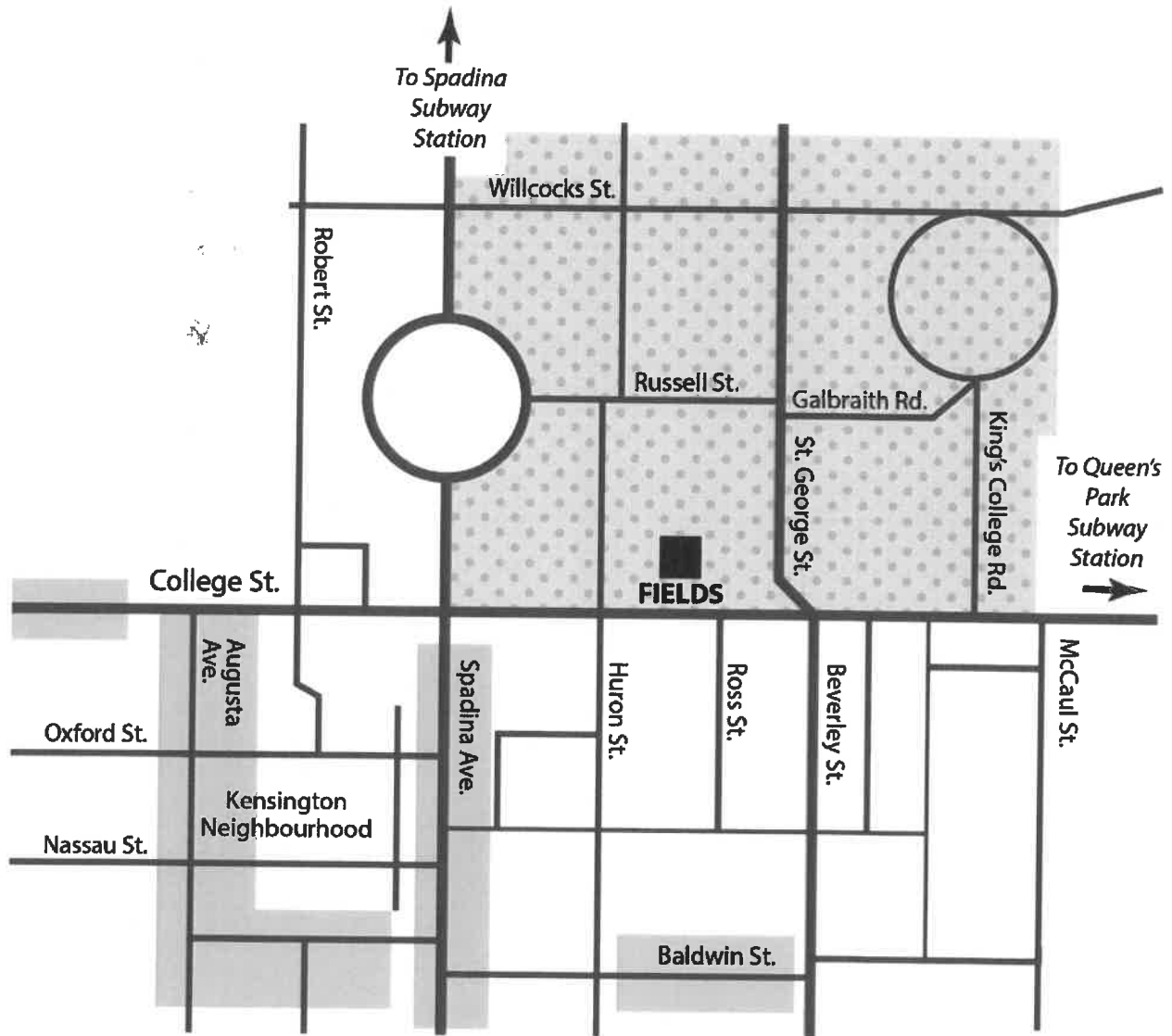
Urban Herbivore

Vegan sandwiches, salads, and soups
64 Oxford St. - 416.927.1231

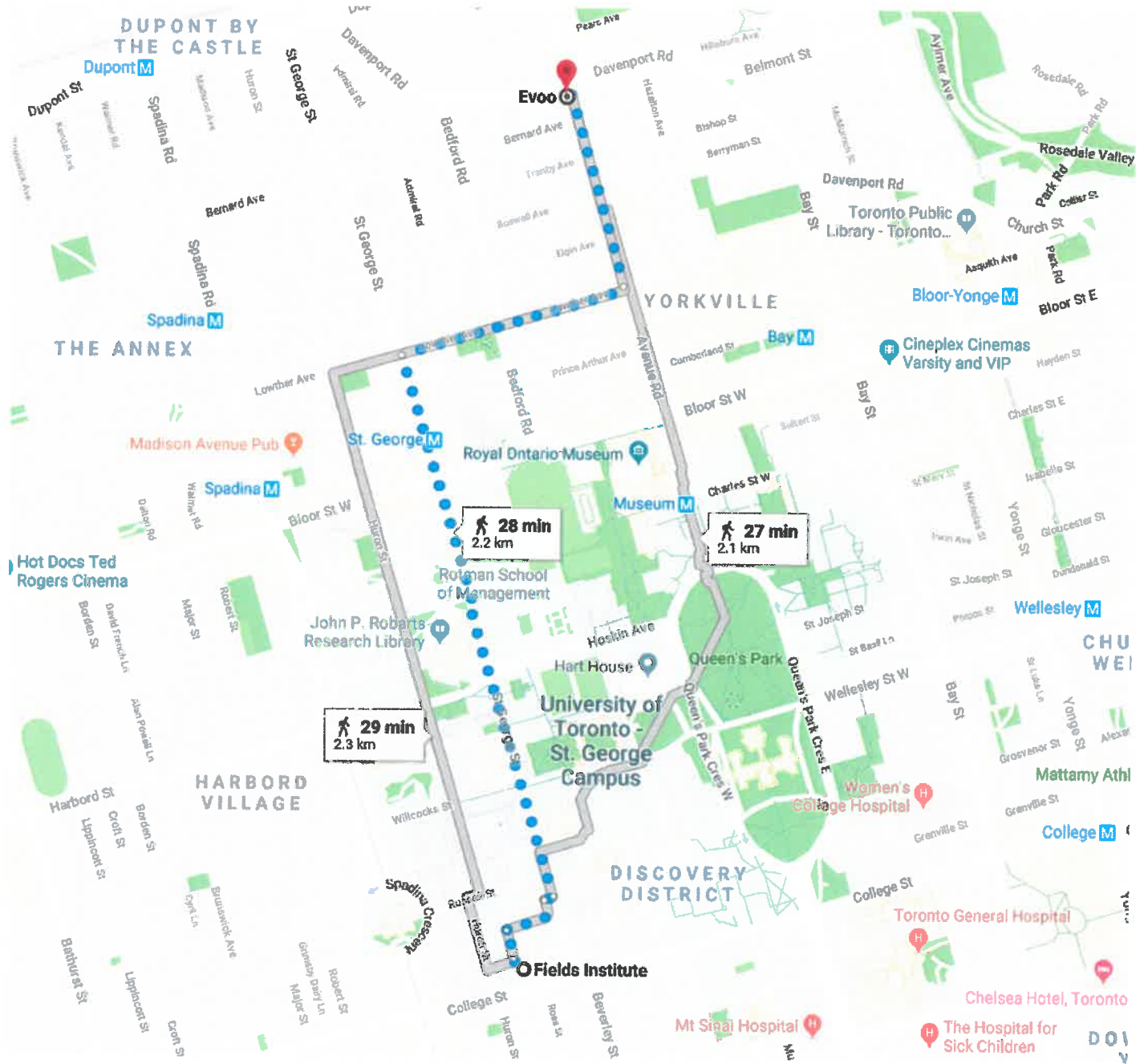
Local area map



3.2 Local Map



Map to EVOO Ristorante (138 Avenue Rd) :



Laptop Connections at The Fields Institute

Connecting to the Wireless Network

1. Choose network **FieldsWiFi**.
2. Enter password **Mathem@ics!** *Note: Do not add a “t” after the @* (here, @ is for “at”)
3. Open up a web browser. You should automatically be directed to an authentication page (if not, see below*). Follow the instructions to register your device. If you do not have an individual Fields Institute account you may use this month’s general access code: **December-gc87** (valid until **December 27** 2018)

*If you are not automatically directed to the authentication page, try manually going to <http://128.100.216.26:82/mycomputer>

Technical note: Some older devices refer to choosing the “SSID” instead of choosing the “network”, and refer to “encryption key” instead of “password”. If you are asked to select the key type, choose “ASCII”. If you are asked for the encryption type, choose “WPA2-Personal” or “WPA2-PSK”. If neither is listed, try “WPA-Personal” or “WPA-PSK”.

Connecting to the Wired Network

1. Connection

There are three laptop stations, and many offices have available connection points.

Laptop stations have 3-4 network cables clipped to the top of the table, and a power bar. Plug one of these cables into your computer. Please do not touch anything underneath the table. Station locations: **4th floor east hallway, 3rd floor west hallway, and 3rd floor east hallway.**

If your office has a free outlet with a six-digit label (like “022-03A”), or a network switch with free ports, you may use it; you will need your own cable (or ask to borrow one from the computing staff).

If your office has a pair of outlets with labels ending in “A” and “B” and a gray cable plugged in to the **B** outlet with the other end free, you may plug the other end of the gray cable into your laptop.

Please do not use any outlets whose labels begin with “V” (these are telephone jacks, not network outlets!) and **please do not disconnect any Fields equipment.**

If there are no free outlets, please ask the computing staff to install a “network switch” which will provide more outlets.

2. Authentication

After plugging in your laptop the first time, authenticate by opening a web browser and follow the same instructions as in step 3 above for a wireless connection. (You only need to do this once).

3.3 Place to Visit in Toronto

Royal Ontario Museum	https://www.rom.on.ca/en
Art Gallery of Ontario	https://ago.ca/
Casa Loma	http://casaloma.ca/
Museum of Contemporary Art	https://museumofcontemporaryart.ca/
High Park	http://www.highparktoronto.com/
Evergreen Brickworks	https://www.evergreen.ca/evergreen-brick-works/
Distillery District	https://www.thedistillerydistrict.com/
St Lawrence Market	http://www.stlawrencemarket.com/
CN Tower	https://www.cntower.ca/intro.html
Roy Thompson Hall	https://www.roythomsonhall.com/
Scotiabank Arena	https://www.scotiabankarena.com/